PHOTOCHEMICAL METHODS FOR NUCLEOPHILIC SUBSTITUTION REACTIONS AND INHIBITION OF CYSTEINE PROTEASES.

by

SHREY PATEL

(Under the Direction of Vladimir Popik)

ABSTRACT

We hereby report the development of the novel photochemical approach to the induction of nucleophilic substitution reactions. This strategy employs a light-activated leaving group based on the 9-aryl-9-fluorene system. 9-fluorenol undergoes efficient photolysis of the C–O bond to generate a fluorenyl cation that is highly reactive. It rapidly undergoes cyclization, activating the leaving group and increasing the electrophilicity of the substrate. Irradiation of 9-aryl-9-fluorenyl derivatives at 300 nm in dichloromethane in the presence of a nucleophile afforded efficient photolysis. The method was applied to form a glycosidic bond between mannosyl sugar and methanol.

o-naphthoquinone methides (o-NQMP) are reactive electrophilic intermediates. Their ability to undergo rapid Michael addition with thiols has developed an interest in protein labeling and modification. Upon irradiation at 350 nm, PEG_4-NQMP and Biotin-NQMP efficiently inhibited cysteine protease papain. In addition, the binding of Biotin-NQMP with papain was confirmed via western blot.

INDEX WORDS: Nucleophilic substitution, HEPFOL-THP, Glycosylation, o- naphthoquinone methide, Thiol-Michael addition, Papain.

PHOTOCHEMICAL METHODS FOR NUCLEOPHILIC SUBSTITUTION REACTIONS AND INHIBITION OF CYSTEINE PROTEASES

by

SHREY PATEL

BS, Georgia Institute of Technology, 2016

A Thesis Submitted to the Graduate Faculty of The University of Georgia in Partial Fulfillment of the Requirements for the Degree

MASTER OF SCIENCE

ATHENS, GEORGIA

2022

PHOTOCHEMICAL METHODS FOR NUCLEOPHILIC SUBSTITUTION REACTIONS AND INHIBITION OF CYSTEINE PROTEASES

by

SHREY PATEL

Major Professor:	Vladimir V. Popik
Committee:	Robert S. Phillips
	Y. George Zheng

Electronic Version Approved:

Ron Walcott
Vice Provost for Graduate Education and Dean of the Graduate School
The University of Georgia
August 2022

DEDICATION

I dedicate this thesis to my family and friends for their support throughout my graduate school.

ACKNOWLEDGEMENTS

I would like to thank my PI Dr. Popik for his support and motivation. I would also like to thank my previous and current lab mates for their assistance. Finally, I would like to thank Dr. Kapil Upadhayaya from the Crich group, Elijah Roberts from the Amster group, and Mengtong Cao and Jiabao Song from the Zheng group for their help with these projects.

TABLE OF CONTENTS

Page

LIST OF TABLES

Page

LIST OF FIGURES

Page

CHAPTER 1

Photoactivable Nucleophilic Substitution Reactions

1.1 Introduction

Nucleophilic substitution reactions play an essential role in organic chemistry. The reaction strategies such as glycosylation, hydrolysis, and ether synthesis are all developed based on the nucleophilic substitution mechanism. But there have not been many reports of light-triggered nucleophilic substitution strategies. In earlier studies, Mayr and co-workers[1] developed photogeneration of benzhydryl cations through irradiation of N-benzhydryl pyridinium salts. But specific reagent requirement limits this strategy's broad application.

The goal is to develop a light-triggered activating system that can be applied to a broad range of substrates. For this purpose, the 9-fluorenyl cation system was chosen. The 9-fluorenyl cation is unstable in the ground-state due to its antiaromatic (4n π) character. Thus, it forms an aromatic 4π cationic system in its excited state. In earlier studies, Wan and Krough[2] showed that irradiation (254 nm) of 9-fluorenol **(1.1)** in the presence of aqueous solvents generated 9-fluorenyl cation via C-O bond cleavage. This was the first benzylic system reported that underwent efficient photolysis without the presence of electron-donating groups.

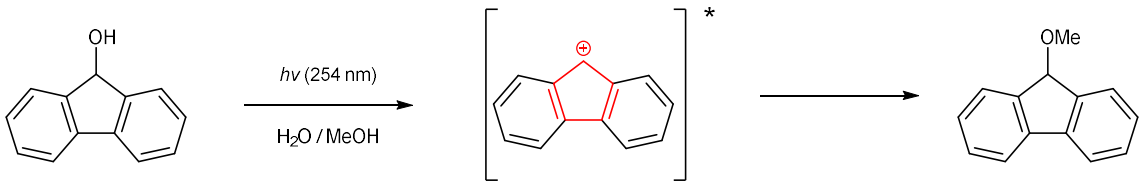

After initial observation, the 9-fluorenyl cation was observed directly via laser flash photolysis in 1989 and found to have a lifetime of fewer than 20 ps in aqueous solutions[3]. It was discovered that the pathway for the cleavage of the C-O bond and cation generation followed both photohomolysis and photoheterolysis[4]. The heterolytic cleavage was preferred in aqueous solutions with a high dielectric constant, whereas homolytic cleavage was preferred in low dielectric constant solvents such as methanol. The 9-fluorenyl cation can be unusually stable in fluorinated alcohols such as 2,2,2-trifluoroethanol **(TFE)** and 1,1,1,3,3,3-Hexafluoropropan-2-ol **(HFIP)** due to their low nucleophilicity but high polarity[5].

The relative ease of formation of the cation formation even with a poor leaving group such as OH^- has been attributed to the internal cyclic array containing 4nπ systems[6]. Alcohols such as diphenylmethanol do not undergo photolysis or do so considerably less efficiently. This shows the importance of the central ring for photolysis.

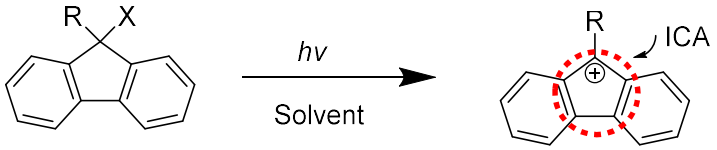

R = H, CH_3, Ph
X = OH, OMe, OAc, Br
Solvent = MeOH:H_2O or ACN:H_2O

1.2 Proposed System for Photochemistry

Herein, we propose a 9-fluorenyl-based system to develop light-induced S_N1/S_N2 reactions. Upon irradiation, heterolytic cleavage of the C-O bond generates a carbocation. The presence of a phenyl ring attached to carbon-9 further stabilizes the carbocation. The generated carbocation is intramolecularly attacked by a heteroatom connected to the system. The six-membered ring transition state ensures a high rate of formation of the intermediate **1.5.** Based on the stability of **1.5**, the onium cation can undergo cleavage with the formation of another carbocation **1.7** (S_N1

pathway) or can be attacked by a nucleophile directly following the S_N2 pathway. This system would also generate spiro product **1.6** as the secondary product.

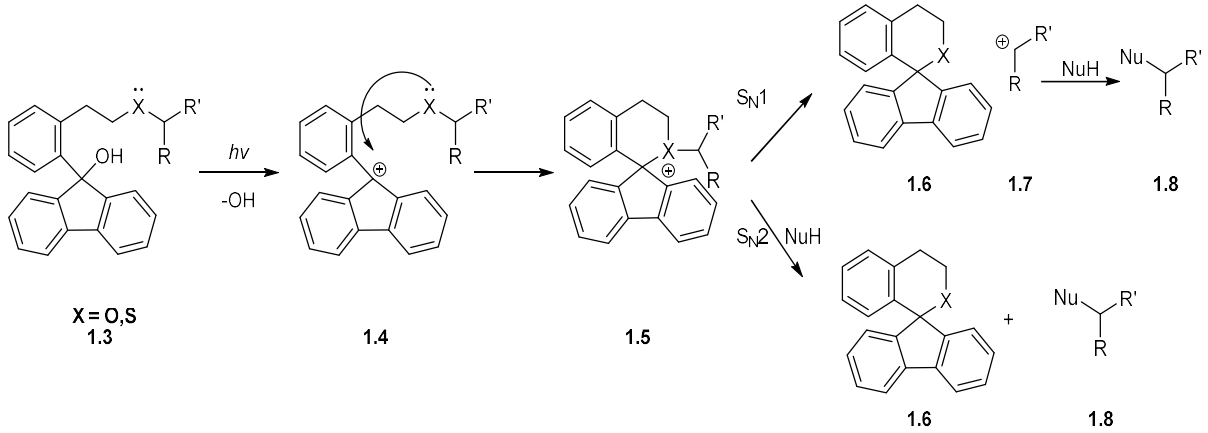

Scheme 1.1. Proposed Strategy for Light-triggered Nucleophilic

We would also like to extend this system toward developing a photochemical glycosylation method. Upon the cation formation, an intramolecular attack by the heteroatom generates oxonium ion **1.11.** It is then trapped by a nucleophile (or another sugar) to give the glycosylated product **1.12** and the secondary product **1.6.**

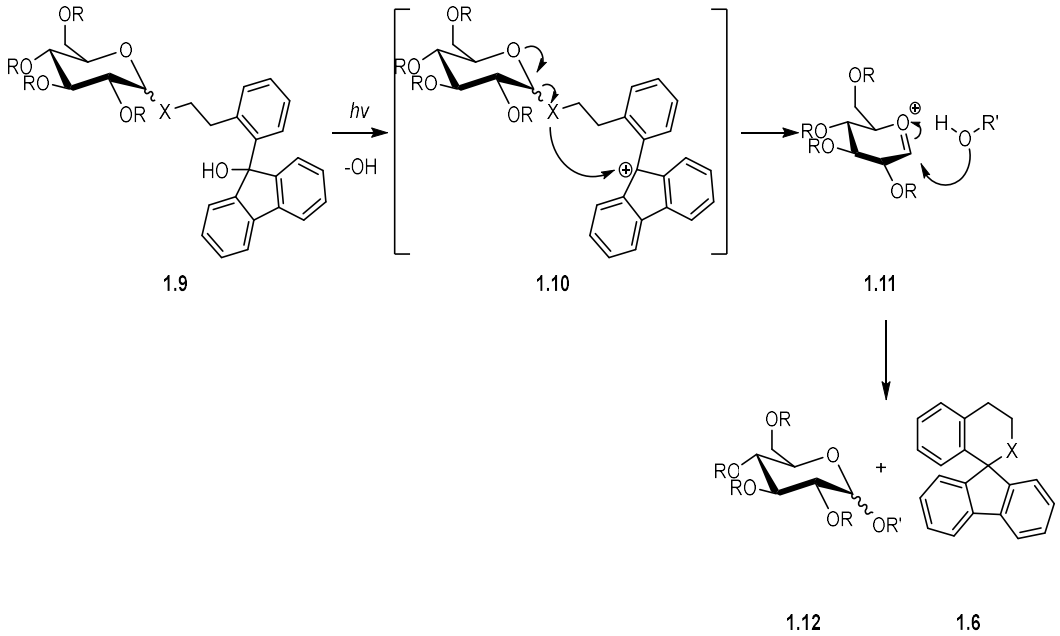

Scheme 1.2. Proposed Mechanism for Light-triggered Glycosylation

1.3 Photochemistry Test of HEPFOL-THP

To test our hypothesis, 9-(2-(2-((tetrahydro-2H-pyran-2-yl)oxy)ethyl)phenyl)-9H-fluoren-9-ol (**HEPFOL-THP**) was used as a model. The tetrahydropyran moiety stabilizes the oxocarbenium ion and gives us a basic idea if this model could be applied to sugars. Photolysis of 2 mM solution of HEPFOL-THP in 1 mL of 2,2,2-trifluoroethanol (TFE) afforded spiro[fluorene-9,1'-isochromane] (**Spiro-FIC)** and 2-(2,2,2-trifluoroethoxy)tetrahydro-2*H*-pyran (**TFE-THP)**. The reaction and the products were followed through GC-MS analysis. The conversion was efficient, with the 95% conversion taking 10 minutes of irradiation.

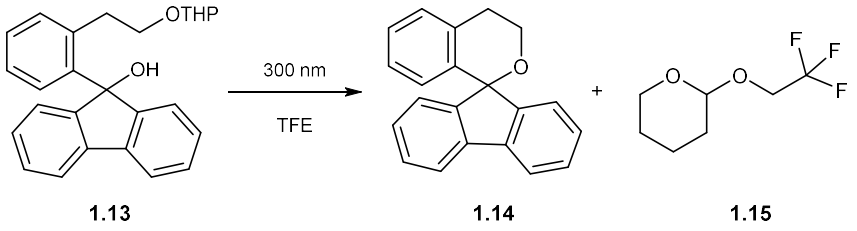

Scheme 1.3. Photolysis of 2 mM HEPFOL-THP in TFE

Similarly, we tested the photolysis in 1,1,1,3,3,3-hexafluoropropan-2-ol **(HFIP)** as well. As expected, 99% conversion happened at 10 min irradiation time. The photolysis afforded the expected products Spiro-FIC **(1.14)** and **1.16.** It was observed that the starting material **1.13** underwent photolysis even under ambient light.

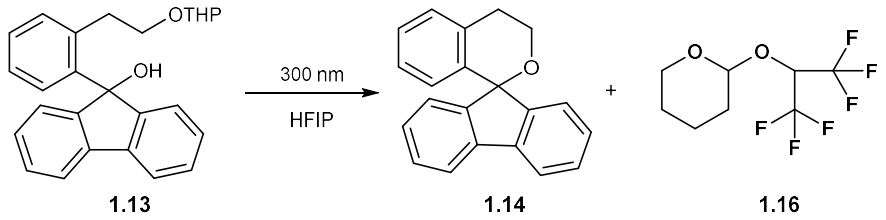

Scheme 1.4. Photolysis of 2 mM HEPFOL-THP in HFIP

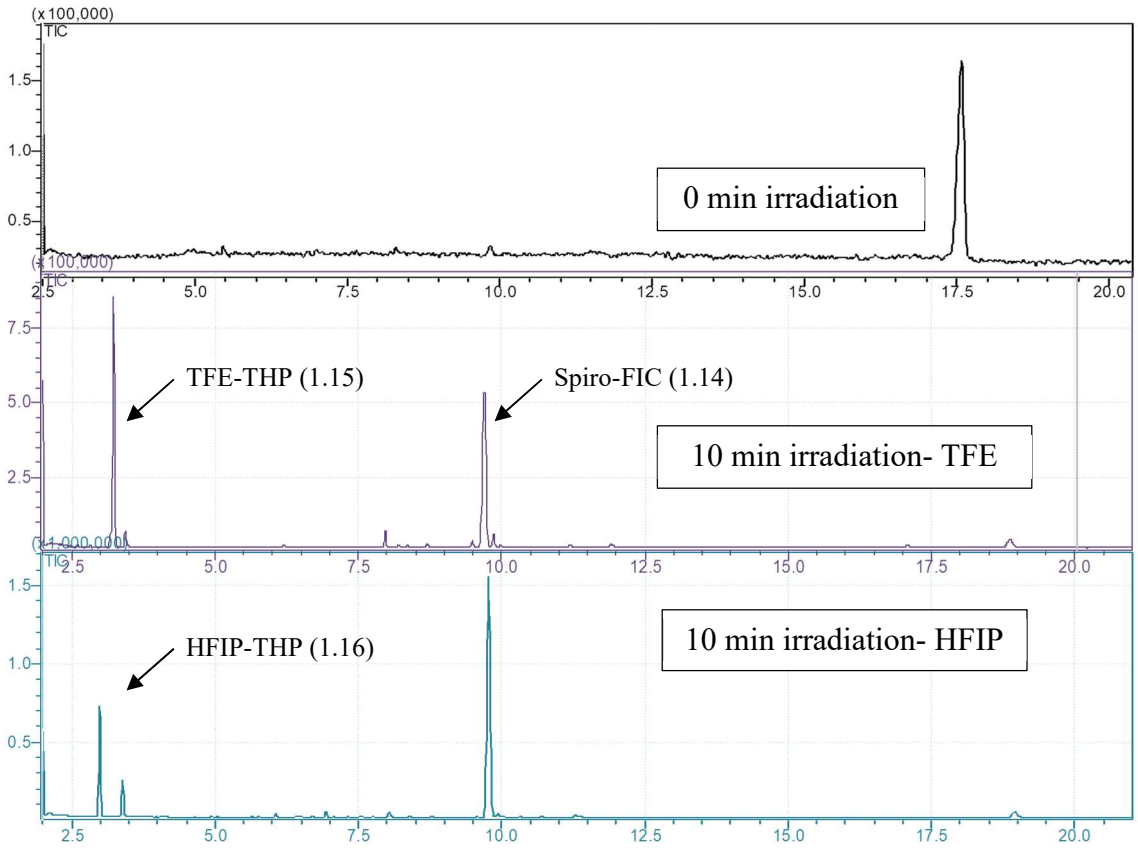

Figure 1.1. GC/MS Analysis of the Photolysis of HEPFOL-THP in TFE/HFIP

After successfully conducting the photochemistry in the fluorinated alcohols, we wanted to test how the photochemistry behaves in more nucleophilic solvents such as methanol. Upon 10 min irradiation of 2 mM of HEPFOL-THP in methanol, only 80% conversion was observed. Even though the expected products **1.14** and **1.17** did form, the compound **1.18** was the major product observed. This product was formed due to nucleophilic methanol trapping the carbocation before it could undergo cyclization. Upon irradiation of **1.18** in methanol**,** it was observed that it could also undergo photolysis to eventually form both Spiro-FIC **(1.14)** and **1.17.** But this additional step increases the required irradiation time for the photolysis of HEPFOL-THP **(1.13).** Even after 30 minutes of irradiation at 300 nm, only 85% conversion was achievable. Upon prolonged irradiation, compound **1.19** started to accumulate. It was theorized that compound **1.19** was the

product of the decomposition of Spiro-FIC **(1.14)**. This was confirmed by irradiating **1.14** at 300 nm and comparing it with a reference. Although Spiro-FIC is a secondary product, it was necessary to limit the irradiation time to 15 min for 2 mM concentration to avoid an accumulation of **1.19** for future experiments.

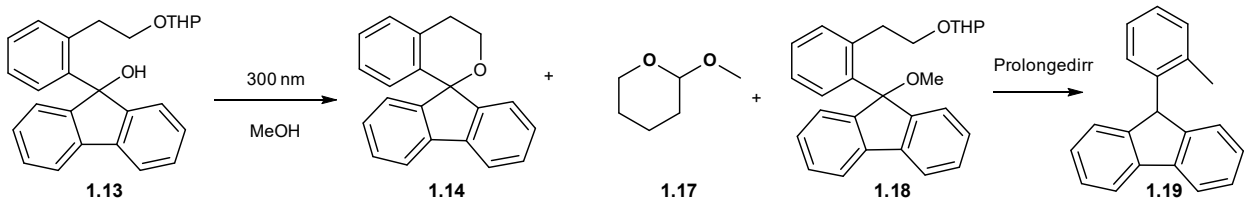

Scheme 1.5. Photolysis of 2 mM HEPFOL-THP in Methanol

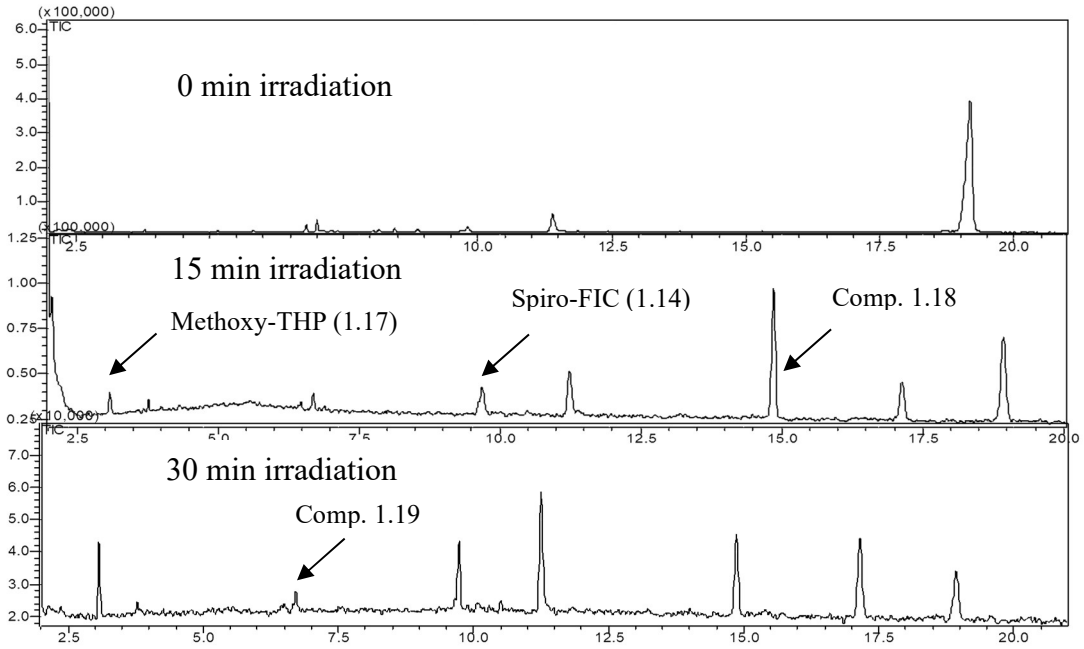

Figure 1.2. GC/MS Analysis of the Photolysis of HEPFOL-THP in MeOH

The target compound HEPFOL-THP **(1.13)** was synthesized as depicted in **Scheme 1.6 (a)** below. 2-bromophenyl ethanol **(1.20)** was protected as the tetrahydropyranyl ether **1.22** with 86% yield. Then, nucleophilic addition of **1.22** to 9-fluorenone **1.23** gave HEPFOL-THP **(1.13)** with 60% yield. We also prepared the references for the expected products. Spiro-FIC **(1.14)** was

prepared by exposing HEPFOL-THP **(1.13)** to strong acidic conditions. 2-Methoxytetrahydro-2*H*-pyran **(1.17)** was prepared by protecting methanol with tetrahydropyran in the presence of copper nitrate as a lewis acid. The byproduct **1.19** was prepared by nucleophilic addition of 1-bromotoluene **(1.26)** to 9-fluorenone **(1.23)**, followed by dehydration. The compound **1.18** was prepared using Williamson ether synthesis.

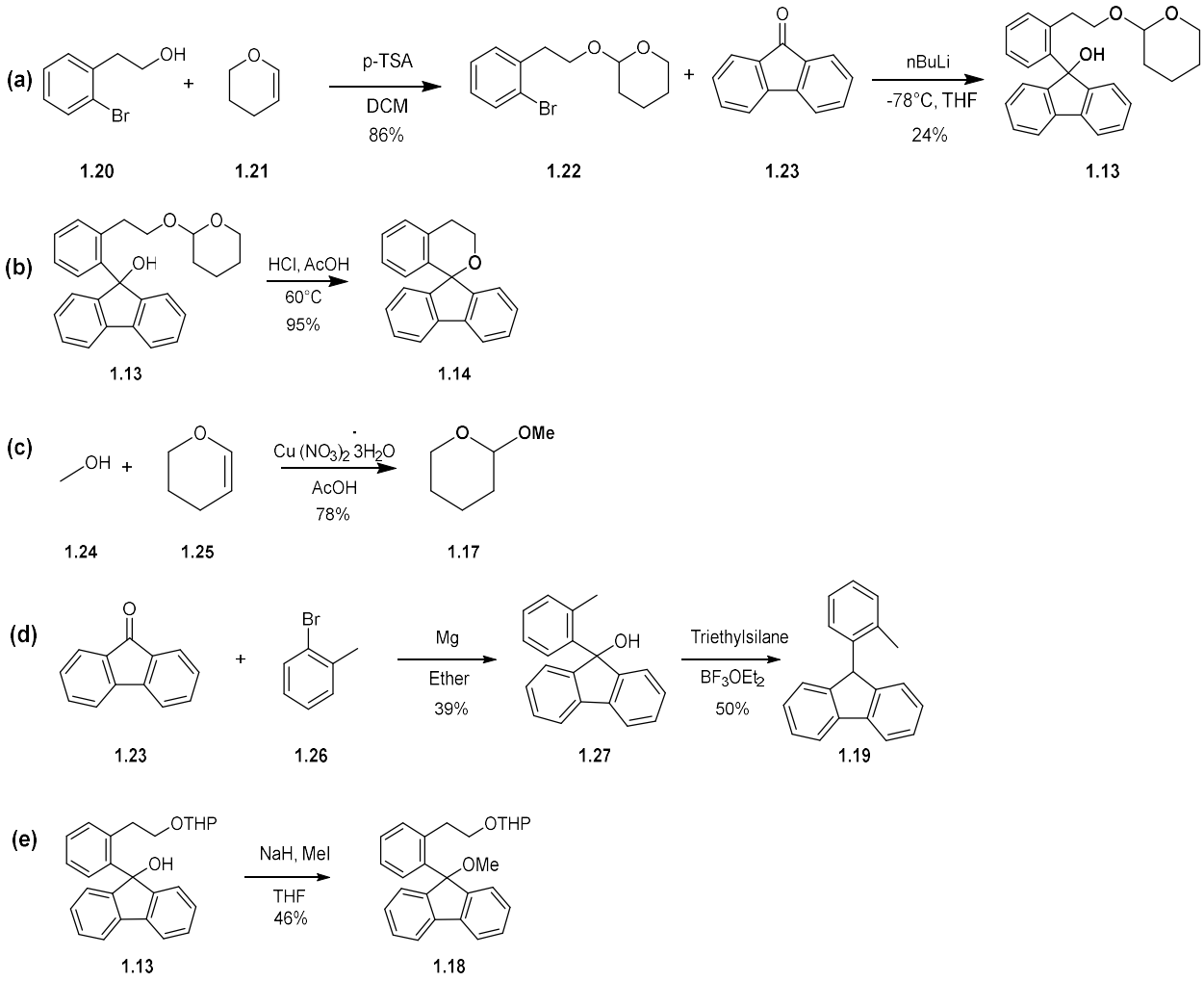

Scheme 1.6. Synthesis of HEPFOL-THP **(1.13)**, Spiro-FIC **(1.14),** Methoxy-THP **(1.17)**

1.4. Non-polar Solvent System

Due to the solvent trapping nature of methanol, we decided to explore non-polar solvents such as dichloromethane **(DCM)**. To our surprise, irradiating 2 mM of HEPFOL-THP with 250

mM of methanol in 1 mL anhydrous DCM gave us Spiro-FIC **(1.14)** and **1.17** in quantitative yield. The use of DCM also eliminated the solvent trapping product **1.18.** These results were unexpected because dichloromethane's non-polar nature is generally unable to stabilize a carbocation. Thus, the photochemistry would prefer to go through homolytic cleavage, generating radicals and byproducts. But that is not seen in the results shown below in **Figure 1.3.** It is possible that the moderately high dielectric constant of dichloromethane makes it an ideal solvent for the presented photochemistry. A similar reaction did not work in tetrahydrofuran **(THF)**, which has a lower dielectric constant.

As shown in **Figure 1.3** and **Table 1.1**, the photolysis of HEPFOL-THP in dichloromethane in the presence of excess nucleophile was very efficient. The chemical yield of the substitution product **1.17** was quantified to be 99% at 15 minutes of irradiation time. The quantum yield of this reaction was determined to be 0.08 (See Appendix C). The chemical yield of the secondary product Spiro-Fic **(1.14)** was only as high as 50%. Spiro-FIC **(1.14)** possibly started to decompose into **1.19,** thus decreasing its yield. Due to excellent results from this experiment, we decided to test a variety of nucleophiles using similar conditions. As shown in **Table 1.2**, they all gave the desired nucleophilic substitution product.

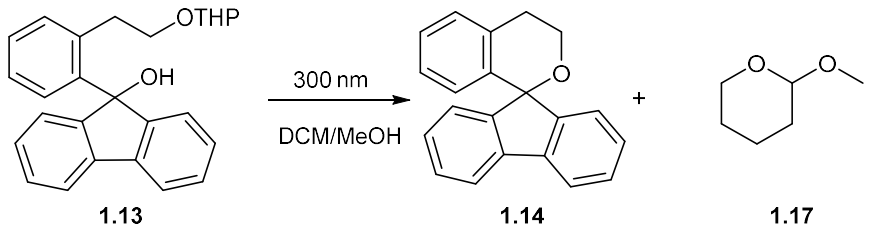

Scheme 1.7. Photolysis of 2 mM HEPFOL-THP in DCM/Methanol

Table 1.1. Chemical Yield of **1.14** and **1.17** in Photolysis of HEPFOL-THP **(1.13)** in DCM/MeOH

Irradiation Time	Conversion Rate	Chemical Yield of Methoxy-THP (1.17)	Chemical Yield of Spiro-FIC (1.14)
5 min	60%	68%	40%
10 min	95%	85%	42%
15 min	99%	99%	50%

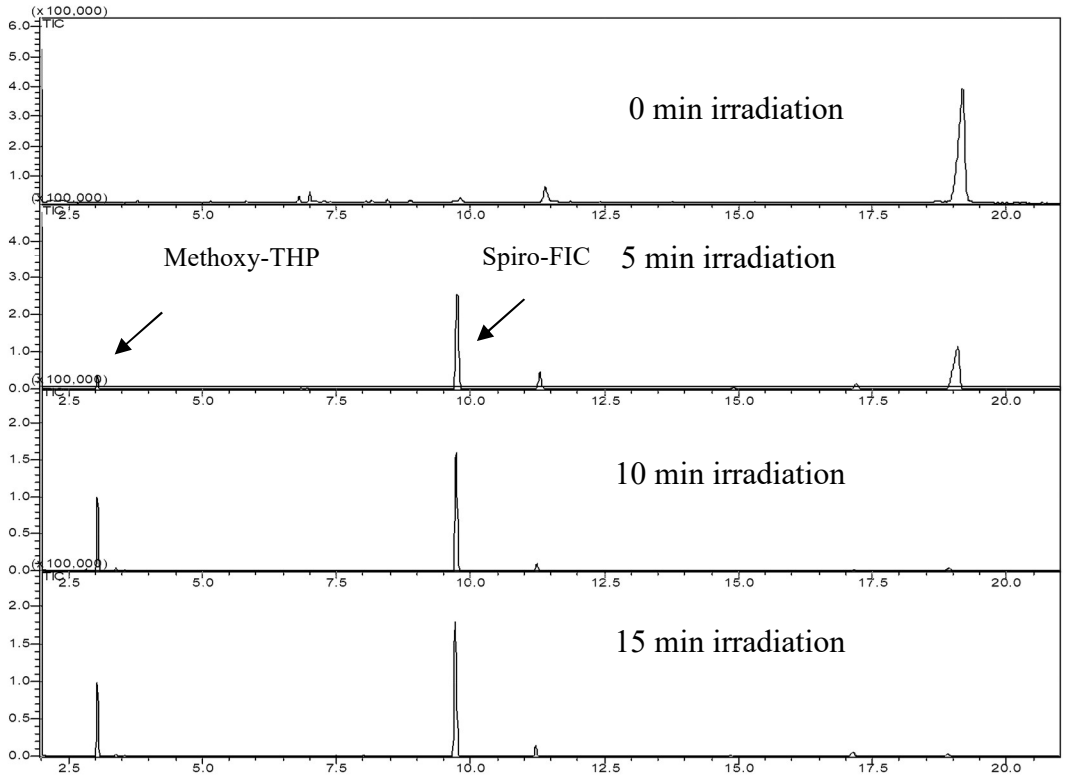

Figure 1.3. GC/MS Analysis of the Photolysis of HEPFOL-THP in DCM/MeOH

Table 1.2. Various Nucleophiles Tested for Photolysis of 2 mM HEPFOL-THP **(1.13)** in DCM. Nucleophile concentration – 250 mM

Nucleophile	**Product**
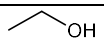 Ethanol	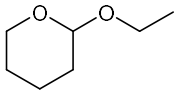
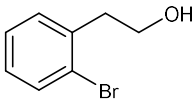 2-bromophenyl ethanol	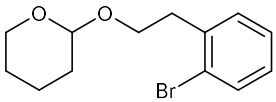
 Ethanethiol	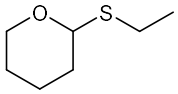

After discovering dichloromethane as a potential solvent, we decided to test our method with sugars. DCM also offers improved solubility of sugars compared to polar solvents such as methanol or TFE. As shown in **Scheme 1.7**, a mannosyl ortho-ester donor attached to our activating group was synthesized by Dr. Kapil Upadhyaya from the Crich group. The ortho-ester offers further stabilization of the carbocation by two oxygens. Irradiating 200 μM of **1.28** with 25 mM methanol in 1 mL of anhydrous DCM for 10 minutes gave us the desired products **1.29** and **1.14.** The product formation was followed by the Orbitrap High-Resolution Mass Spectrometer (HR-MS) in the Crich lab. This was the first successful light-triggered glycosylation using our strategy.

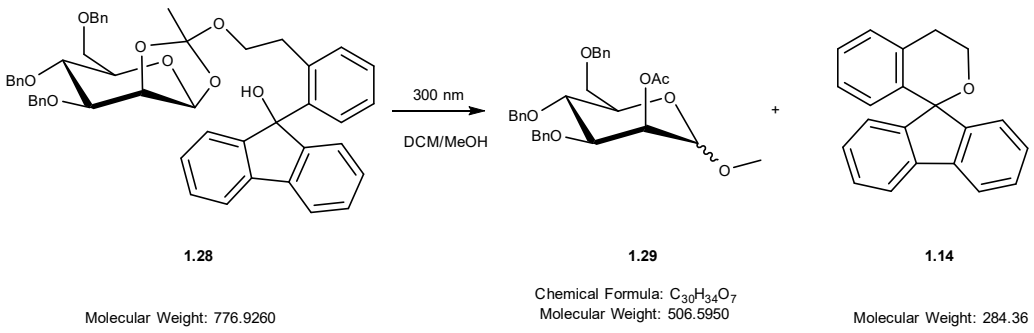

Scheme 1.8. Photolysis of Mannosyl O*rtho*-Ester Donor in DCM/MeOH

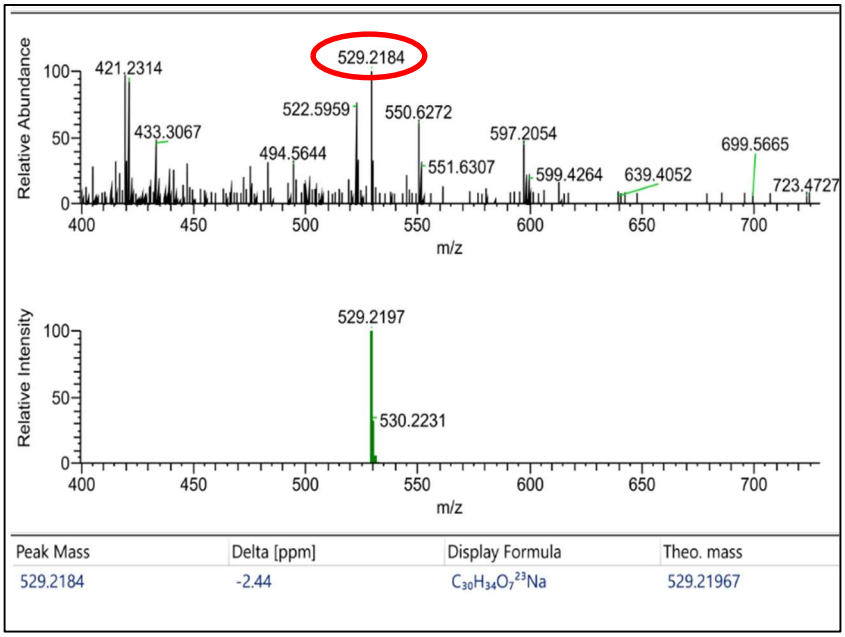

Figure 1.4. Orbitrap HR-MS of Photolysis of **1.28** in DCM/MeOH. Exact Mass- 529.2184

We further tested our strategy with another sugar as a nucleophile in DCM. As shown in **Scheme 1.8**, an acetal-protected sugar with alcohol at the C6 position **(1.30)** was obtained from the Crich group to use as an acceptor. For the reaction, 200 µM of **1.28** in DCM with 5 mM of **1.30** in 1 mL anhydrous DCM was irradiated at 300 nm for 10 minutes. But we did not observe glycosylated sugars. Instead, we observed hydrolysis of **1.28** along with Spiro-FIC **(1.14)**. It was theorized that water (OH^-) that acts as the leaving group from our activating group upon irradiation was hydrolyzing the sugar. This wasn't an issue with higher methanol nucleophilicity, but acetal-

protected sugar's **(1.30)** low nucleophilicity allowed water to trap the oxocarbenium ion. This issue presented a limitation to our strategy.

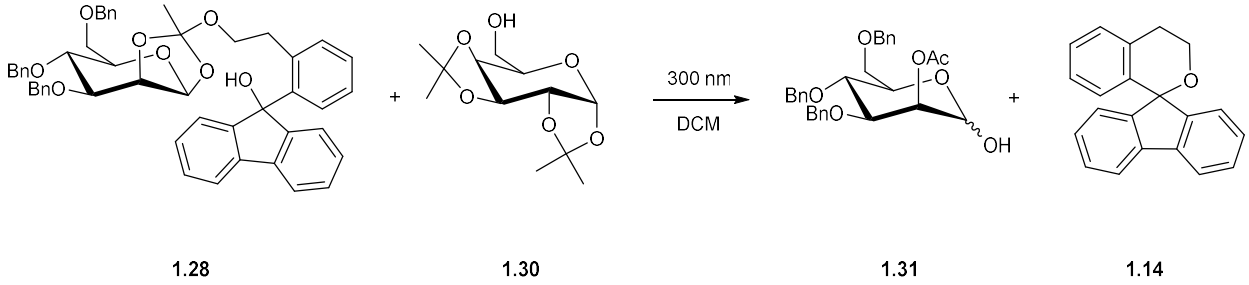

1.28 1.30 1.31 1.14

Scheme 1.8. Photolysis of Mannosyl O*rtho*-Ester Donor **(1.28)** with Acetal Protected Sugar **(1.30)** in DCM

1.5. Expanding the S_N1 Strategy to Different Groups

We further wanted to test the scope of our method with different protecting groups other than tetrahydropyran. The success with other groups would allow us to apply the strategy to a broad range of substrates. For this purpose, tert-butyl and benzyl ether protecting groups were chosen. Like THP, these groups can also stabilize a carbocation. Thus, 9-(2-(2-(tert-butoxy)ethyl)phenyl)-9H-fluoren-9-ol (HEPFOL-tbu, **1.34**) and 9-(2-(2-(benzyloxy)ethyl)phenyl)-9H-fluoren-9-ol (HEPFOL-Bz, **1.39**) were synthesized.

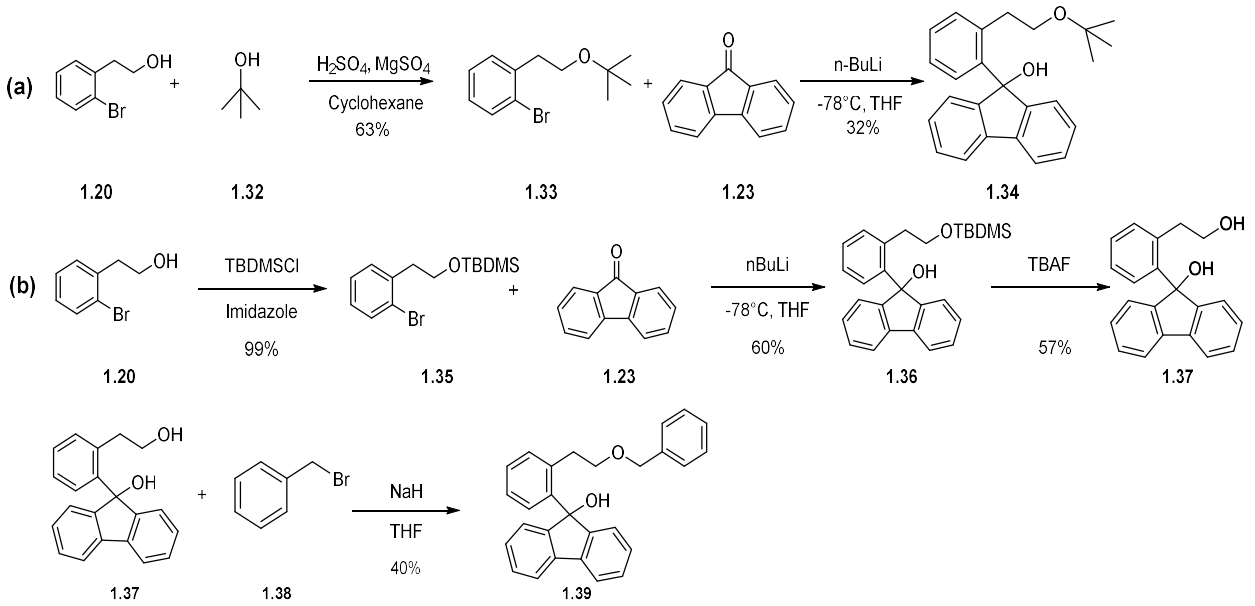

Scheme 1.9. Synthesis of HEPFOL-tbu **(1.34)** and HEPFOL-Bz **(1.39)**

For the synthesis, 2-bromophenyl ethanol **(1.20)** was protected with tert-butyl group under strongly acidic conditions to yield **1.33** with a 63% yield. Then, nucleophilic addition to 9-fluorenone **(1.23)** yielded the final product HEPFOL-tbu **(1.34)** with a 32% yield. For the synthesis of HEPFOL-Bz, the conventional route of protecting 2-bromophenyl ethanol **(1.20)** followed by nucleophilic addition yielded a very low yield. Thus, the benzyl ether group was added at the last step. First, 2-bromophenyl ethanol **(1.20)** was protected with the TBDMS group, followed by nucleophilic addition to 9-fluorenone **(1.23)** to give **1.36** with a 60% yield. Then, the TBDMS group was deprotected with TBAF to yield 9-(2-(2-hydroxyethyl)phenyl)-9*H*-fluoren-9-ol (HEPFOL, **1.37**) with a 80% yield. For the last step, the primary alcohol was protected with benzyl ether under basic conditions to yield the desired product HEPFOL-Bz **(1.39)** with a 60% yield**.**

For the photolysis of HEPFOL-tbu **(1.34)** and HEPFOL-Bz **(1.39)**, dichloromethane was used as the solvent with excess amounts of the nucleophile. A larger nucleophile was needed for HEPFOL-tbu **(1.34)** because the products with smaller nucleophiles such as methanol were too volatile to be detected by GC/MS. As shown in **Scheme 1.10**, 2-bromophenyl ethanol was used as

the nucleophile. The 2 mM samples with 200 mM nucleophile concentration in 1 mL DCM were irradiated for 15 min. In the case of HEPFOL-tbu **(1.34)**, we were able to detect both the substitution product **1.33** and Spiro-FIC **(1.14).** But in the case of HEPFOL-Bz, the substitution product was not detected, and only Spiro-FIC **(1.14)** was detected as the known product. It was apparent that cyclization did occur with HEPFOL-Bz, but substitution did not happen.

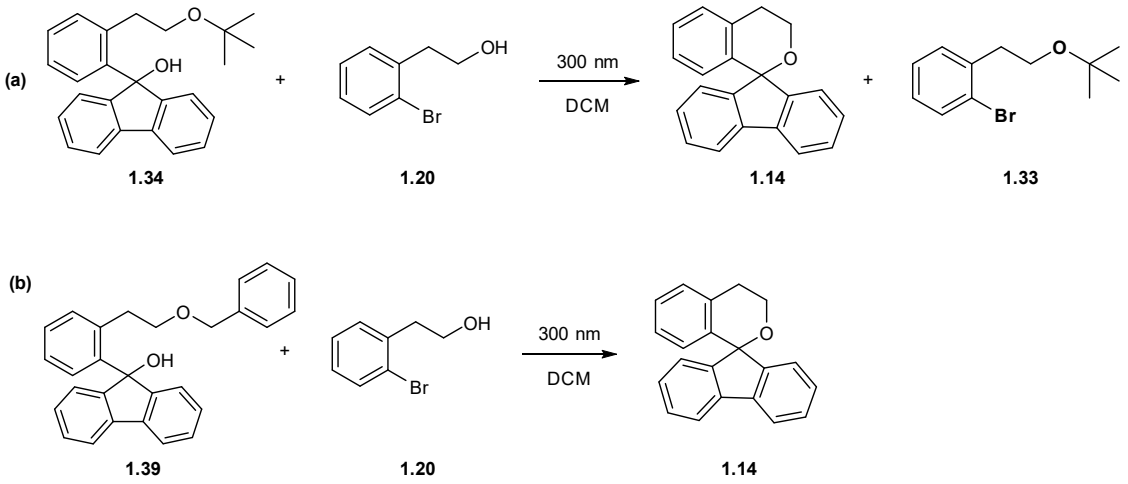

Scheme 1.9. Photolysis of HEPFOL-tbu **(1.34)** and HEPFOL-Bz **(1.39)** in DCM

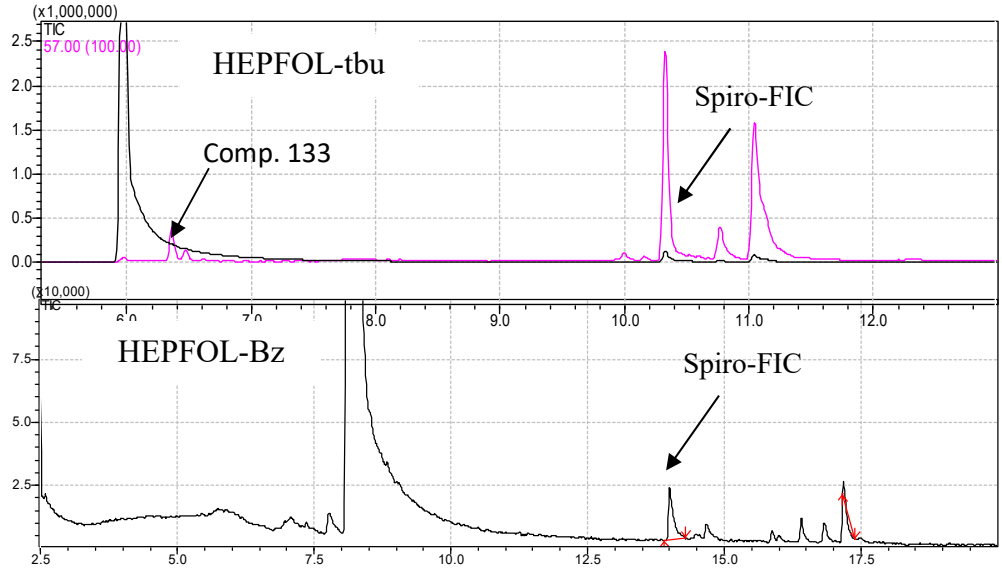

Figure 1.5. GC/MS Analysis of the Photolysis of HEPFOL-tbu **(1.34)** and HEPFOL-Bz **(1.39)** in DCM

1.6. Potential S_N2 Approach:

To push the mechanism towards S_N2 mechanism, the intermediate **1.5** in **Scheme 1.1** needs increased lifetime and stability. One way we thought to achieve this was to replace the heteroatom with sulfur. The sulfonium ion has increased stability compared to an oxonium ion. Sulfur contains an empty d-orbital which can spread the positive charge easily to stabilize it. Thus to test the photolysis, we synthesized 9-(2-(2-((tetrahydro-2*H*-pyran-2-yl)thio)ethyl)phenyl)-9*H*-fluoren-9-ol (TEPFOL-THP).

As shown in **Scheme 1.10,** 2-bromophenyl ethanol **(1.20)** was reacted with thioacetic acid under Mitsunobu reaction conditions to yield **1.41** with a 45% yield. It was followed up by DIBAL-H reduction to thiol to yield **1.42** with a 70% yield. Next, the thiol was protected with tetrahydropyran group under acidic conditions to obtain **1.43** with a 57% yield. Then, nucleophilic addition to 9-fluorenone **(1.23)** yielded the final desired product TEPFOL-THP **(1.44),** with a 15% yield.

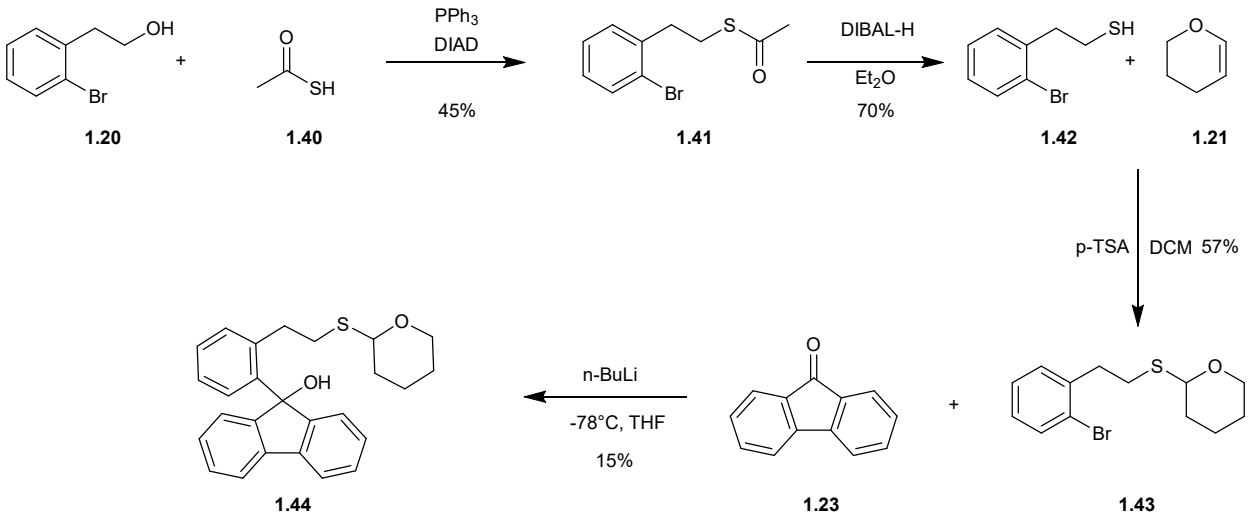

Scheme 1.10. Synthesis of TEPFOL-THP **(1.44)**

The photolysis experiment for TEPFOL-THP **(1.44)** was conducted in dichloromethane with 2,2,2-trifluoroethanol as the nucleophile. As shown in **Scheme 1.11**, photolysis of 2 mM solution of **1.44** in DCM with 250 mM TFE afforded both the expected products **1.17** and **1.45.** The photochemistry was efficient with 10 minutes of irradiation, without any significant byproducts. Similar photolysis also worked with methanol as the nucleophile.

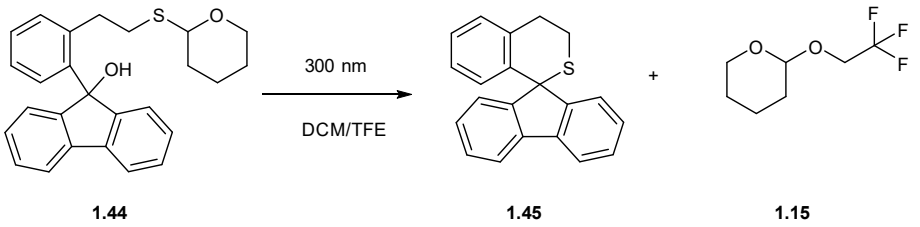

Scheme 1.10. Photolysis of TEPFOL-THP **(1.44)** DCM/TFE

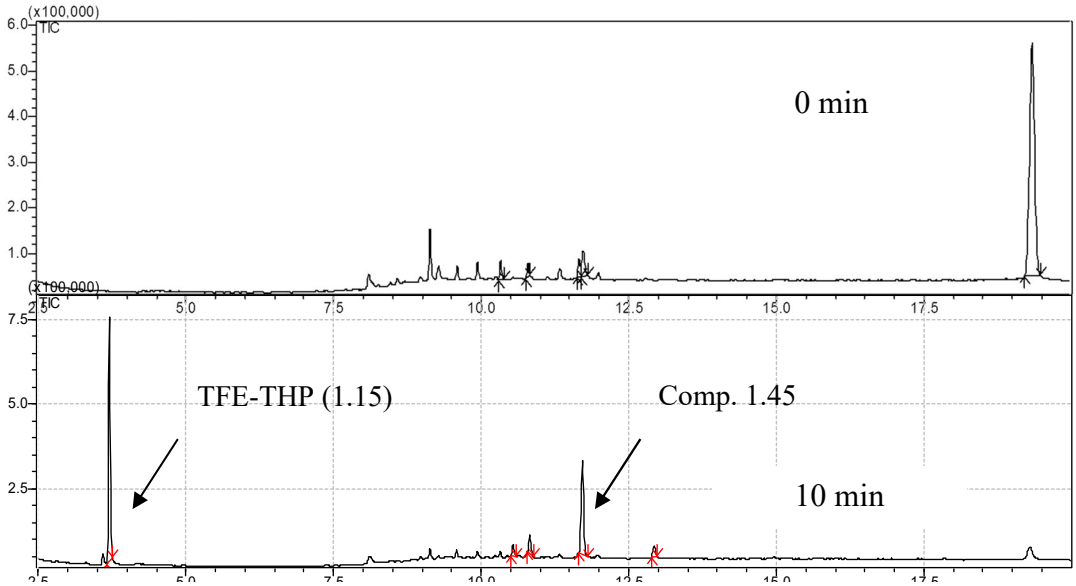

Figure 1.6. GC/MS Analysis of the Photolysis of TEPFOL-THP **(1.44)** in DCM/TFE

1.7 Stability of Sulfonium Intermediate:

We analyzed the stability of the sulfonium intermediate by adding the nucleophile after irradiation. A 2 mM sample of TEPFOL-THP **(1.44)** in DCM was irradiated for 10 minutes at 300 nm. After irradiation, TFE (250 mM) was added to the sample after a delay and stirred in the dark

for 5 minutes. We observed that even after 10 minutes of delay, there was no significant decrease in the yield of the substitution product **1.15.**

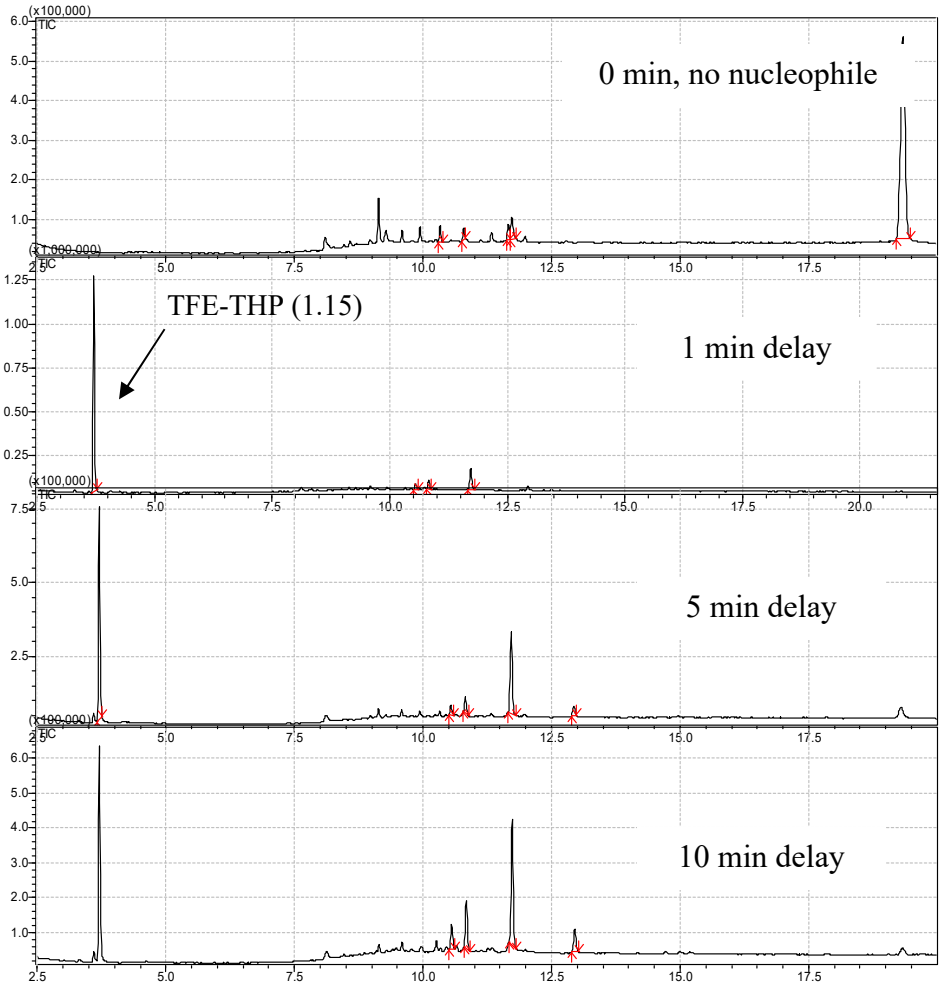

1.8 Conclusion and Future Works:

This chapter discussed a novel strategy to perform light-triggered nucleophilic substitution reactions using 9-aryl-9-fluorenol system. The photolysis of HEPFOL-THP **(1.13)** was efficient in fluorinated alcohols as expected. In polar and nucleophilic solvents such as methanol, the solvent trapping effect was observed. Dichloromethane proved to be an excellent non-polar solvent with

small amounts of nucleophile present. This was a fascinating discovery as DCM is generally not known to stabilize carbocations.

Applying our strategy to glycosylation, we were able to generate a glycosylated product with methanol as the nucleophile. But when a sugar was used as a nucleophile, the initial acceptor underwent hydrolysis due to water being a byproduct of our system. An alternative approach for glycosylation could be to substitute hydroxy at C9 position of fluorene. The low nucleophilicity of fluorene should allow donor sugar to attack the oxocarbenium ion.

We also explored the scope of our method with HEPFOL-tbu **(1.34)** and HEPFOL-Bz **(1.39)**. Although the photolysis of HEPFOL-tbu did work as expected, the photolysis of HEPFOL-Bz failed to afford the substitution product. It is possible that the presence of an aromatic ring near the heteroatom oxygen is affecting the efficiency of cyclization. It could be solved by inducing faster cyclization by going through a five-membered ring transition state instead of six.

At last, we explored a possible way to conduct photo-S_N2 reactions by substituting oxygen with sulfur. We have shown that the photolysis is not affected by the substitution. Future work would include a way to detect the sulfonium ion intermediate through UV-Vis or NMR experiments.

1.9 Experimental Section

All the reagents that were commercially purchased were used as is without purification. The GC/MS analysis was performed on Shimadzu QP-2010 instrument. Photo reactions were done in small Rayonet photo reactor with 300 nm light tubes (7 tubes). The photo reactions were carried out in 3 mL Quartz cuvette with 1 cm path length. The reactions were stirred with an air stirrer.

2-(2-bromophenethoxy)tetrahydro-2*H*-pyran (1.22): Catalytic amount of pTSA (0.14 g, 0.73 mmol) was added to a solution of 2-bromophenyl ethanol (5 mL, 1.48 g/mL, 36.7 mmol) and 3,4-

dihydro-2*H*-pyran (6.7 mL, 0.922 g/mL, 73,4 mmol) in 50 mL THF at room temperature. The resulting mixture was stirred at room temperature for 2 hours. The solvent was evaporated with rotovap and the resulting product was purified via column chromatography with DCM (0.1% TEA). The product was obtained as colorless liquid (9.05 g, 31.7 mmol, 86% yield). ^{1}H NMR (400 MHz, $CDCl_3$): δH = 7.56 (d, 1H), 7.30 (m, 2H), 7.09 (t, 1H), 4.63 (t, 2H), 3.98 (m, 1H), 3.78 (m, 1H), 3.68 (m, 1H), 3.50 (m, 1H), 3.09 (t, 2H), 1.84 (m, 1H), 1.72 (m, 1H), 1.53 (m, 4H).

9-(2-(2-((tetrahydro-2*H*-pyran-2-yl)oxy)ethyl)phenyl)-9*H*-fluoren-9-ol (1.13): To a solution of **1.22** (5.0 g, 17.5 mmol) in 100 mL dry THF, n-BuLi in hexane (2.3 M, 16 mL, 36.8 mmol) was added slowly at -78° C under nitrogen and stirred for 30 minutes. A light green color was observed. Then, a solution of 9-fluorenone (3.48 g, 19.3 mmol) **(1.23)** in 20 mL dry THF was added under nitrogen and the mixture was stirred for 30 minutes at room temperature. The reaction was quenched with 100 mL conc. Ammonium chloride and the organic layer was separated. The aqueous layer was extracted with ethyl acetate (50 mL x 2). The organic layers were dried with brine and magnesium sulfate and the solvent was evaporated under vacuum. The crude was purified on neutral alumina with 5% ethyl acetate: DCM to obtain the final product as white solid (1.65 g, 24% yield). ^{1}H NMR (500 MHz, DMSO-d, 100° C): δH = 8.07 (s, 1H), 7.79 (d, 2H), 7.37 (m, 1H), 7.23 (m, 3H), 7.09 (m, 2H), 5.77 (s, 1H), 4.10 (s, 1H), 3.49 (m, 1H), 3.26 (m, 1H), 3.10 (m, 1H), 2.98 (m, 2H), 2.77 (m, 1H), 2.18 (s, 2H), 1.62 (m, 2H), 1.41-1.28 (m, 4H). ^{13}C NMR (DMSO-d): δC ppm 151.9, 142.18, 140.23, 136.36, 131.32, 128.91, 128.43, 127.6, 127.27, 126.00, 124.83, 120.63, 98.32, 82.77, 67.47, 61.76, 32.82, 30.72, 25.47, 19.55. HRMS m/z: (409.1771, $(M+Na)^{+}$).

spiro[fluorene-9,1'-isochromane] (1.14): 0.1 g (0.259 mmol) of 1 was added in 3 mL of glacial acetic acid at 60° C and stirred until dissolved. Then, 1 mL of concentrated HCl was added to the

mixture dropwise and stirred for 10 minutes. The mixture turned dark brown/black color. The solvent was evaporated on rotovap and the remaining crude was purified via column chromatography with 5 % Ethyl Acetate: Hexane. The final product, 2, was obtained as sticky white solid (70 mg, 95% yield). ^{1}H NMR (400 MHz, $CDCl_3$): δH = 7.60 (d, 2H), 7.29 (t, 2H), 7.20-7.06 (m, 6H), 6.85 (t, 1H), 6.35 (d, 1H), 4.29 (t, 2H), 3.08 (t, 2H).

2-methoxytetrahydro-2*H*-pyran (1.17): 500 mg (5.94 mmol) of 3,4-DHP was added to 0.2 mL (4.95 mmol) methanol. Then, 0.11 mL (1.98 mL) acetic acid and 25 mg of Cu $(NO_3)_2 \cdot 3H_2O$ were added to the mixture and then stirred for 1 hour. The reaction mixture was washed with saturated $NaHCO_3$ and extracted with 2 x 10 mL DCM. The organic layer was then washed with brine and dried over $MgSO_4$. The solvent was evaporated in rotovap carefully to obtain the final product as clear liquid (0.45 g, 78% yield). 1H NMR (400 MHz, $CDCl_3$): δH = 1.47-1.74 (m, 6H), 3.34 (s, 3H), 3.47 (m, 1H), 3.79 (m, 1H), 4.49 (m, 1H).

9-(o-tolyl)-9*H*-fluoren-9-ol (1.27): 100 mg of magnesium powder (4.12 mmol) was added to 6 mL of anhydrous diethyl ether with 3 mg iodine. Then, 550 mg of 1-bromo-2-methylbenzene **(1.26)** (3.21 mmol) was added dropwise to the mixture and refluxed for 1 hour with vigorous stirring until the solution became clear color. Then, 426 mg of 9-fluorenone (2.36 mmol) was added to the reaction mixture and refluxed for 3 hours. The reaction was quenched with 10 mL water and extracted with 2 x 10 mL diethyl ether. The solvent was evaporated, and the crude was recrystallized in hexane (impurities are soluble). The final product was obtained as white crystals (0.25 g, 39% yield). ^{1}H NMR (400 MHz, $CDCl_3$): δ 8.36 (d, 1H), 7.71 (d, 2H), 7.41 (m, 3H), 7.26-7.21 (m, 5H), 6.99 (d, 1H), 2.38 (s, 1H), 1.34 (s, 3H).

9-(o-tolyl)-9*H*-fluorene (1.19): 0.13 g of **1.27** (0.47 mmol) was dissolved in 5 mL DCM and cooled to 0° C. Then, 0.055 g of triethylsilane (0.47 mmol) and 0.068 g of boron trifluoride diethyl

etherate (0.48 mmol) were added to the mixture and stirred for 1 hour at 0° C. The reaction was quenched with 5 mL of saturated NaHCO3, and the product was extracted with 2 x 5 mL of diethyl ether. The solvent was evaporated, and the crude was purified on short silica plug with hexane to obtain the final product as white crystals (0.60 g, 50% yield). ^{1}H NMR (400 MHz, $CDCl_3$): δ 7.80 (d, 2H), 7.60 (d, 0.5 H), 7.37-7.10 (m, 9H), 6.97-6.90 (m, 1H), 6.37 (d, 0.5H), 5.41 (s, 0.5H), 5.02 (s, 0.5H), 2.77 (s, 2H).

2-(2-(9-methoxy-9*H*-fluoren-9-yl)phenethoxy)tetrahydro-2*H*-pyran (1.18): To a solution containing 100 mg of **1.13** (0.26 mmol) in 4 mL of dry THF was cooled to 0°C under argon. Then 34 mg of sodium hydride (60% dispersion in mineral oil, 0.85 mmol) was added to the solution and stirred at 0°C for 10 minutes. To this solution was added 44 mg of iodomethane (0.32 mmol) and the mixture was stirred overnight at room temperature. The reaction was quenched with water and extracted with 2 x 5 mL diethyl ether. The organic layer was washed with brine and dried over $MgSO_4$. The solvent was evaporated under reduced pressure and the crude product was purified with 15% ethyl acetate: hexane over silica gel to yield **1.18** (50 mg, 46% yield) as white solid. ^{1}H NMR (400 MHz, $CDCl_3$): δ ppm 1.18-1.64 (m, 7H), 2.70 (s, 3H), 3.25 (m, 1H), 3.51 (m, 1H), 7.05-7.30 (m, 9H), 7.60 (d, 2H). ^{13}C NMR ($CDCl_3$): δ ppm 19.5, 25.5, 30.6, 49.9, 62.0, 98.5, 119.9, 125.4, 125.5, 125.9, 127.1, 127.3, 128.3, 128.4, 129.1, 129.2, 141.5, 146.9. HRMS m/z: (423.1932, $(M+Na)^{+}$).

1-bromo-2-(2-(tert-butoxy)ethyl)benzene (1.33): In 3 mL of cyclohexane, 48 mg of magnesium sulfate was added and stirred vigorously. To the mixture, 55 µL of concentrated sulfuric acid (1.0 mmol) was added and stirred at room temperature for 15 minutes. Then, a solution of 2-bromophenyl ethanol **(1.20)** (200 mg, 1.0 mmol) and tert-butanol **(1.32)** (0.47 mL, 5.0 mmol) in 1 mL cyclohexane was added to the reaction mixture and stirred at room temperature overnight.

Upon completion, 10 mL of 5% sodium bicarbonate solution was added and stirred until all of magnesium sulfate was dissolved. The organic layer was separated and the solvent was removed under reduced pressure to yield the final product **1.33** as colorless oil (0.163 g, 63% yield). 1H NMR (CDCl3): δ ppm: 1.16 (s, 9H, t-butyl), 2.97 (t, 2H), 3.56 (t, 2H), 7.06 (m, 1H), 7.22-7.27 (m, 2H), 7.51 (d, 1H).

9-(2-(2-(tert-butoxy)ethyl)phenyl)-9*H*-fluoren-9-ol (1.34): A mixture of **1.33** (50 mg, 0.19 mmol) in 5 mL of dry THF was cooled to -78°C under argon. Then, 0.15 mL of n-BuLi (2.5 M in hexane, 0.38 mmol) was added dropwise to the mixture while stirring. The reaction was stirred at -78°C for 30 minutes. Afterwards, 41 mg of 9-fluorenone **(1.23)** (0.23 mmol) dissolved in 1 mL dry THF was added dropwise to the reaction mixture at -78°C. The reaction was warmed to room temperature and stirred for 24 hours. Upon completion, the reaction was quenched with 5 mL of saturated ammonium chloride. The mixture was extracted with 2 x 5 mL of diethyl ether and then the organic layer was washed with brine. After drying over magnesium sulfate, the solvent was evaporated under reduced pressure and the crude solid was purified over silica with 10-15% diethyl ether: hexane to yield the final product **1.34** as white solid (20 mg, 32% yield). ^{1}H NMR (DMSO-d6, 120° C): δ ppm 0.91 (s, 9H), 2.15 (t, 2H), 2.80 (t, 2H), 7.11 (m, 3H), 7.23 (m, 4H), 7.37 (m, 2H), 7.78 (d, 2H), 8.01 (m, 1H). ^{13}C NMR (DMSO-d6, 120° C): δ ppm 152.04, 142.11, 140.24, 137.15, 131.64, 128.87, 128.35, 127.55, 127.13, 125.84, 124.80, 120.60, 83.01, 72.30, 62.19, 34.11, 27.84. HRMS m/z: (359.2038, $(M+H)^{+}$).

(2-bromophenethoxy)(tert-butyl)dimethylsilane (1.35): To a solution of 2-bromophenyl ethanol (5.0 g, 24.9 mmol) in 25 mL DMF and imidazole (3.37 g, 49.5 mmol), TBDMSCl (4.12 g, 27.3 mmol) was added at 0° C. The mixture was stirred at room temperature overnight. The reaction was diluted with 200 mL water and then extracted with ethyl acetate (2 x 100 mL). The

solvent was evaporated, and the crude product was purified via column chromatography (5% ether: hexane). The final product **1.35** was obtained as colorless liquid (7.86 g, 99% yield). ^{1}H NMR (400 MHz, CDCl3): δH = 7.53 (d, 1H), 7.27 (m, 2H), 7.08 (m, 1H), 3.85 (t, 2H), 3.00 (t, 2H), 0.89 (s, 9H), 0.00 (s, 6H).

9-(2-(2-((tert-butyldimethylsilyl)oxy)ethyl)phenyl)-9*H*-fluoren-9-ol (1.36): To a solution of **1.35** (9.1 g, 28.9 mmol) in 230 mL dry THF, n-BuLi in hexane (2.5 M, 23.2 mL, 57.2 mmol) was added slowly at -78° C under nitrogen and stirred for 30 minutes. Then, a solution of 9-fluorenone (7.3 g, 40.5 mmol) in 40 mL dry THF was added under nitrogen and the mixture was stirred for 30 minutes. The reaction was quenched with 500 mL conc. Ammonium chloride and the organic layer was separated. The aqueous layer was extracted with ethyl acetate (200 mL x 2). The organic layers were dried with brine and magnesium sulfate and the solvent was evaporated under vacuum. The resulting crude was purified on deactivated silica (with TEA) with 5-15% ether: petroleum ether to afford the final product **1.36** as white solid (7.2 g, 60% yield). ^{1}H NMR (500 MHz, DMSO-d): δH = 8.08 (2H, s), 7.77 (3H, d), 7.37 (3H, m), 7.23-7.11 (6H, m). 7.07 (4H, m), 5.76 (OH), 2.99 (14H, m), 2.12 (8H, s), 0.78 (9H, s), -0.20 (6H, s). ^{13}C NMR (DMSO-d): δC ppm 151.83, 142.12, 140.22, 136.36, 131.56, 128.92, 128.41, 127.55, 127.09, 125.98, 124.8, 120.62, 82.76, 63.19, 35.91, 26.2, 18.17, -4.98. HRMS m/z: (439.2061, $(M+Na)^{+}$).

9-(2-(2-hydroxyethyl)phenyl)-9*H*-fluoren-9-ol (1.37): 12.4 mL of TBAF was added dropwise to a mixture of 4.87 g of **1.36** (11.7 mmol) and 70 mL of dry THF at 0° C. The mixture was stirred at room temperature for 30 minutes. The reaction was quenched with 100 mL of conc. Ammonium chloride and the organic layer was separated. The aqueous layer was extracted with ethyl acetate (2 x 50 mL). The combined organic layers were washed with brine and dried over magnesium sulfate. The solvent was evaporated and the crude was purified on alumina with 40% EtOAc :

Hexane. The final product **1.37** was obtained as white solid (2.01 g, 57% yield). ^{1}H NMR (500 MHz, DMSO-d6, 120° C): δH = 7.95 (1H, s), 7.80 (1H, d), 7.37 (1H, m), 7.23-7.13 (4H, m), 5.81 (OH), 3.78 (OH), 3.00 (2H, m), 2.21 (2H, s). ^{13}C NMR (DMSO-d6, 120° C): δC ppm 153.00, 142.14, 140.21, 137.28, 131.42, 128.88, 128.40, 127.50, 127.20, 125.75, 124.80, 120.64, 83.08, 61.91, 36.06. HRMS m/z: (325.1196, $(M+Na)^{+}$).

9-(2-(2-(benzyloxy)ethyl)phenyl)-9*H*-fluoren-9-ol (1.39): To 2.5 mL of anhydrous THF was added 40 mg of NaH (60% in mineral oil, 1 mmol) under argon and cooled to 0°C. While stirring, 200 mg of **1.37** (0.66 mmol) dissolved in 2.5 mL anhydrous THF was added dropwise to the reaction flask. The mixture was stirred at room temperature for 30 min and then at 50°C for 30 min. After cooling the reaction mixture to 0°C, 0.1 mL of benzyl bromide **(1.38)** (0.80 mmol) was added and then the mixture was stirred at room temperature overnight. The reaction was quenched with 5 mL of water and then extracted with 2 x 5 mL diethyl ether. The organic layer was washed with brine and then dried over MgSO4. The crude was purified with 25% ether: hexane over silica gel to yield **1.39** as white solid. (100 mg, 40% yield). ^{1}H NMR (500 Mhz, DMSO-d6, 120°C): δ ppm: 2.23 (t, 2H), 2.94 (t, 2H), 4.08 (s, 2H), 5.66 (s, 1H), 7.11-7.37 (m, 13H), 7.78 (d, 2H), 8.11 (d, 1H). ^{13}C NMR (500 Mhz, DMSO-d6, 120° C): δ ppm 151.91, 142.27, 140.28, 139.23, 136.25, 131.31, 128.92, 128.43, 128.42, 127.67, 127.61, 127.48, 127.30, 126.02, 124.84, 120.62, 82.85, 72.06, 70.68, 32.74. HRMS m/z: (415.1673, $(M+Na)^{+}$).

S-(2-bromophenethyl) ethanethioate (1.41): To a solution of 1.0 g of 2-bromophenyl ethanol **(1.20)** (4.97 mmol) in 35 mL THF were added 1.97 g PPH_3 (7.47 mmol) and DIAD (1.47 mL, 7.47 mmol) successively. To the yellow solution, 0.74 mL of thioacetic acid **(1.40)** (96%, 9.96 mmol) was added dropwise which turned the solution dark brown. The mixture was stirred overnight at room temperature. The solution was concentrated to 10 mL and then diluted in 40 mL of hexane

and cooled in ice to precipitate triphenylphosphine oxide as white powder. After filtration, the solvent was evaporated under reduced pressure and the crude was purified on silica with 30% DCM: hexane to yield **1.41** as clear oil (0.58 g, 45% yield). ^{1}H NMR ($CDCl_3$): δ 2.33 (s, 3H), 3.00 (t, 2H3.13 (t, 2H), 7.08 (m, 1H), 7.26 (m, 2H), 7.54 (d, 1H).

2-(2-bromophenyl)ethane-1-thiol (1.42): To a solution of 0.58 g of **1.41** (2.24 mmol) in 20 mL anhydrous ether, 5.6 mL of DIBAL-H (1 M in hexane, 5.60 mmol) was added dropwise at -78° C under nitrogen. The mixture was stirred at room temperature for 2 hours. It was quenched with 5 mL methanol at 0° C, followed by 15 mL of 2 M HCl. The organic layer was washed with saturated NaHCO3 and dried with brine and sodium sulfate. The solvent was evaporated under reduced pressure and the crude was purified on short silica plug with hexane to yield **1.42** as colorless oil (0.35 g, 70% yield). 1H NMR (400 Mhz, CDCl3): δ 1.42 (t, 1H), 2.81 (q, 2H), 3.05 (t, 2H), 7.09 (m, 1H), 7.24 (m, 2H), 7.53 (d, 1H).

2-((2-bromophenethyl)thio)tetrahydro-2H-pyran (1.43): To a mixture of 50 mg of **1.42** (0.23 mmol) and 38.7 mg of 3,4-dihydro-2H-pyran **(1.21)** (0.46 mmol) in 2.5 mL DCM was added 2 mg of p-Toluenesulfonic acid. The solution was stirred for 3 hours at room temperature and the solvent was evaporated under reduced pressure. The crude was purified with 10% ether: hexane to obtain **1.41** as colorless oil (40 mg, 57% yield). ^{1}H NMR ($CDCl_3$): δ 1.57-1.92 (m, 6H), 2.83-3.07 (m, 2H), 3.51 (m, 1H), 4.07 (m, 1H), 4.89 (m, 1H), 7.06 (m, 1H), 7.24 (m, 2H), 7.51 (m, 1H). ^{13}C NMR ($CDCl_3$) δ 21.8, 25.6, 30.04, 31.4, 37.09, 64.7, 82.5, 124.3, 127.4, 128.0, 130.7, 132.8, 139.9. HRMS m/z: (323.0068, $(M+Na)^+$).

9-(2-(2-((tetrahydro-2*H*-pyran-2-yl)thio)ethyl)phenyl)-9*H*-fluoren-9-ol (1.44): To a solution of 100 mg of **1.43** (0.33 mmol) in 5 mL dry THF was added 0.26 mL of n-BuLi (1 M in hexane, 0.66 mmol) at -78°C under nitrogen gas. The mixture was allowed to stir for 30 minutes at -78°C.

Then, 72 mg of 9-fluorenone (0.40 mmol) was added dropwise to the reaction mixture by dissolving in 0.5 mL dry THF. The reaction was allowed to stir for 1 hour and then quenched with 10 mL of saturated ammonium chloride solution. The aqueous layer was extracted with 2 x 5 mL of ethyl acetate, and the organic layer was washed with brine and dried with sodium sulfate. The solvent was evaporated under reduced pressure and the crude was purified on silica with 5-10% ethyl acetate: hexane. The final product **1.44** was obtained as yellow oil (20 mg, 15% yield). ^{1}H NMR (500 Mhz, DMSO-d6, 120°C): δ ppm: 1.46 (m, 4H), 1.69 (m, 2H), 2.08 (m, 2H), 2.20 (m, 2H), 3.34 (m, 1H), 3.79 (m, 1H), 4.46 (m, 1H), 5.66 (s, 1H), 7.12-7.38 (m, 9H), 7.79 (d, 2H), 8.08 (d, 1H). ^{13}C NMR (500 Mhz, DMSO-d6, 120° C): δ ppm 21.6, 25.7, 30.8, 31.8, 33.5, 64.1, 82.13, 82.8, 120.7, 124.8, 126.1, 127.5, 127.7, 128.4, 128.9, 130.8, 138.4, 140.3, 141.9, 151.8. HRMS m/z: (425.1540, $(M+Na)^{+}$).

1.10. References:

1. Nigst, T. A.; Ammer, J.; Mayr, H., Photogeneration of Benzhydryl Cations by Near-UV Laser Flash Photolysis of Pyridinium Salts. *The Journal of Physical Chemistry A* **2012,** *116* (33), 8494-8499.

2. Wan, P.; Krogh, E., Evidence for the generation of aromatic cationic systems in the excited state. Photochemical solvolysis of fluoren-9-ol. *Journal of the Chemical Society, Chemical Communications* **1985,** (17), 1207.

3. Mecklenburg, S. L.; Hilinski, E. F., Picosecond spectroscopic characterization of the 9-fluorenyl cation in solution. *Journal of the American Chemical Society* **1989,** *111* (14), 5471-5472.

4. Gaillard, E.; Fox, M. A.; Wan, P., A kinetic study of the photosolvolysis of 9-fluorenol. *Journal of the American Chemical Society* **1989,** *111* (6), 2180-2186.

5. McClelland, R. A.; Mathivanan, N.; Steenken, S., Laser flash photolysis of 9-fluorenol. Production and reactivities of the 9-fluorenol radical cation and the 9-fluorenyl cation. *Journal of the American Chemical Society* **1990,** *112* (12), 4857-4861.

6. Wan, P.; Krogh, E., Contrasting photosolvolytic reactivities of 9-fluorenol vs. 5-suberenol derivatives. Enhanced rate of formation of cyclically conjugated four .pi. carbocations in the excited state. *Journal of the American Chemical Society* **1989,** *111* (13), 4887-4895.

Chapter 2

Photoinhibition of Cysteine Protease with o-Naphthoquinone Methide Precursors (NQMP)

2.1 Introduction

o-Quinone methides (o-QMs) and *o*-Naphthoquinone Methide (o-NQMs) are highly reactive electrophilic intermediates. The first conclusive evidence of o-QM was proved by Gardner and Sarrafizadeh in 1959[1]. Since then, the high reactivity of o-QM and o-NQM has led to extensive applications in DNA methylation, protein labeling, and organic synthesis[2-6]. Generally, o-QM and o-NQM are generated through thermal activation, oxidation, acid or base catalysis, or light **(Scheme 2.1)**[7-16].

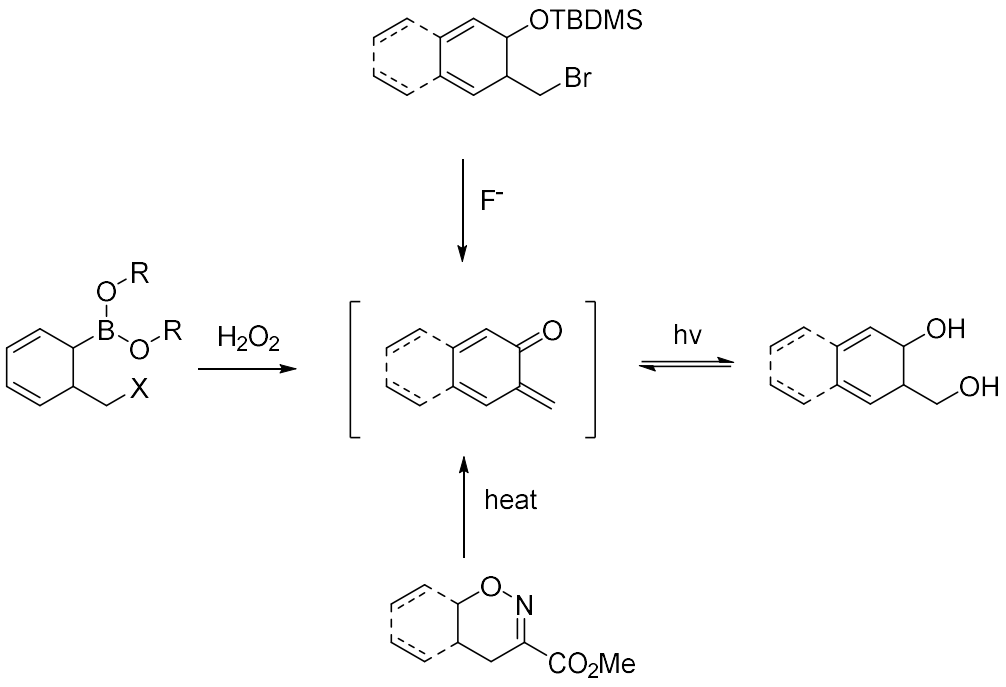

Scheme 2.1. Generation o-QM and o-NQM via Different Methods

o-NQM can be efficiently generated via photochemical dehydration of 3-(hydroxymethyl)-2-naphthols (Φ = 0.20). The lifetime of o-NQM **(2.2)** in neutral aqueous solutions is only 7 ms. It rapidly adds water ($k_{H2O} \sim 2.6\ M^{-1}\ s^{-1}$) to regenerate the starting naphthoquinone methide precursor (NQMP) **(2.1)**[16]. Among endogenous nucleophiles, only thiols are reactive enough ($k_{RSH} \sim 2.2 \times 10^5\ M^{-1}\ s^{-1}$) to outcompete water in a Michael addition[17]. The thioether produced in the reaction can be cleaved with irradiation back to **2.2.** Compared to o-QM, o-NQM is also a stronger chromophore above 300 nm, making it suitable for biological applications[18]. In addition, the 8th position of its naphthalene backbone is more suitable for functionalization without significantly impacting the reactivity.

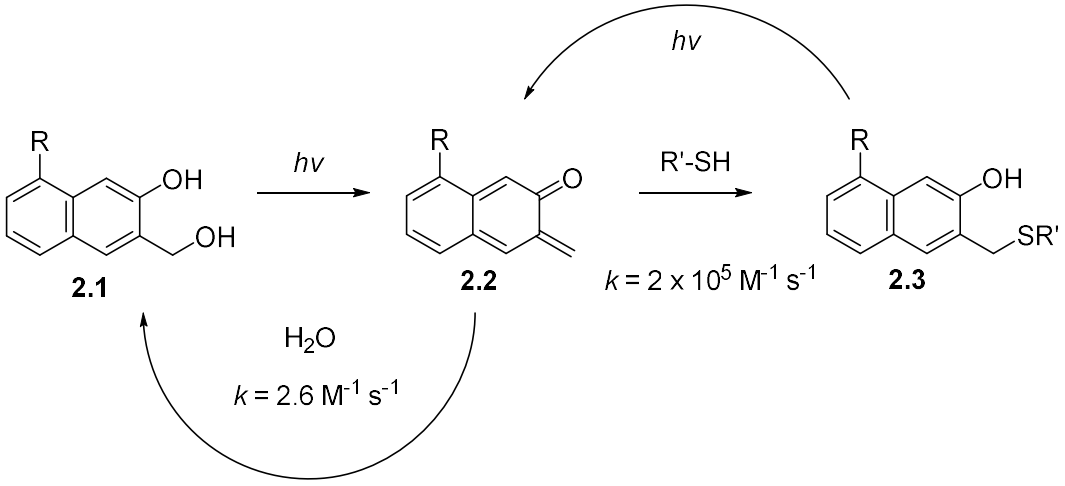

Scheme 2.2. Photochemistry of o-NQMP in the Presence of Thiols

The thiol-QM photo click reaction is an important reaction for protein labeling and modification when combined with cysteine chemistry. Cysteine is a sulfur-containing amino acid that can be present as free thiol (RSH) in proteins or can create disulfide bonds to construct protein structure. Previously, our group used o-NQMP derivatives to reversibly label Bovine Serum Albumin (BSA) via photo-induced Michael addition[18].

Cysteine proteases play multifaceted roles in every aspect of physiology and development. They are a class of enzymes that hydrolyze a peptide bond in proteins by the nucleophilic attack and subsequent hydrolysis. Cysteine proteases contain cysteine residue in their catalytic sites as the nucleophile, along with a histidine residue that enhances the nucleophilicity of cysteine. Cysteine proteases from parasites and viruses have become promising targets for major diseases such as arthritis, AIDS, cancer, and immunogenic disorders[19-20]. Thus, the free cysteine residue in the catalytic site is a good target for the inhibitors via thiol reactions.

We hypothesized that the thiol-QM reaction of o-NQMP derivatives could be used to develop a novel photoinhibition method for cysteine proteases. We decided to use PEG_4-NQMP **(2.13)** and Biotin-NQMP **(2.14)** which have been synthesized by our group. The introduction of polyethylene glycol (PEG) to the naphthalene backbone increases the compound's aqueous solubility. In addition, the alkoxy substituent extends the absorbance wavelength of the chromophore past 360 nm, making this compound suitable for activation using 350 nm wavelength[18].

2.2. Protein and Substrate Used

Papain is a very commonly used cysteine protease for inhibitor studies and drug design. It is one of the four cysteine proteases isolated from papaya latex. Papain contains two subunits that contain 212 amino acids and are stabilized through three disulfide bonds. The catalytic center is created by Cys-25, His-159, and Asn-175[21-22]. It has a wide pH range (5-8) and thermostability, making it an ideal cysteine protease model for research purposes. Its molecular weight is 23.4 kDa.

The most commonly used papain substrate is Nα-Benzoyl-L-arginine-4-nitroanilide hydrochloride (L-BAPNA). Upon getting hydrolyzed by papain, p-nitroaniline **(2.5)** is released,

which is bright yellow. Since the substrate and the secondary product **2.4** are colorless, the reaction can be monitored spectrophotometrically at 400 nm[23].

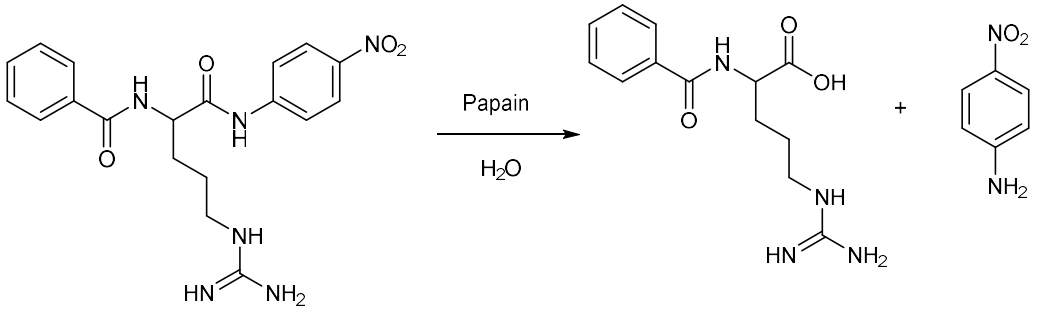

2.4 2.5 2.6

Scheme 2.3. Hydrolysis of L-BAPNA **(2.4)** by Papain

2.3 Synthesis of the Inhibitors

The synthesis of PEG_4-NQMP and Biotin-NQMP in this chapter followed the procedure previously published by our group[24-25]. The compounds were synthesized by Dr. Nannan Lin. The first step is the Fischer esterification of 3,5-dihydroxy-2-naphthoic acid **(2.7)** to afford **2.8.** This was followed by LAH reduction to generate NQMP **2.9.** The diols were protected using 2,2-dimethoxypropane to afford **2.10.** The acetal compound was then reacted with I-PEG_4-OH to afford **2.11,** which can be further reacted with biotin through EDC coupling to form **2.12.** As the last step, compounds **2.11** and **2.12** underwent acidic deprotection to remove the acetal group to yield PEG_4-NQMP **(2.13)** and Biotin-NQMP **(2.14).**

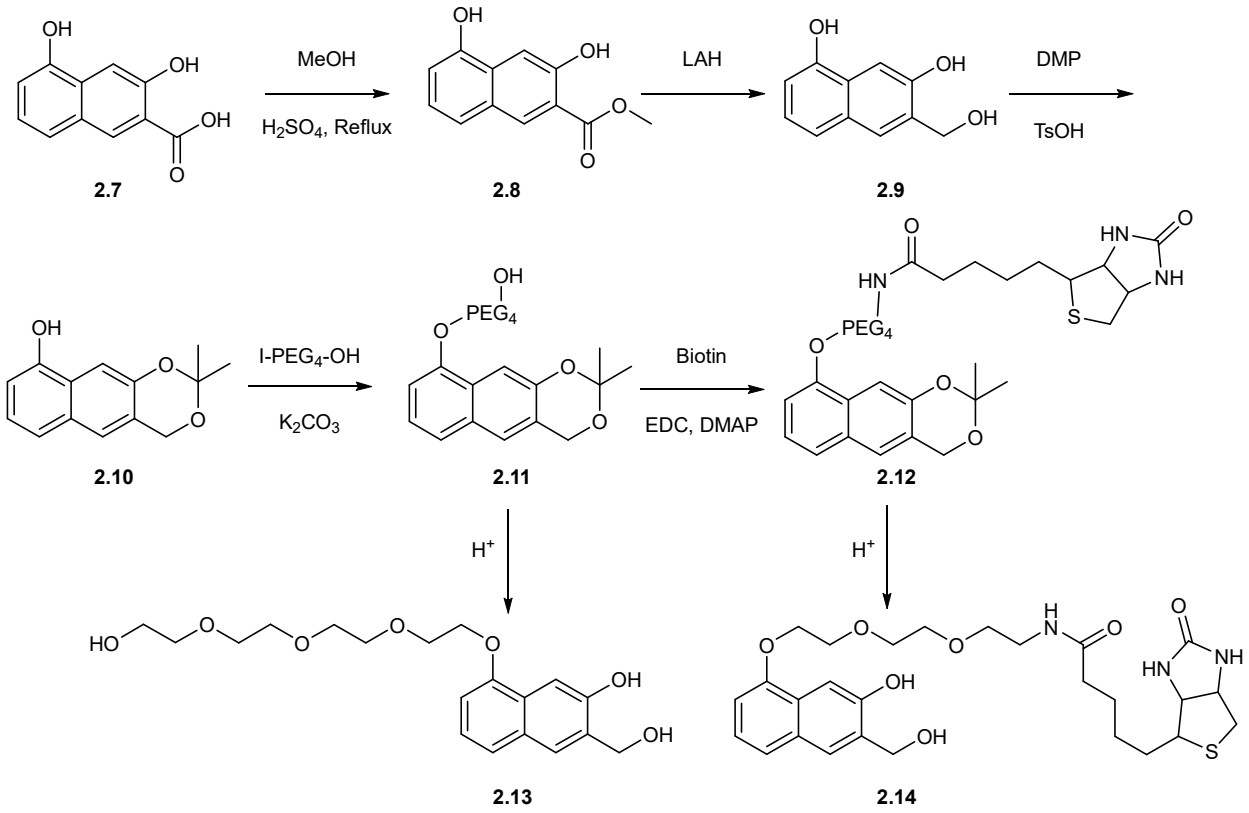

Scheme 2.1. Synthesis of PEG_4-NQMP **(2.13)** and Biotin-NQMP **(2.14)**

2.4 Inhibition Studies of Papain

For a sample containing 5.7 μM of activated papain and 67 μM of PEG_4-NQMP inhibitor, complete inhibition was achieved after 5 minutes of 350 nm irradiation. Previously, Dr. Nannan Lin from our group had discovered that the inhibition efficiency of PEG_4-NQMP does not substantially increase by increasing the concentration of the inhibitor beyond a certain point[26]. In order to achieve similar inhibition efficiency and irradiation time, 120 μM of Biotin-NQMP was required. The data suggested that Biotin-NQMP was less efficient at the inhibition of papain.

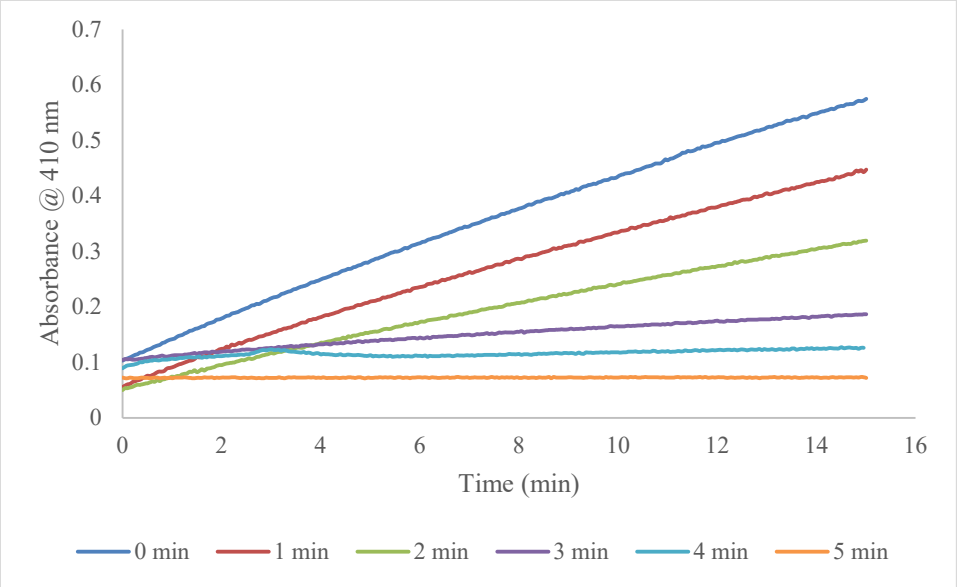

Figure 2.1. UV/Vis Kinetics of Papain Activity with PEG_4-NQMP Inhibitor

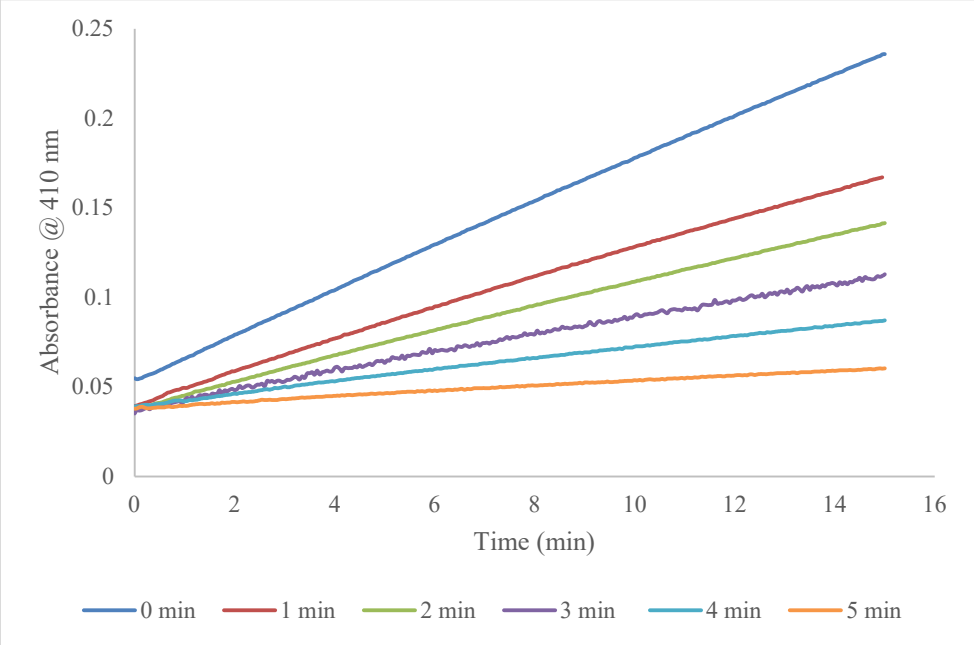

Figure 2.2. UV/Vis Kinetics of Papain Activity with Biotin-NQMP Inhibitor

2.5. Detection of Biotin-NQMP Tag on Papain

After achieving efficient inhibition with both the inhibitors, we sought to prove the binding of the inhibitors to cysteine in the active site of papain. First, we decided to check the presence of the inhibitor on the protein via western blotting. We used Biotin-NQMP due to its binding capability with Streptavidin-Horseradish Peroxidase (HRP). The samples were submitted to Dr. Zheng's group to conduct the experiment. As shown in **Figure 2.3,** a clear band shows up near 23 kDa in the samples that were irradiated, indicating the presence of biotin on papain.

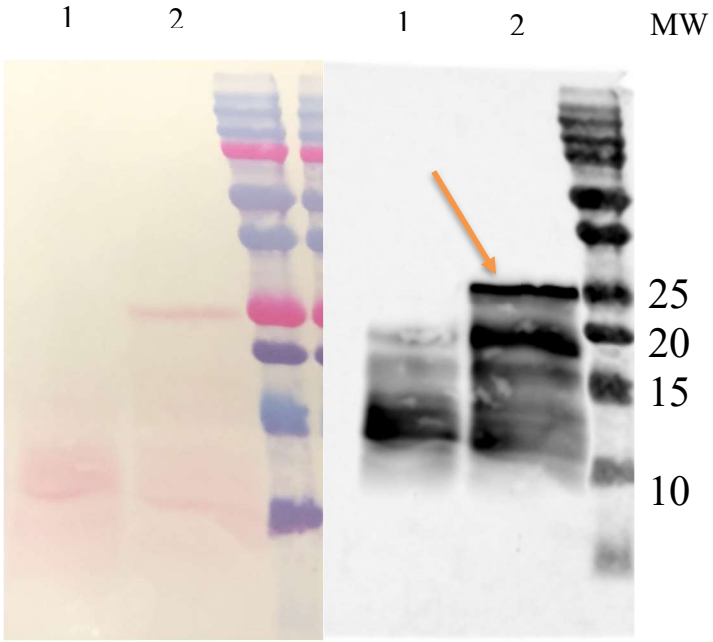

Figure 2.3. Western Blotting Analysis of Papain Inhibition with Biotin-NQMP.

The image on the left is Ponceau S staining. The image on the right is visualization under the western blot scanner.

Lane 1- Sample with inhibitor; no irradiation

Lane 2- Sample with inhibitor and irradiation

2.6 High-res ESI and Tandem Mass Spectrometry Analysis

We decided to use the high-resolution tandem mass spectrometry (MS/MS) technique to further prove our theory of how the inhibitors bind to the protein. If the inhibitors are bound to papain, we will notice a change in the mass of the protein. Then using MS/MS, the protein sequence can be analyzed to see which residue the inhibitors are bound to. The inhibited protein samples were sent to the Amster group for mass spec analysis. As shown in **Figure 2.4,** there was no significant change in the mass of papain detected with either of the inhibitors.

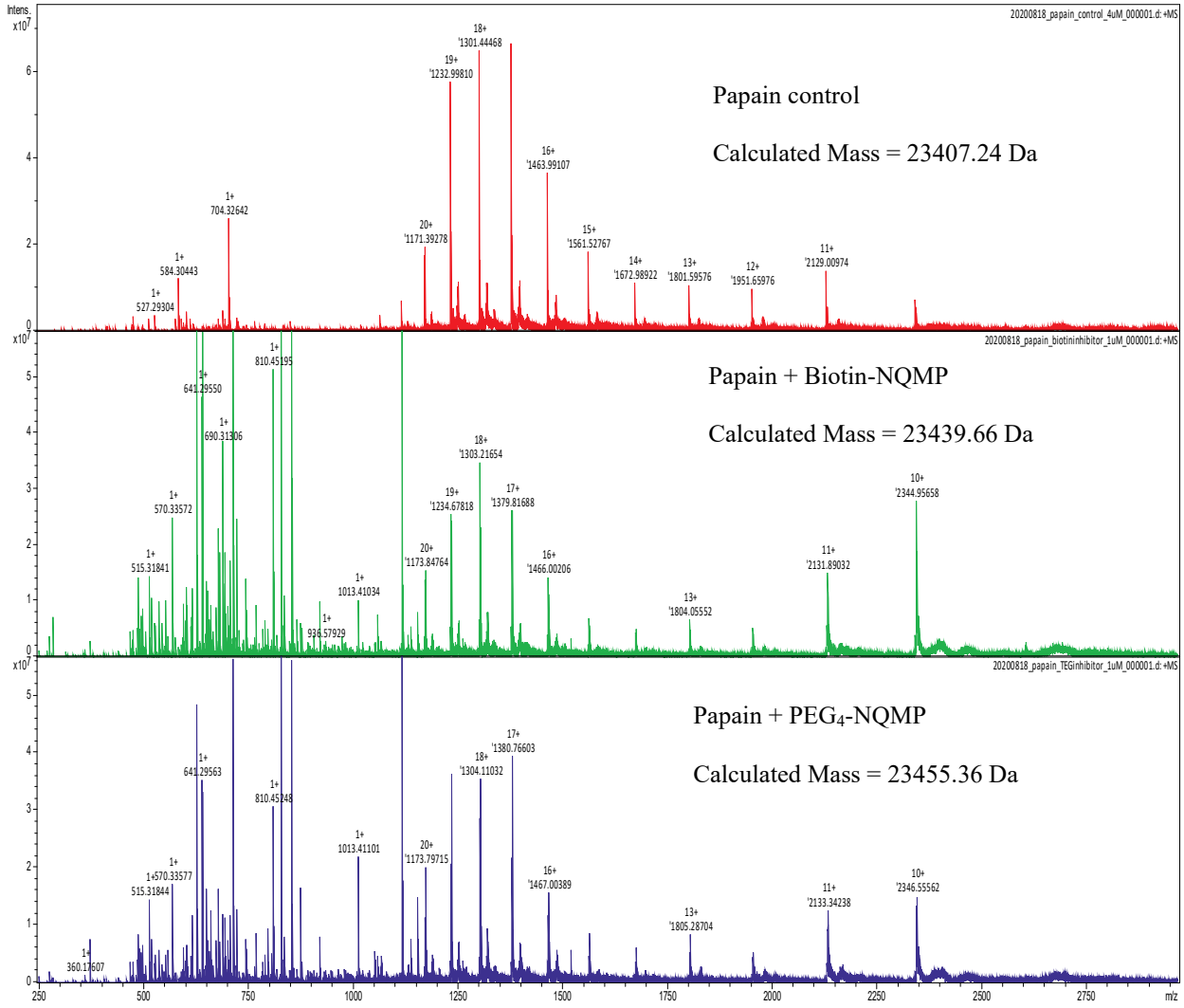

Figure 2.4. ESI Analysis of Papain with PEG_4-NQMP and Biotin-NQMP

2.7. Conclusion and Future Works

The compounds PEG_4-NQMP and Biotin-NQMP proved to be effective at inhibiting the activity of papain. This was a novel photo-induced inhibition method for a cysteine protease. We were able to show the presence of Biotin-NQMP on the protein with western blotting. The tandem mass spectrometry experiment did not show appropriate mass for papain + inhibitor complex.

It is possible that the desalting procedure before taking the mass spec affected the protein-inhibitor complex. Therefore, we plan to use a different buffer such as ammonium acetate instead of PBS to avoid the desalting step. We also plan to submit the protein band from SDS-PAGE gel for a mass spec experiment to see if we can observe the papain + inhibitor complex mass.

2.8 Experimental Section

UV/Vis spectra and kinetic traces were measured using a CARY-300 Bio UV-Vis spectrophotometer. Photo reactions were done in a big Rayonet photo reactor with 4 W 350 nm tubes (16 tubes). The reactions were carried out in a 3 mL quartz cuvette with a path length of 1 cm. Papain was purchased from Sigma Aldrich (Suspension in sodium acetate, 27 mg/mL protein). The buffer used was phosphate-buffered silane with an adjusted pH of 6.1.

Papain Activation: The commercially purchased papain contains a pro-peptide region that needs to be removed by a reducing agent. The stock solution of papain (250 µL) was incubated in 10 mM Dithiothreitol (DTT) / 1 mM Ethylenediaminetetraacetic acid (EDTA) solution prepared in PBS at 6.1 pH for 40 minutes. The protein activity was measured using L-BAPNA as a substrate.

Papain Sample Preparation: DTT was removed from the protein using PD-10 desalting columns after the incubation period. The stock solution of L-BAPNA was 10 mM in Dimethylsulfoxide (DMSO). The final concentration of L-BAPNA in the sample was 167 µM. The first fifteen minutes of kinetic trace were analyzed for protein activity.

2.9 References

1. Gardner, P. D.; Sarrafizadeh R, H.; Brandon, R. L., o-Quinone Methide. *Journal of the American Chemical Society* **1959**, 81 (20), 5515-5515.
2. Wang, H., Quinone Methides and Their Biopolymer Conjugates as Reversible DNA Alkylating Agents. *Curr Org Chem* **2014**, 18 (1), 44-60.
3. Percivalle, C.; Doria, F.; Freccero, M., Quinone Methides as DNA Alkylating Agents: An Overview on Efficient Activation Protocols for Enhanced Target Selectivity. *Curr Org Chem* **2014**, 18 (1), 19-43.
4. Arumugam, S.; Orski, S. V.; Mbua, N. E.; McNitt, C.; Boons, G. J.; Locklin, J.; Popik, V. V., Photo-click chemistry strategies for spatiotemporal control of metal-free ligation, labeling, and surface derivatization. *Pure Appl Chem* **2013**, 85 (7), 1499-1513.
5. Arumugam, S.; Orski, S. V.; Mbua, N. E.; McNitt, C.; Boons, G. J.; Locklin, J.; Popik, V. V., Photo-click chemistry strategies for spatiotemporal control of metal-free ligation, labeling, and surface derivatization. *Pure Appl Chem* **2013**, 85 (7), 1499-1513.
6. Pathak, T. P.; Sigman, M. S., Applications of ortho-Quinone Methide Intermediates in Catalysis and Asymmetric Synthesis. *J Org Chem* **2011**, 76 (22), 9210- 9215.
7. Willis, N. J.; Bray, C. D., ortho-Quinone Methides in Natural Product Synthesis. *Chem-Eur J* **2012**, 18 (30), 9160-9173.
8. Jones, R. M.; Van De Water, R. W.; Lindsey, C. C.; Hoarau, C.; Ung, T.; Pettus, T. R. R., A Mild Anionic Method for Generating o-Quinone Methides: Facile Preparations of

Ortho-Functionalized Phenols. *The Journal of Organic Chemistry* **2001**, 66 (10), 3435-3441.

9. Sugimoto, H.; Nakamura, S.; Ohwada, T., Retro-Diels−Alder Reaction of 4H-1,2-Benzoxazines to Generate o-Quinone Methides: Involvement of Highly Polarized Transition States. *The Journal of Organic Chemistry* **2007**, 72 (26), 10088-10095.

10. Caruana, L.; Fochi, M.; Bernardi, L., The Emergence of Quinone Methides in Asymmetric Organocatalysis. *Molecules* **2015**, 20 (7), 11733-11764.

11. Yang, Q. Q.; Xiao, W. J., Catalytic Asymmetric Synthesis of Chiral Dihydrobenzofurans through a Formal [4+1] Annulation Reaction of Sulfur Ylides and In Situ Generated ortho-Quinone Methides. *Eur J Org Chem* **2017**, (2), 233-236.

12. Jiang, X. L.; Liu, S. J.; Gu, Y. Q.; Mei, G. J.; Shi, F., Catalytic Asymmetric [4+1] Cyclization of ortho-Quinone Methides with 3-Chlorooxindoles. *Adv Synth Catal* **2017**, 359 (19), 3341-3346.

13. El-Sepelgy, O.; Haseloff, S.; Alamsetti, S. K.; Schneider, C., Bronsted Acid Catalyzed, Conjugate Addition of beta-Dicarbonyls to In Situ Generated ortho-Quinone Methides-Enantioselective Synthesis of 4-Aryl-4H-Chromenes. *Angew Chem Int Edit* **2014**, 53 (30), 7923-7927.

14. Jaworski, A. A.; Scheidt, K. A., Emerging Roles of in Situ Generated Quinone Methides in-Metal-Free Catalysis. *J Org Chem* **2016**, 81 (21), 10145-10153.

15. Saha, S.; Schneider, C., Bronsted Acid-Catalyzed, Highly Enantioselective Addition of Enamides to In Situ-Generated ortho-Quinone Methides: A Domino Approach to Complex Acetamidotetrahydroxanthenes. *Chem-Eur J* **2015**, 21 (6), 2348- 2352.

16. Alamsetti, S. K.; Spanka, M.; Schneider, C., Synergistic Rhodium/Phosphoric Acid Catalysis for the Enantioselective Addition of Oxonium Ylides to ortho-Quinone Methides. *Angew Chem Int Edit* **2016**, 55 (7), 2392-2396.

17. Arumugam, S.; Popik, V. V., Photochemical Generation and the Reactivity of o-Naphthoquinone Methides in Aqueous Solutions. *Journal of the American Chemical Society* **2009,** *131* (33), 11892-11899.

18. Arumugam, S.; Guo, J.; Mbua, N. E.; Friscourt, F.; Lin, N.; Nekongo, E.; Boons, G.-J.; Popik, V. V., Selective and reversible photochemical derivatization of cysteine residues in peptides and proteins. *Chem. Sci.* **2014,** *5* (4), 1591-1598.

19. Siklos, M., BenAissa, M., & Thatcher, G. R. Cysteine proteases as therapeutic targets: does selectivity matter? A systematic review of calpain and cathepsin inhibitors. *Acta Pharmaceutica Sinica*. **2015,** B, 5(6), 506–519.

20. Verma, S.; Dixit, R.; Pandey, K. C., Cysteine Proteases: Modes of Activation and Future Prospects as Pharmacological Targets. *Front Pharmacol* **2016**, 7.

21. Anson, M. L., The estimation of papain with hemoglobin. *J Gen Physiol* **1937**, 20 (4), 561-563.

22. Vernet, T.; Tessier, D. C.; Chatellier, J.; Plouffe, C.; Lee, T. S.; Thomas, D. Y.; Storer, A. C.; Menard, R., Structural and Functional Roles of Asparagine-175 in the Cysteine Protease Papain. *Journal of Biological Chemistry* **1995**, 270 (28), 16645-16652.

23. Cornely, K.; Crespo, E.; Earley, M.; Kloter, R.; Levesque, A.; Pickering, M.. Kinetics of Papain: An Introductory Biochemistry Laboratory Experiment. *Journal of Chemical Education* **1999**, 76 (5), 644.

24. Arumugam, S.; Popik, V. V., Attach, Remove, or Replace: Reversible Surface Functionalization Using Thiol–Quinone Methide Photoclick Chemistry. *Journal of the American Chemical Society* **2012,** *134* (20), 8408-8411.

25. Arumugam, S.; Popik, V. V., Bichromophoric fluorescent photolabile protecting group for alcohols and carboxylic acids. *Photochem. Photobiol. Sci.* **2012,** *11* (3), 518-521.

26. Lin, N. DESIGN, SYNTHESIS and APPLYCATION of O-NAPHTHOQUINONE METHIDE PRECURSOR for BIOCHEMISTRY and NANOMATERIAL SCIENCE. Thesis, University of Georgia.

APPENDIX A

^{1}H NMR and ^{13}C NMR

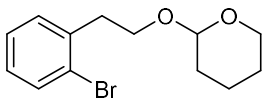

1.22

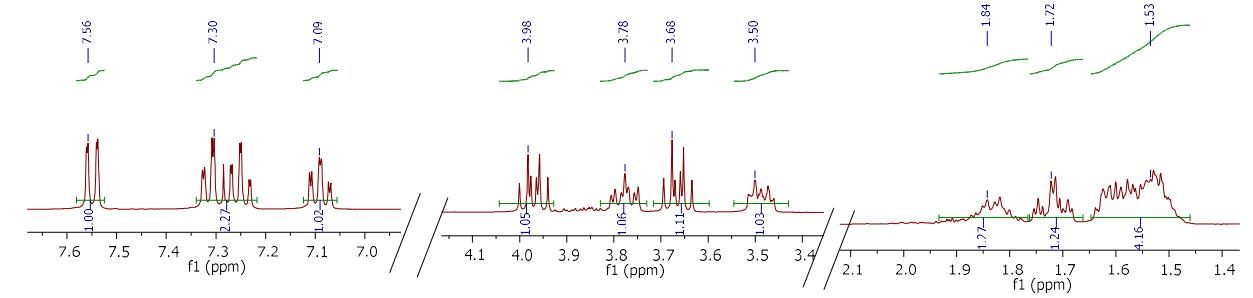

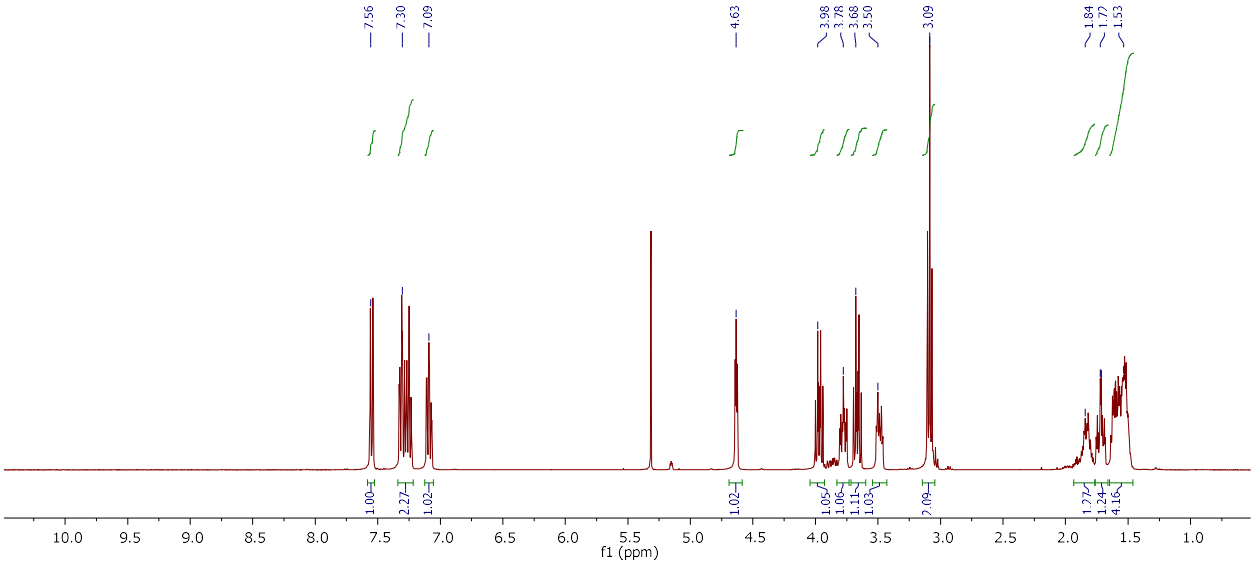

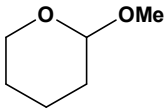
O
OMe

1.17

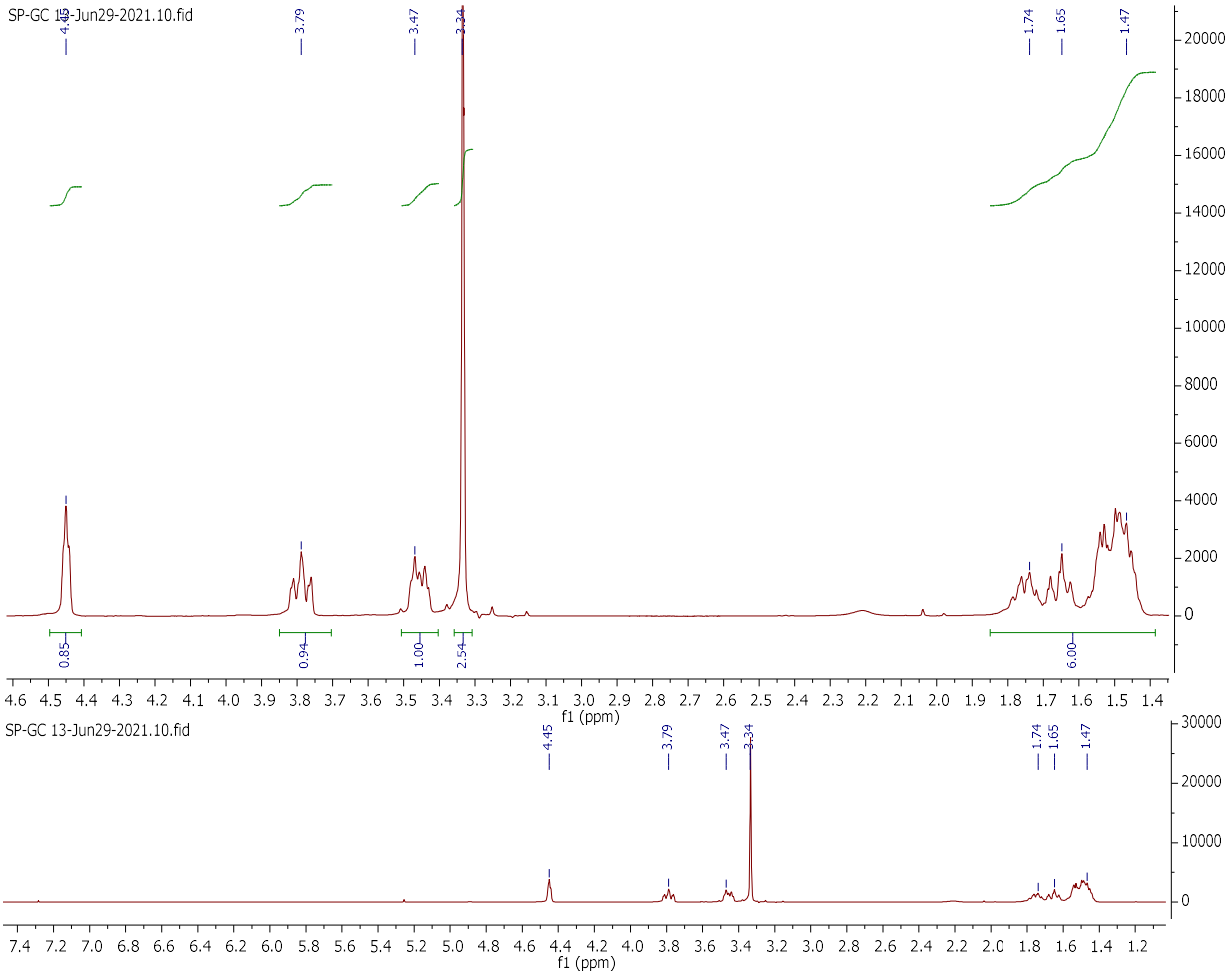
SP-GC 13-Jun29-2021.10.fid
4.45
3.79
3.47
3.34
1.74
1.65
1.47
0.85
0.94
1.00
2.54
6.00
f1 (ppm)
SP-GC 13-Jun29-2021.10.fid
f1 (ppm)

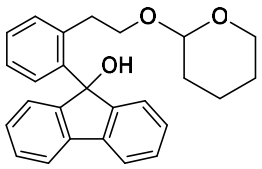
O
O
OH

1.13

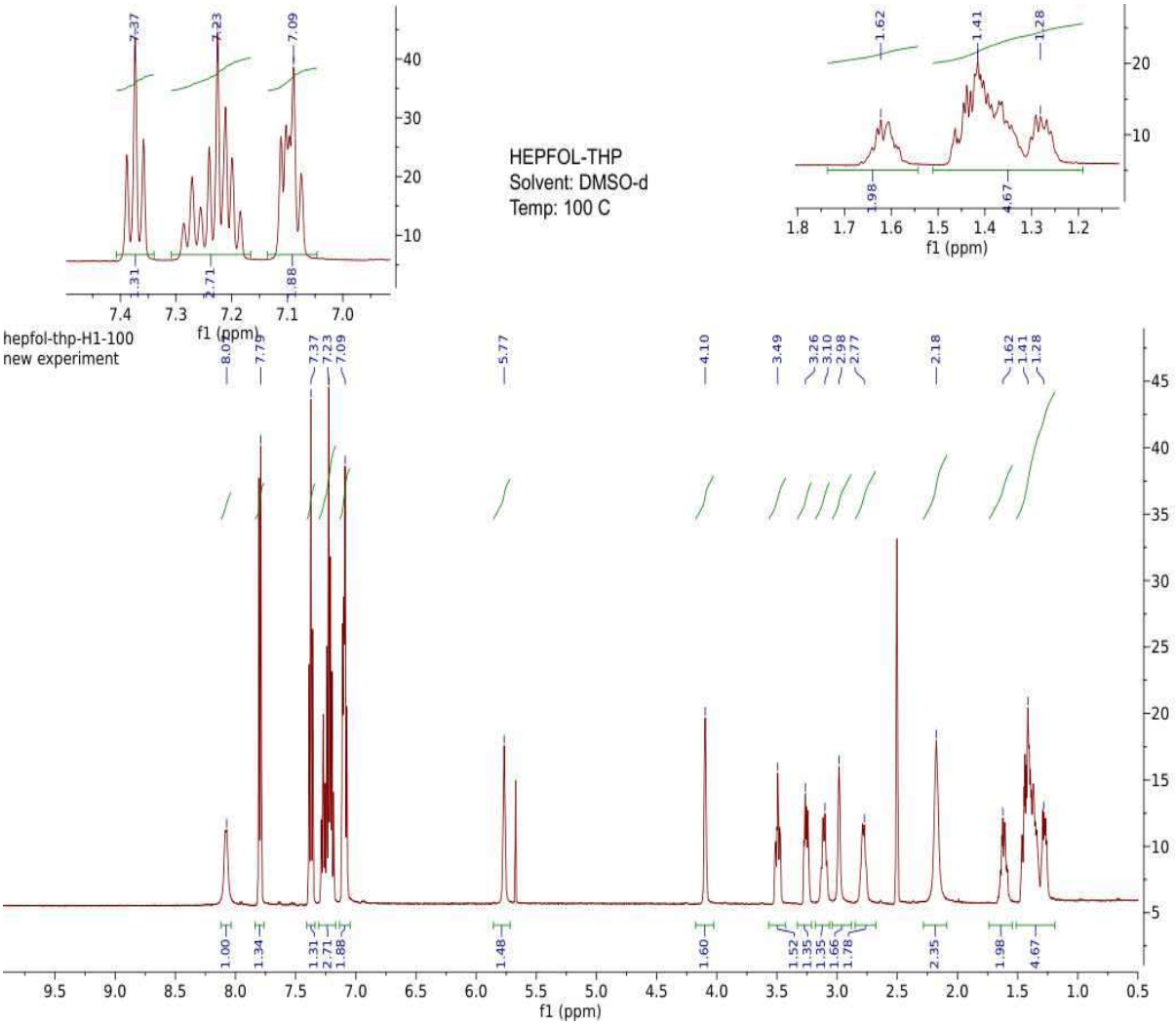
HEPFOL-THP
Solvent: DMSO-d
Temp: 100 C
hepfol-thp-H1-100
new experiment
f1 (ppm)

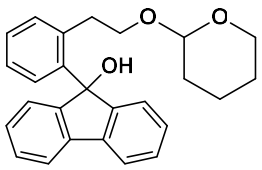
O
O
OH

1.13

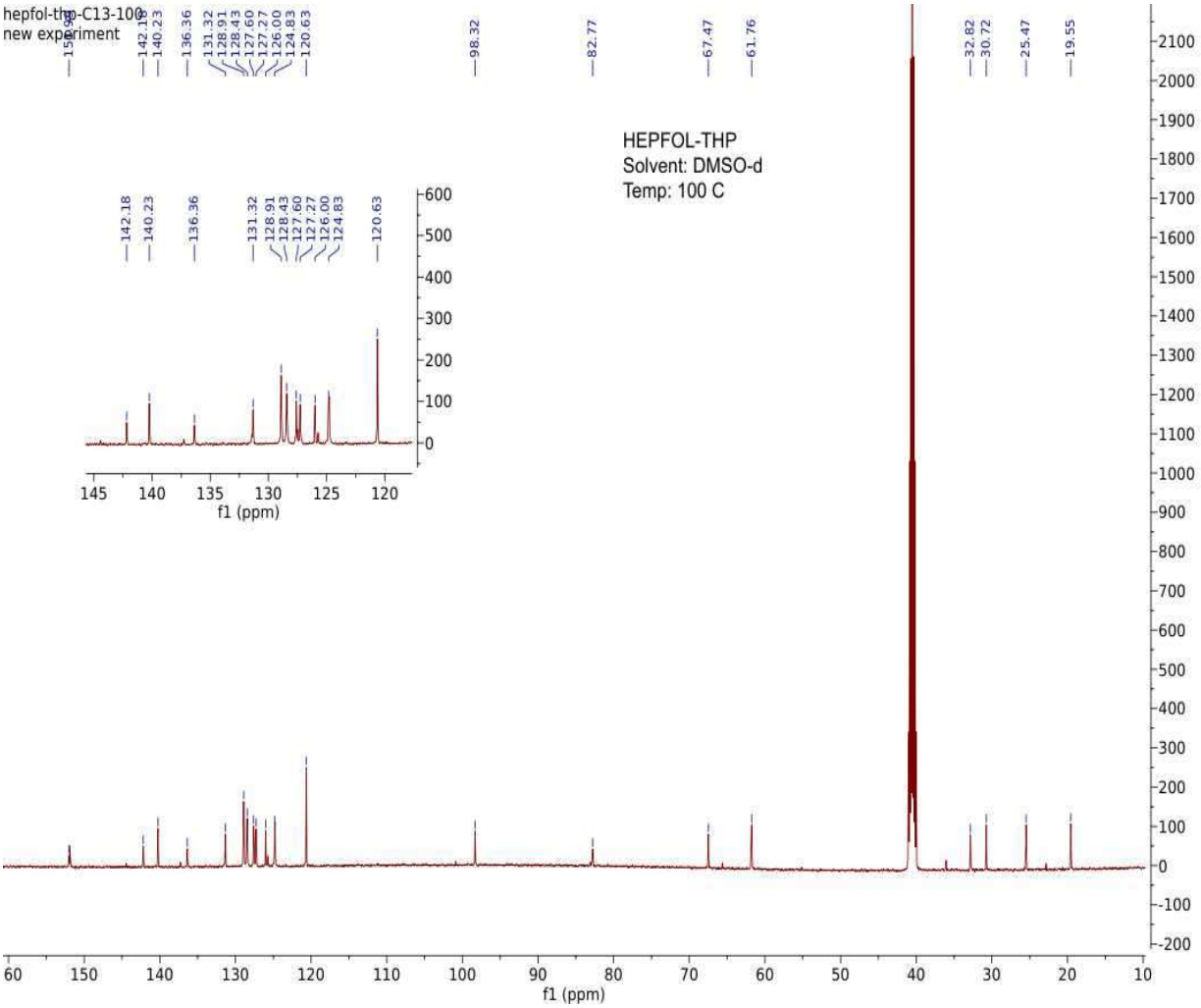
hepfol-thp-C13-100
new experiment
HEPFOL-THP
Solvent: DMSO-d
Temp: 100 C
f1 (ppm)

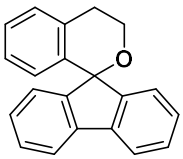

1.14

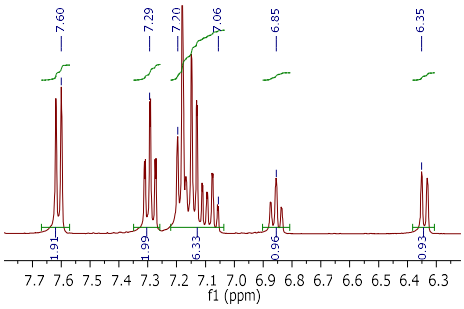
7.60
7.29
7.20
7.06
6.85
6.35
1.91
1.99
6.33
0.96
0.93
7.7 7.6 7.5 7.4 7.3 7.2 7.1 7.0 6.9 6.8 6.7 6.6 6.5 6.4 6.3
f1 (ppm)

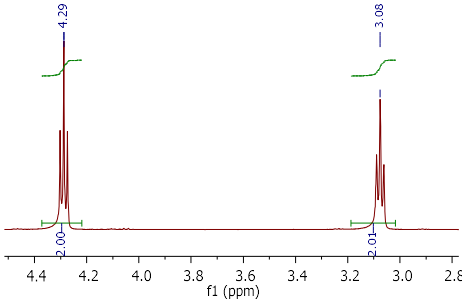
4.29
3.08
2.00
2.01
4.4 4.2 4.0 3.8 3.6 3.4 3.2 3.0
f1 (ppm)

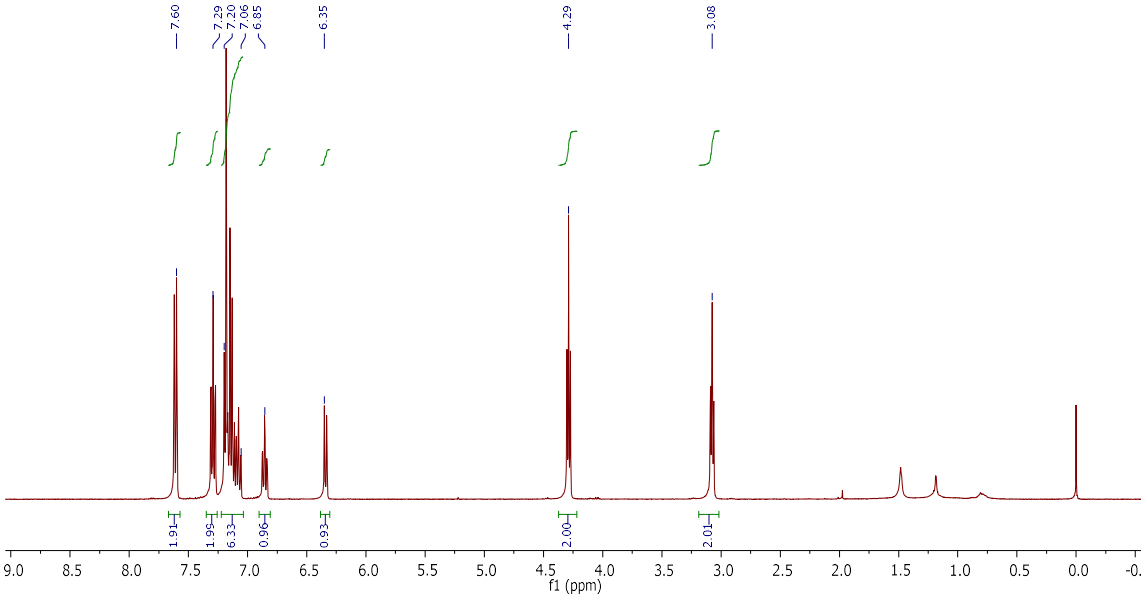
7.60
7.29
7.20
7.06
6.85
6.35
4.29
3.08
1.91
1.99
6.33
0.96
0.93
2.00
2.01
9.0 8.5 8.0 7.5 7.0 6.5 6.0 5.5 5.0 4.5 4.0 3.5 3.0 2.5 2.0 1.5 1.0 0.5 0.0
f1 (ppm)

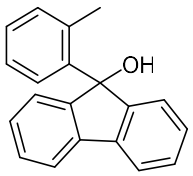
OH

1.27

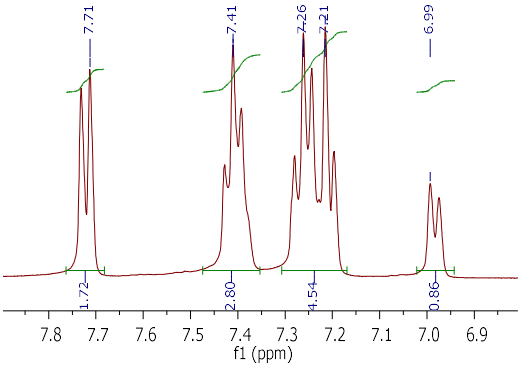
7.71
7.41
7.26
7.21
6.99
1.72
2.80
4.54
0.86
7.8 7.7 7.6 7.5 7.4 7.3 7.2 7.1 7.0 6.9
f1 (ppm)

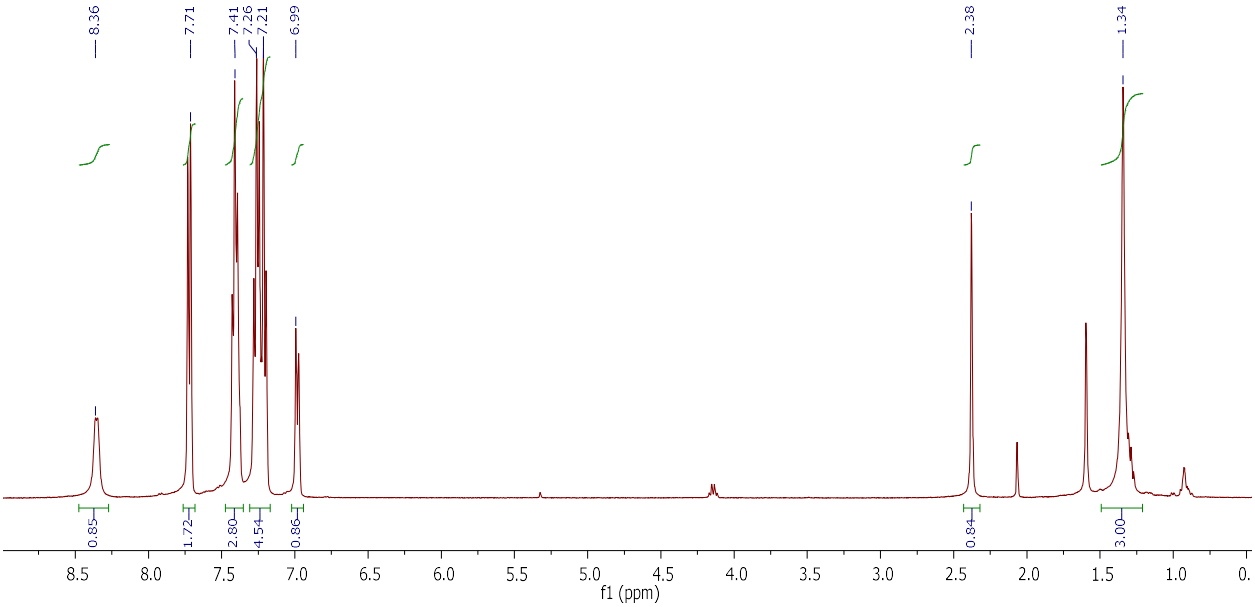
8.36
7.71
7.41
7.26
7.21
6.99
2.38
1.34
0.85
1.72
2.80
4.54
0.86
0.84
3.00
8.5 8.0 7.5 7.0 6.5 6.0 5.5 5.0 4.5 4.0 3.5 3.0 2.5 2.0 1.5 1.0 0.
f1 (ppm)

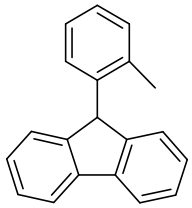

1.19

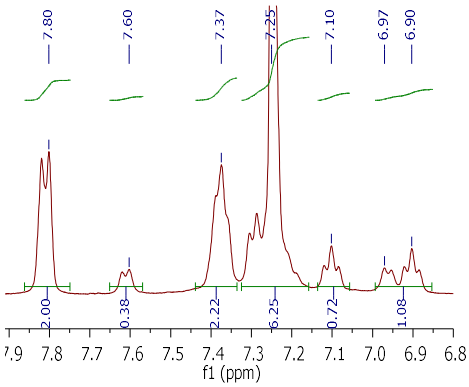
7.80
7.60
7.37
7.25
7.10
6.97
6.90
2.00
0.38
2.22
6.25
0.72
1.08
f1 (ppm)

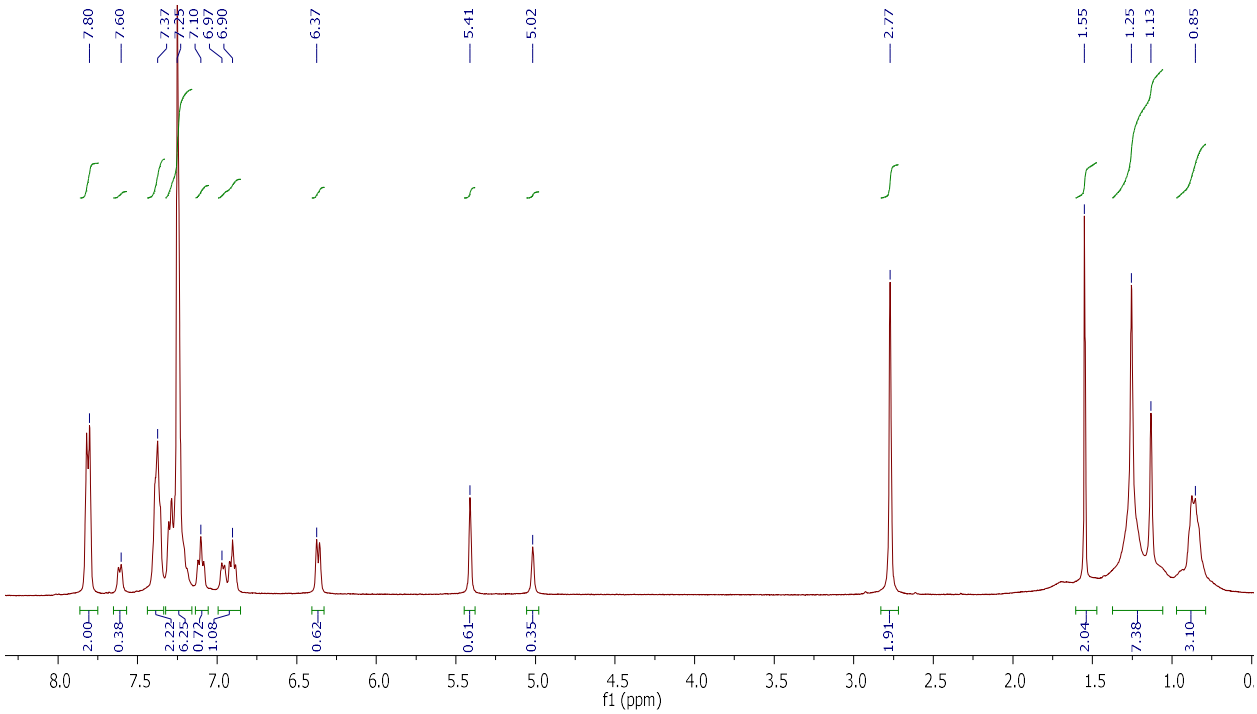
7.80
7.60
7.37
7.25
7.10
6.97
6.90
6.37
5.41
5.02
2.77
1.55
1.25
1.13
0.85
2.00
0.38
2.22
6.25
0.72
1.08
0.62
0.61
0.35
1.91
2.04
7.38
3.10
f1 (ppm)

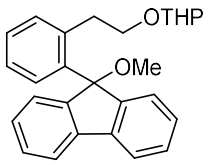
OTHP
OMe

1.18

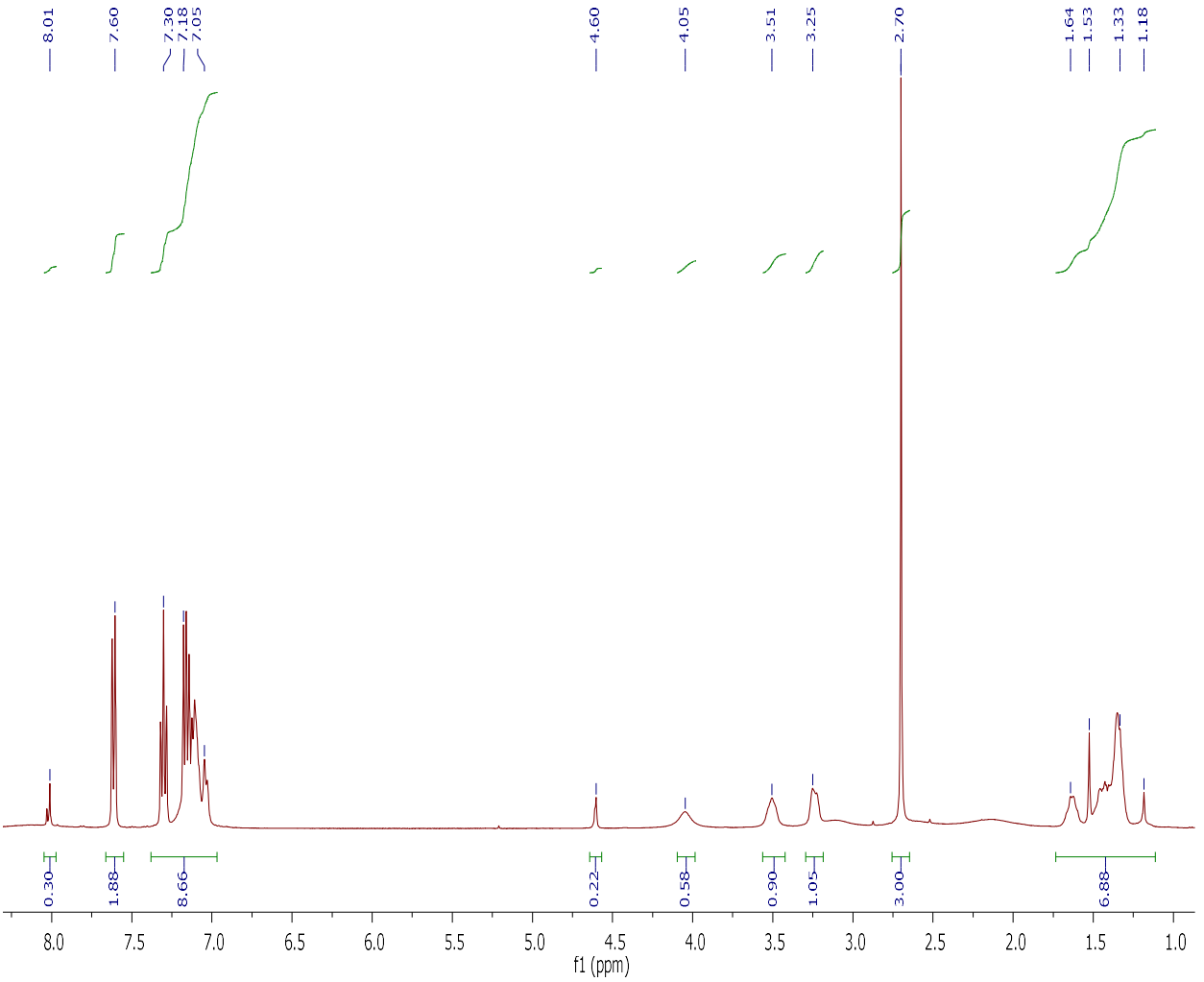
8.01
7.60
7.30
7.18
7.05
4.60
4.05
3.51
3.25
2.70
1.64
1.53
1.33
1.18
0.30
1.88
8.66
0.22
0.58
0.90
1.05
3.00
6.88
f1 (ppm)

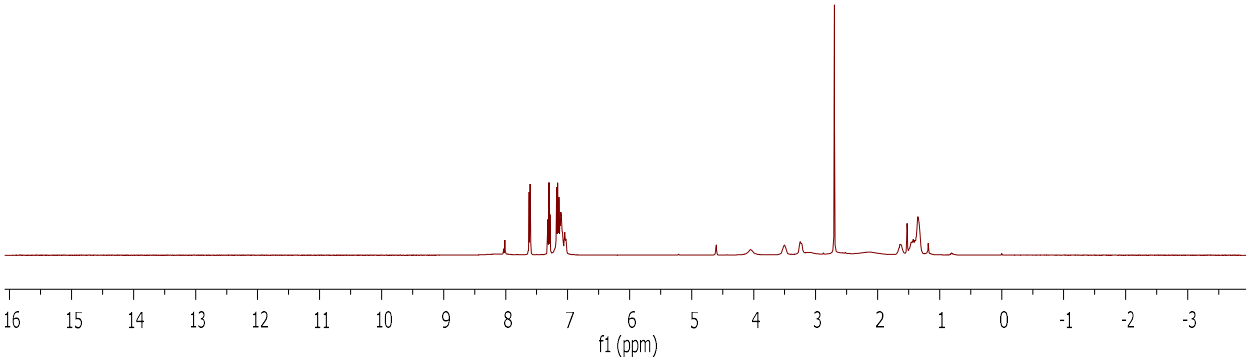
f1 (ppm)

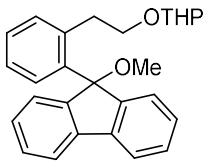
OTHP
OMe

1.18

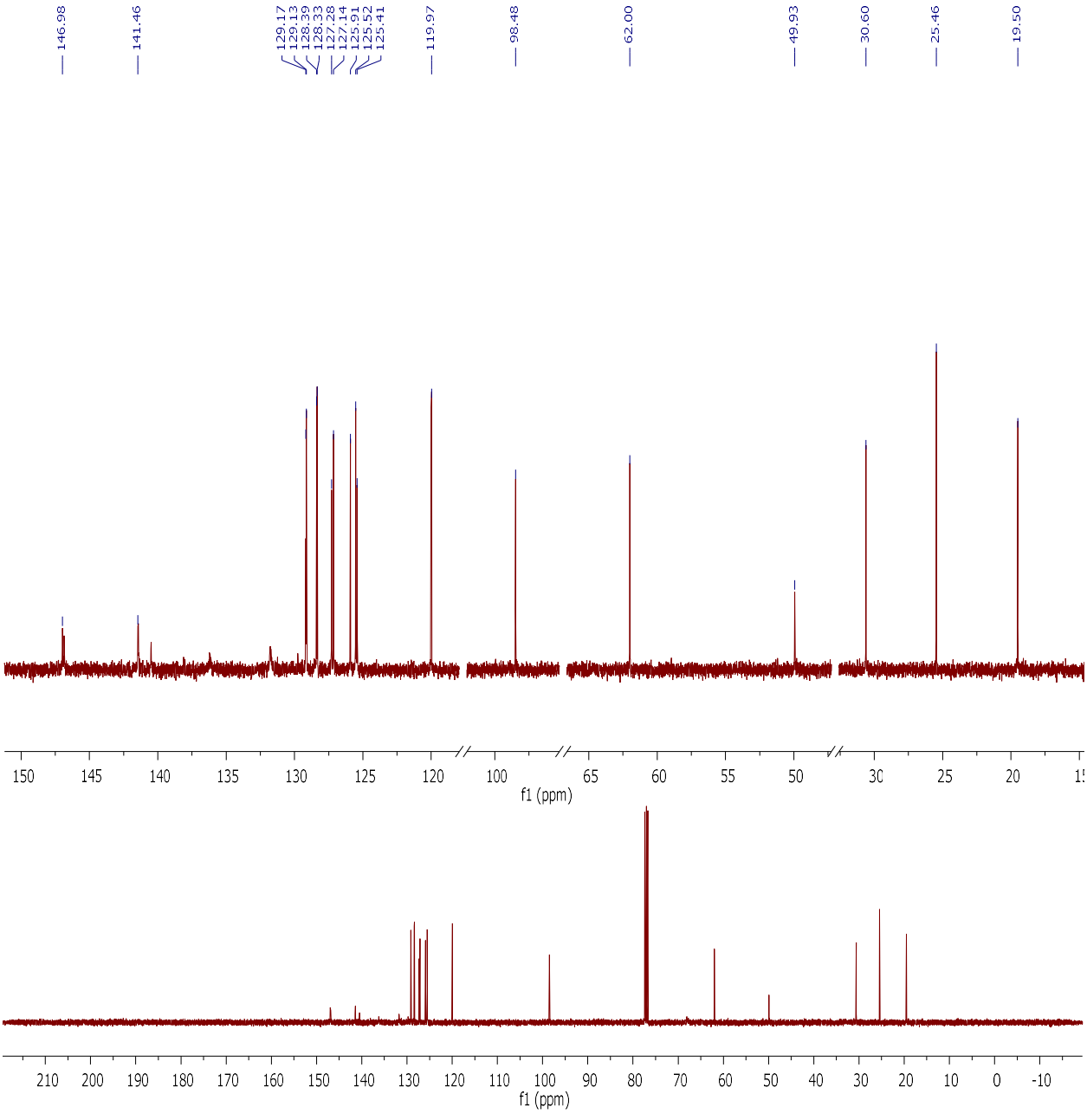
146.98
141.46
129.17
129.13
128.39
128.33
127.28
127.14
125.91
125.52
125.41
119.97
98.48
62.00
49.93
30.60
25.46
19.50
150 145 140 135 130 125 120 100 65 60 55 50 30 25 20
f1 (ppm)
210 200 190 180 170 160 150 140 130 120 110 100 90 80 70 60 50 40 30 20 10 0 -10
f1 (ppm)

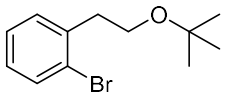
O
Br

1.33

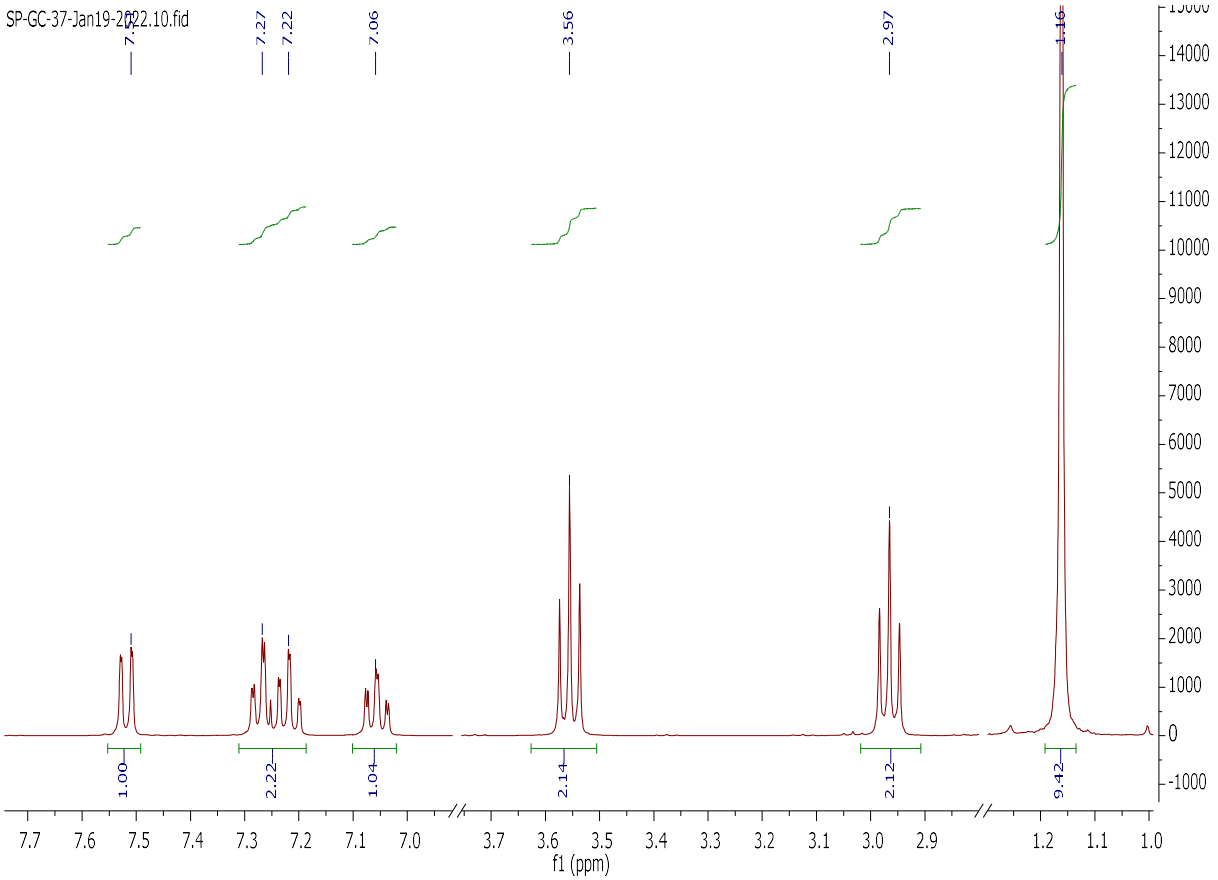
SP-GC-37-Jan19-2022.10.fid
7.27
7.22
7.06
3.56
2.97
1.16
1.00
2.22
1.04
2.14
2.12
9.42
f1 (ppm)

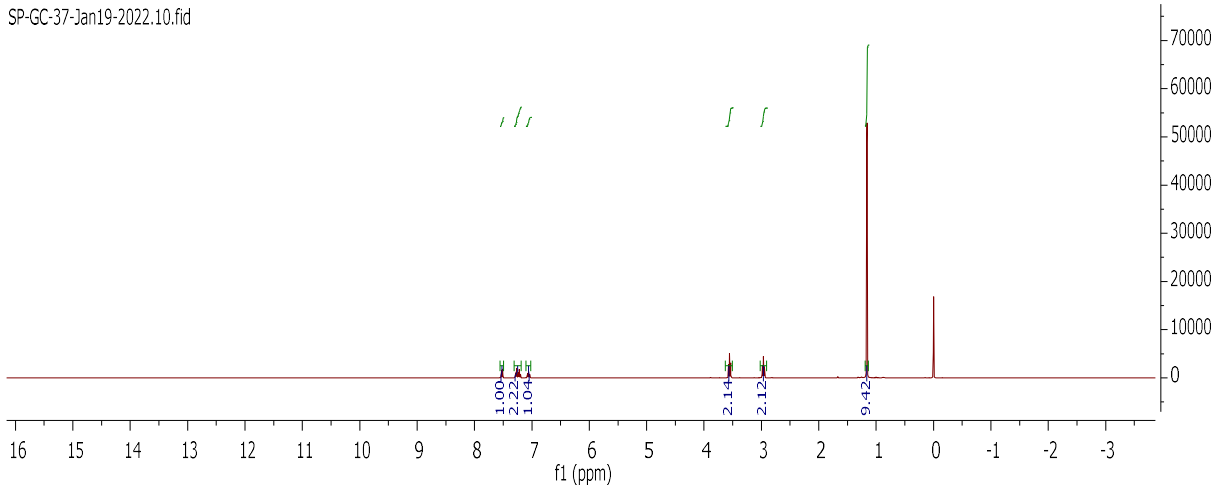
SP-GC-37-Jan19-2022.10.fid
1.00
2.22
1.04
2.14
2.12
9.42
f1 (ppm)

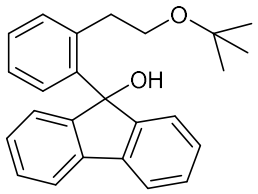
O
OH

1.34

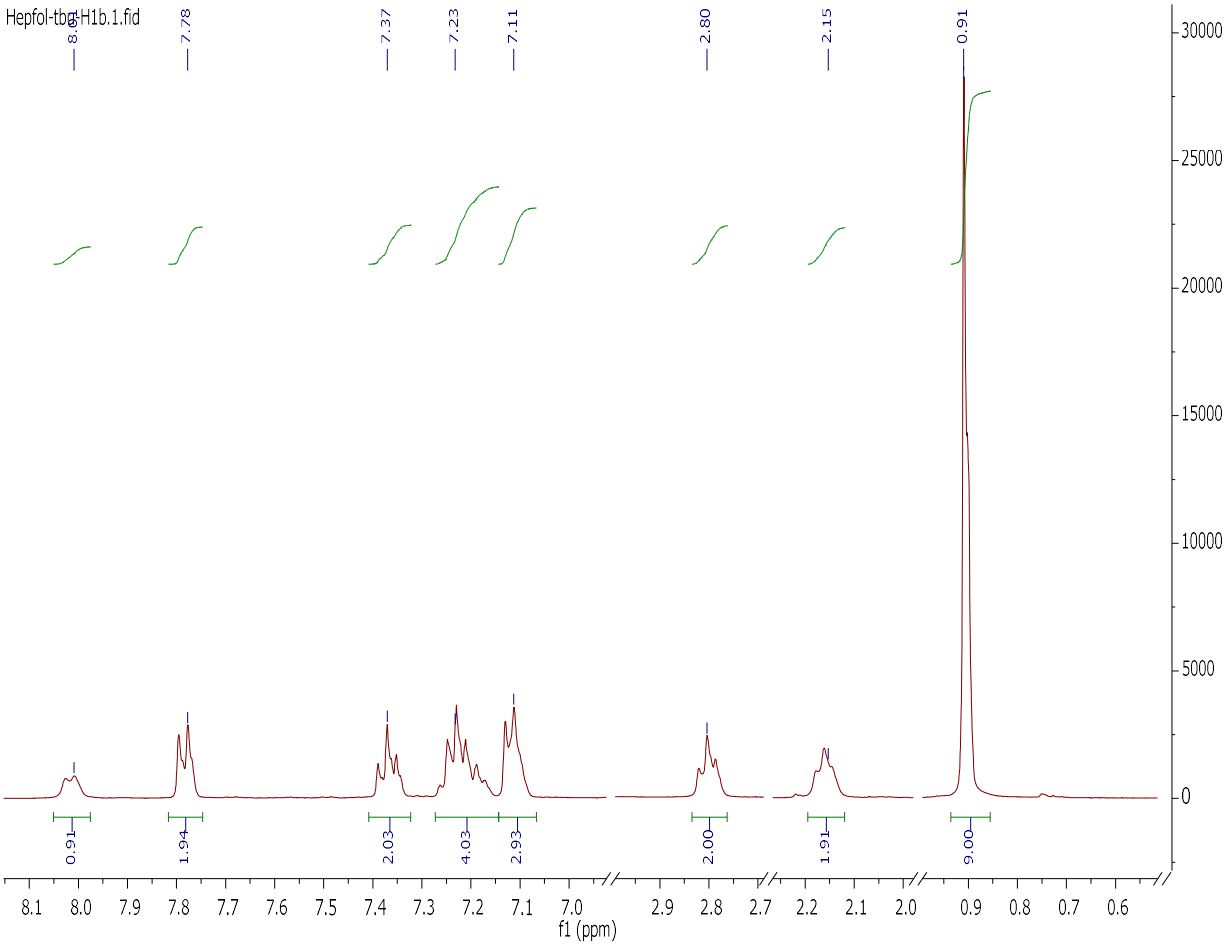
Hepfol-tbu-H1b.1.fid
8.09
7.78
7.37
7.23
7.11
2.80
2.15
0.91
0.91
1.94
2.03
4.03
2.93
2.00
1.91
9.00
f1 (ppm)

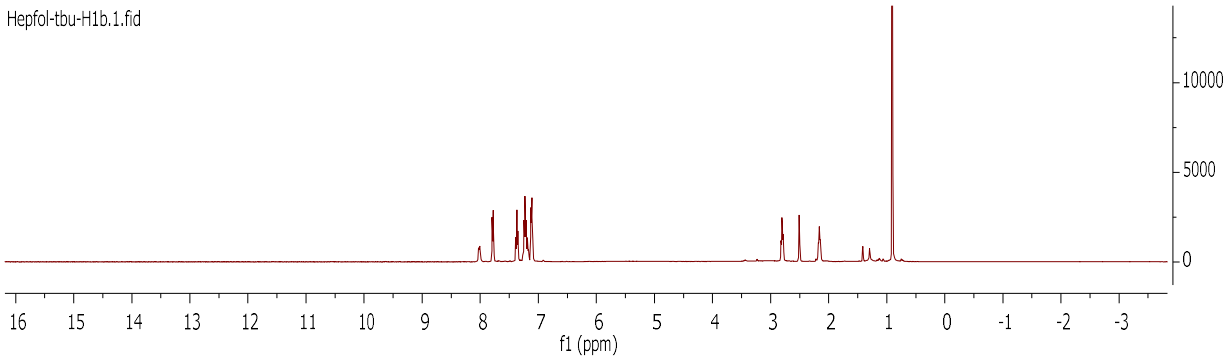
Hepfol-tbu-H1b.1.fid
f1 (ppm)

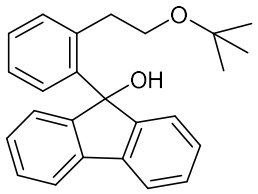
O
OH

1.34

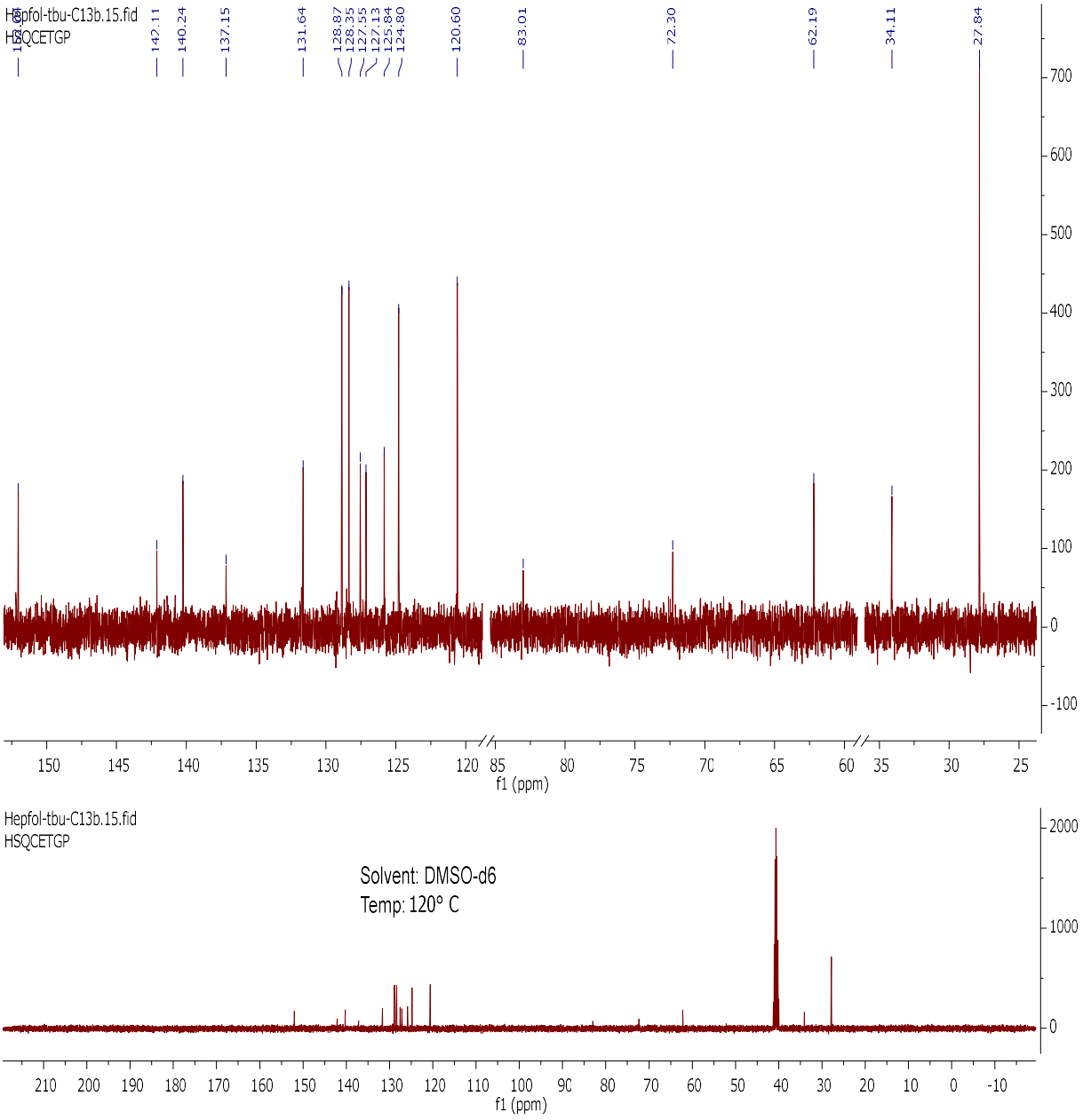
Hepfol-tbu-C13b.15.fid
HSQCETGP
142.11
140.24
137.15
131.64
128.87
128.35
127.55
127.13
125.84
124.80
120.60
83.01
72.30
62.19
34.11
27.84
f1 (ppm)
Hepfol-tbu-C13b.15.fid
HSQCETGP
Solvent: DMSO-d6
Temp: 120° C
f1 (ppm)

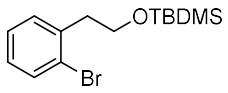
OTBDMS
Br

1.35

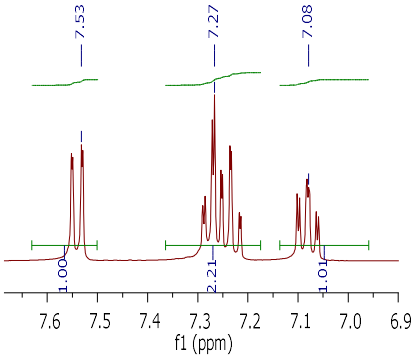
7.53
7.27
7.08
1.00
2.21
1.01
7.6 7.5 7.4 7.3 7.2 7.1 7.0 6.9
f1 (ppm)

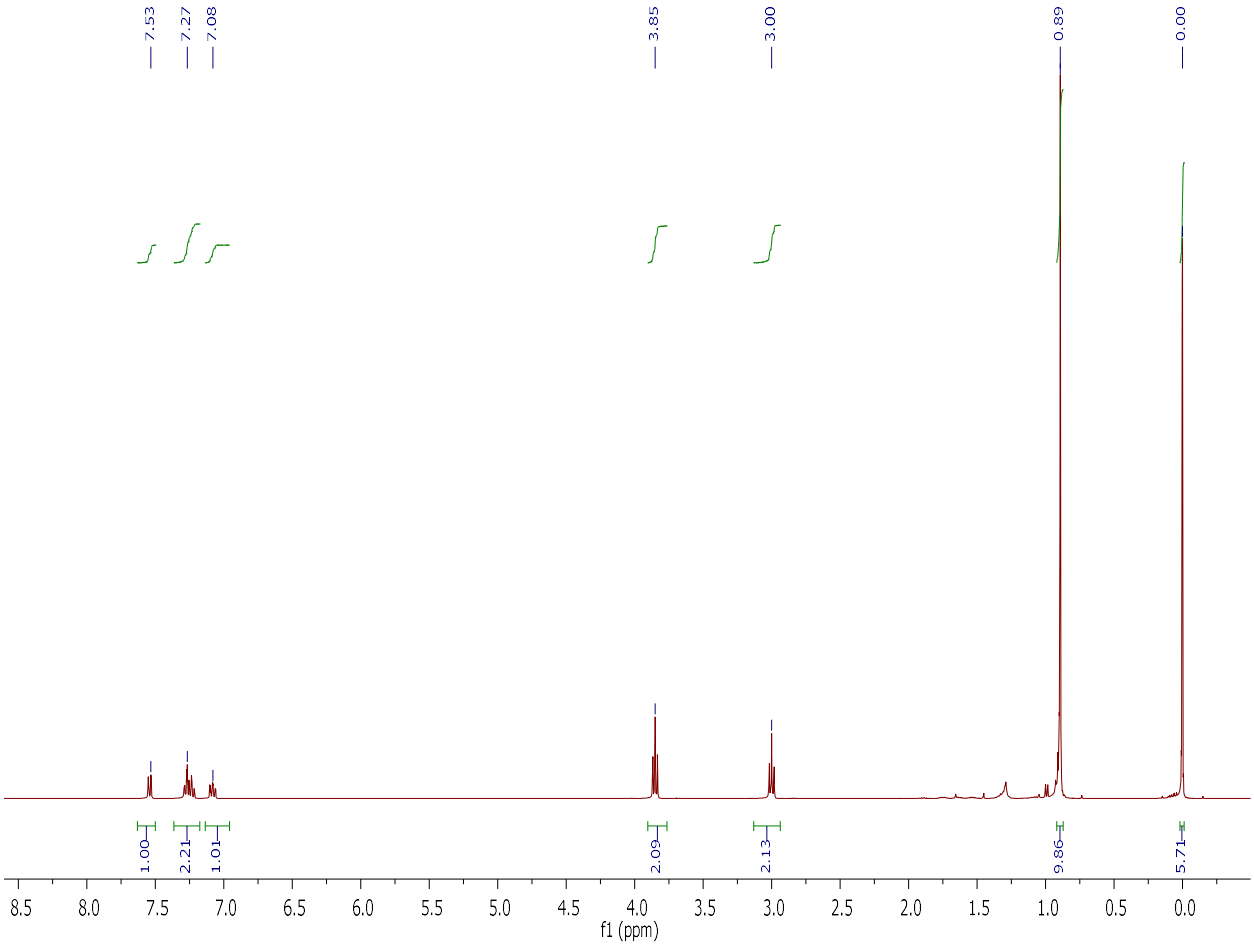
7.53
7.27
7.08
3.85
3.00
0.89
0.00
1.00
2.21
1.01
2.09
2.13
9.86
5.71
8.5 8.0 7.5 7.0 6.5 6.0 5.5 5.0 4.5 4.0 3.5 3.0 2.5 2.0 1.5 1.0 0.5 0.0
f1 (ppm)

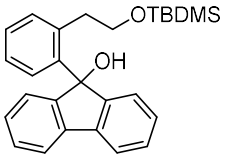
OTBDMS
OH

1.36

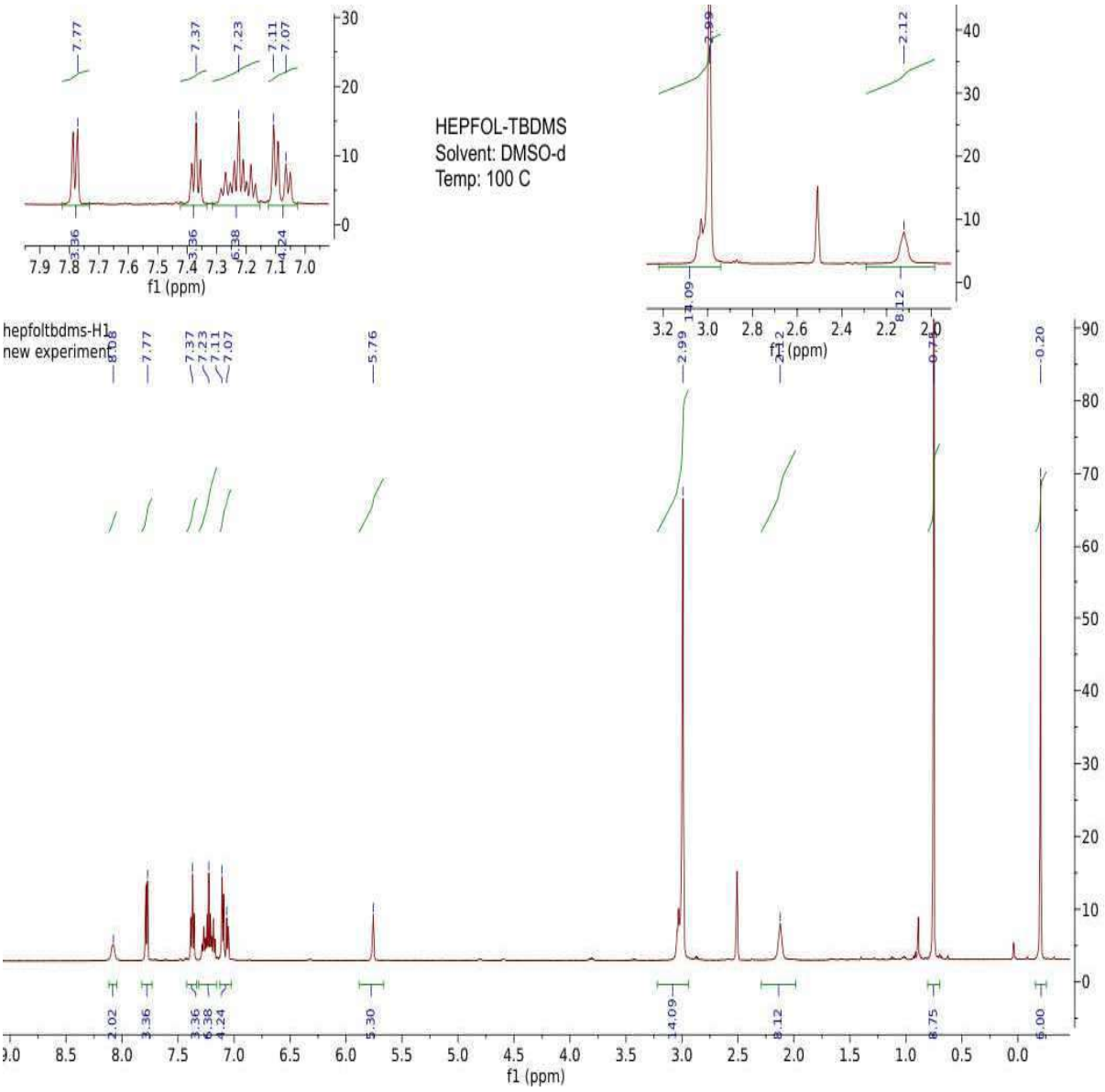
HEPFOL-TBDMS
Solvent: DMSO-d
Temp: 100 C
hepfoltbdms-H1
new experiment
f1 (ppm)

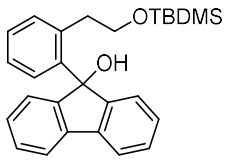
OTBDMS
OH

1.36

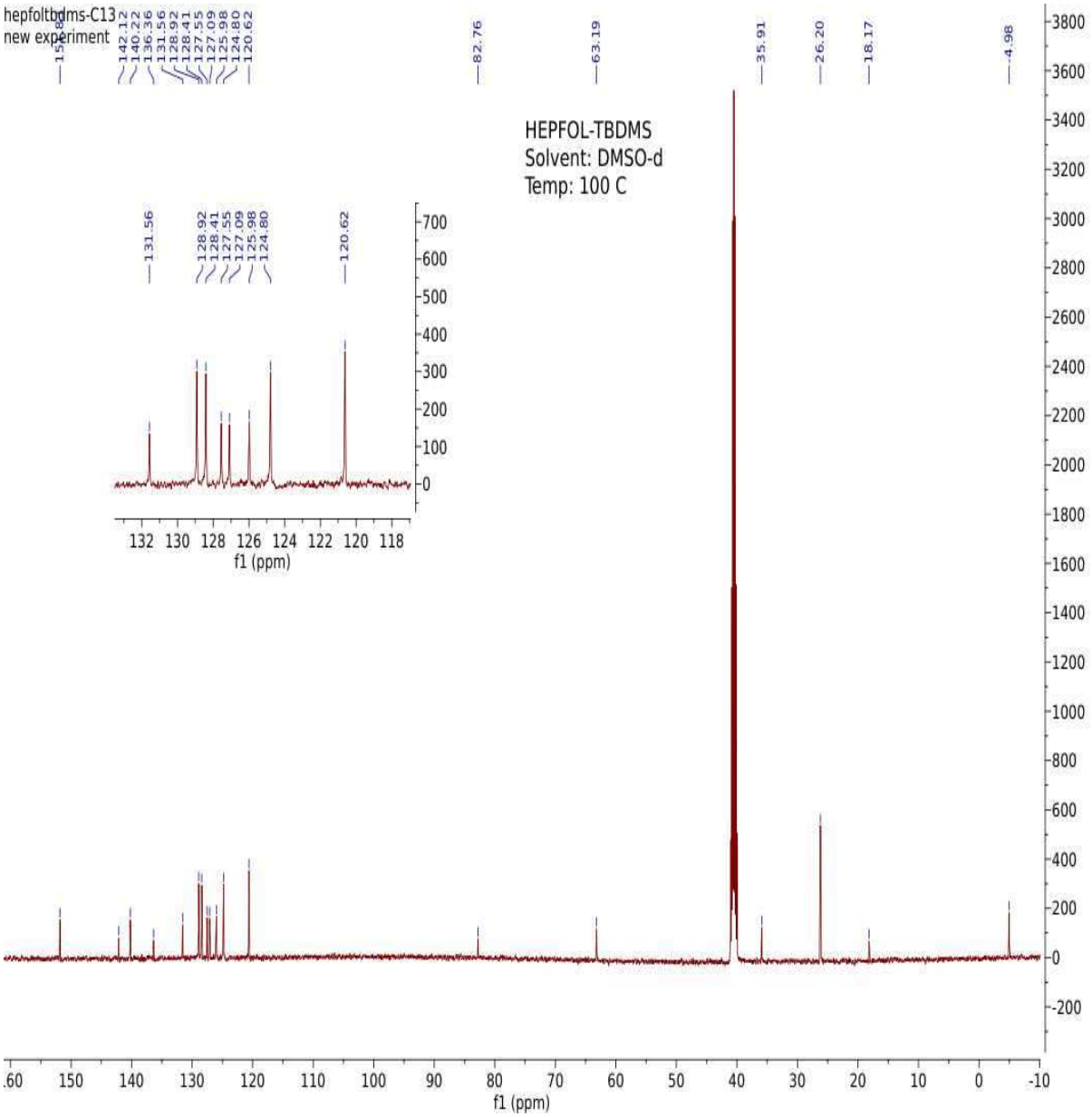
hepfoltbdms-C13
new experiment
HEPFOL-TBDMS
Solvent: DMSO-d
Temp: 100 C
f1 (ppm)

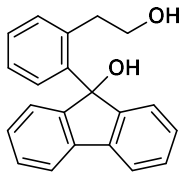
OH
OH

1.37

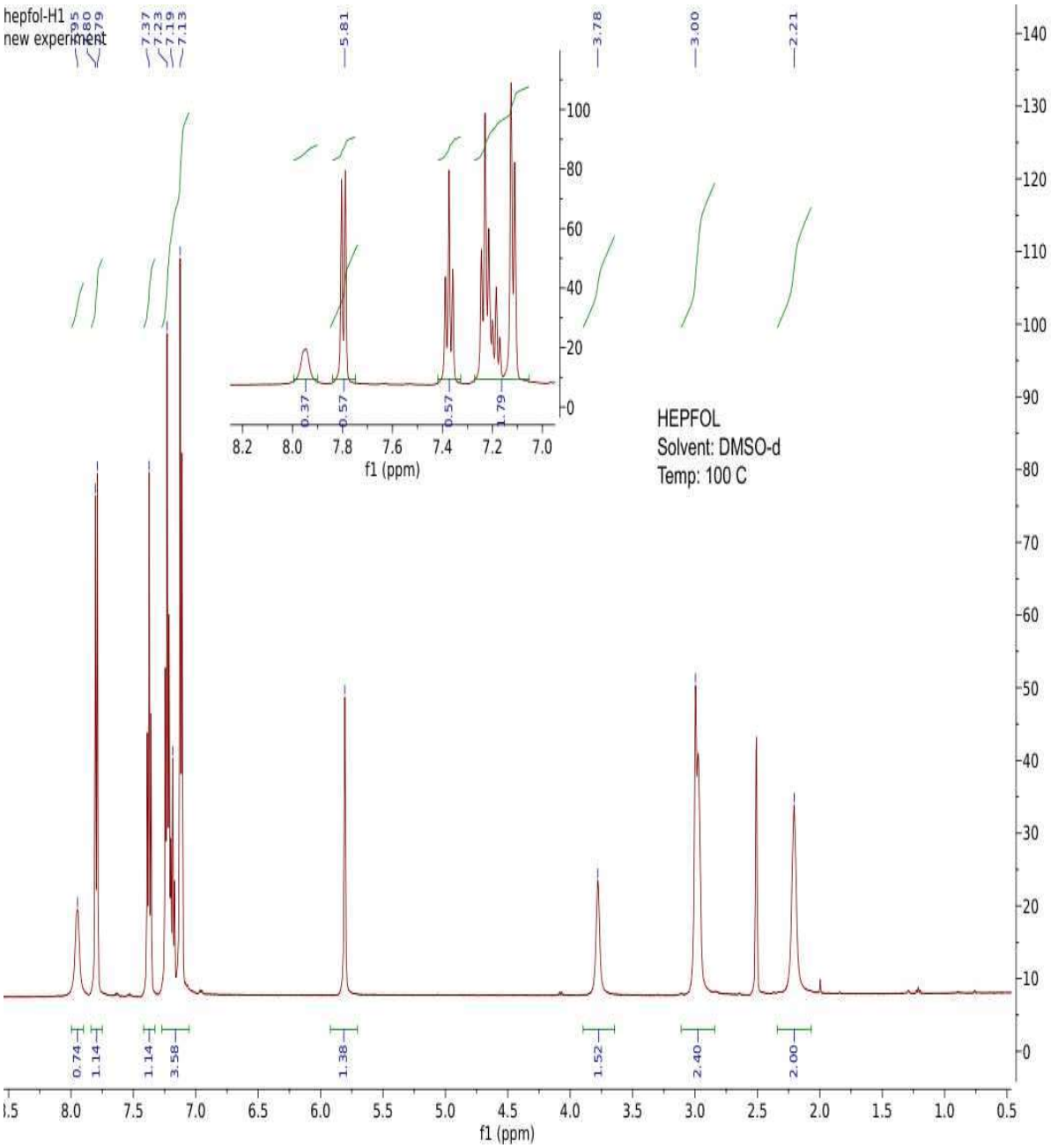
hepfol-H1
new experiment
HEPFOL
Solvent: DMSO-d
Temp: 100 C
f1 (ppm)

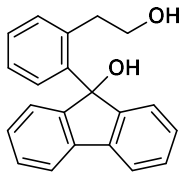
OH
OH

1.37

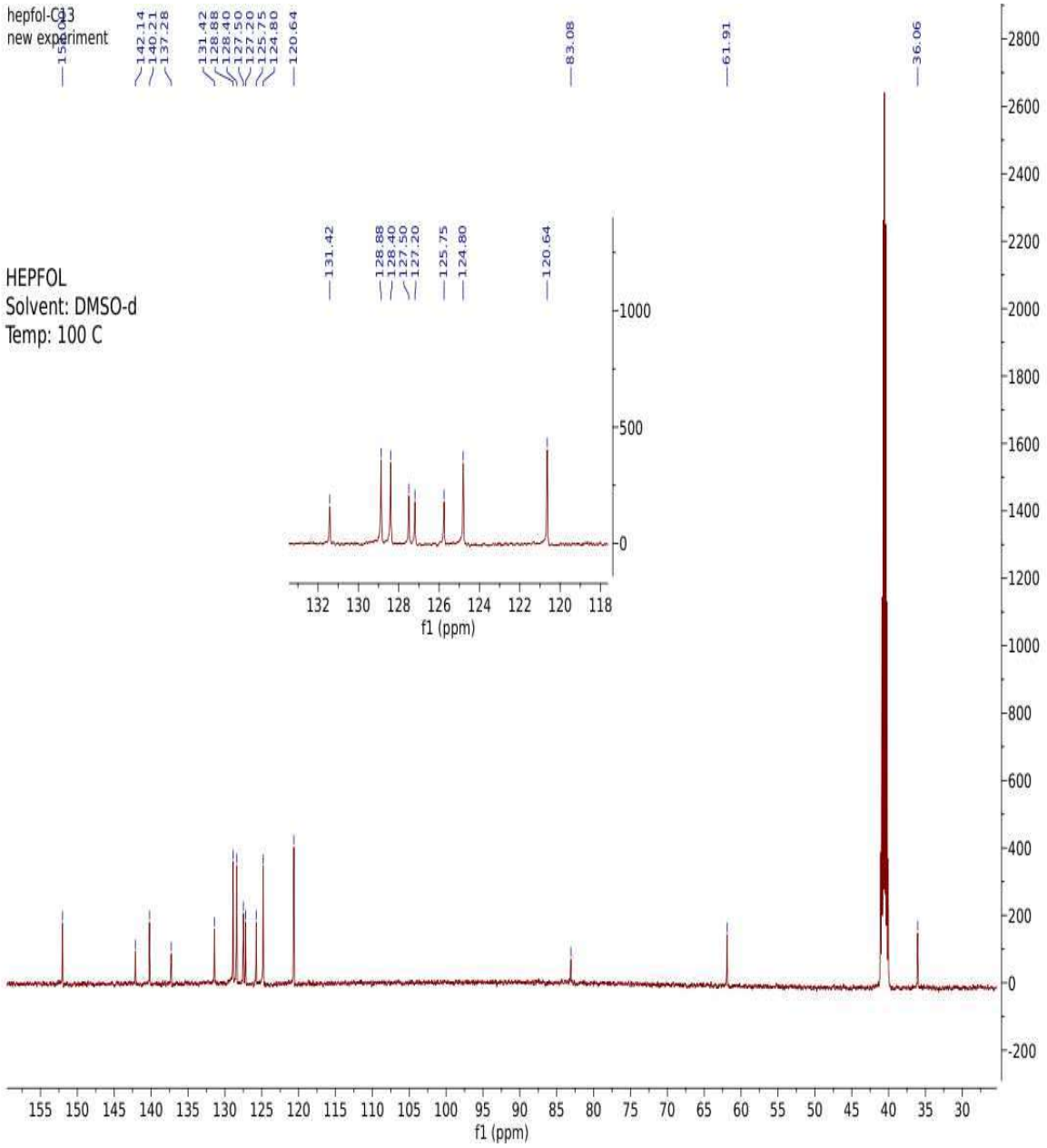
hepfol-C13
new experiment
150.04
142.14
140.21
137.28
131.42
128.88
128.40
127.50
127.20
125.75
124.80
120.64
83.08
61.91
36.06
HEPFOL
Solvent: DMSO-d
Temp: 100 C
f1 (ppm)
f1 (ppm)

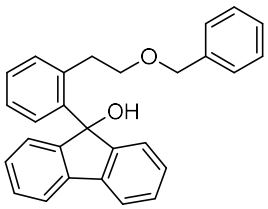
O
OH

1.39

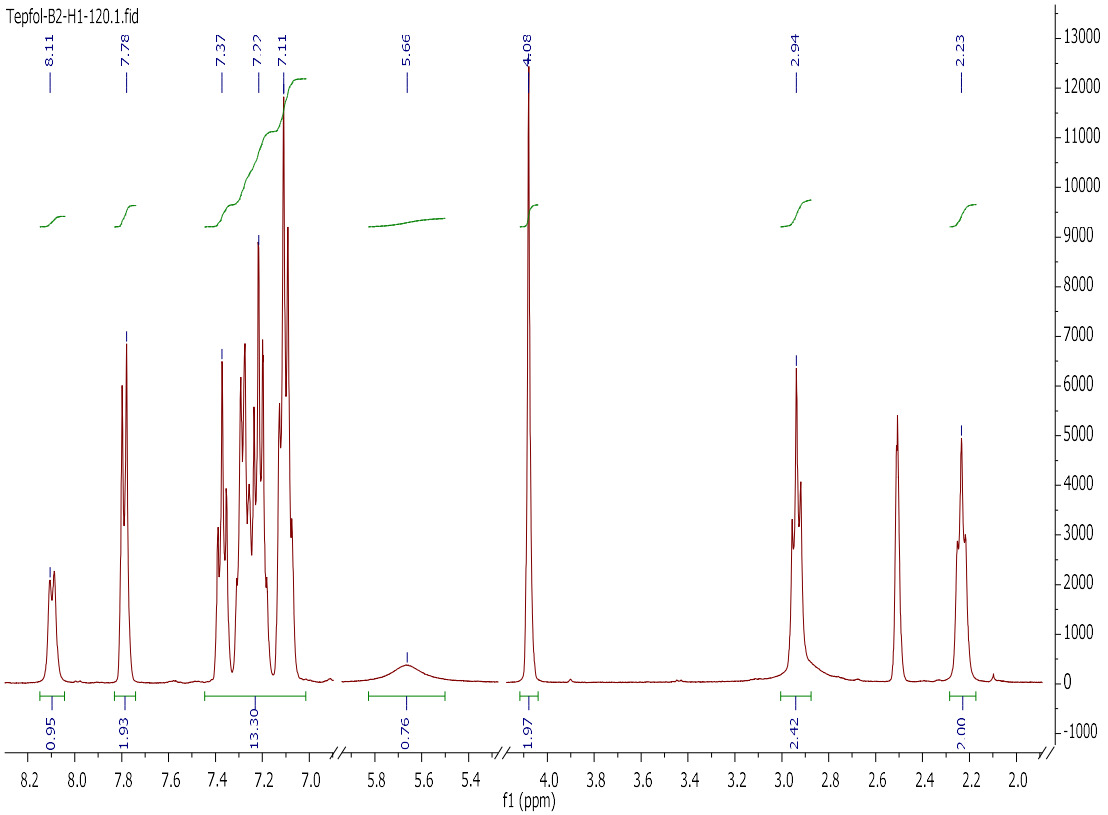
Tepfol-B2-H1-120.1.fid
8.11
7.78
7.37
7.22
7.11
5.66
4.08
2.94
2.23
0.95
1.93
13.30
0.76
1.97
2.42
2.00
f1 (ppm)

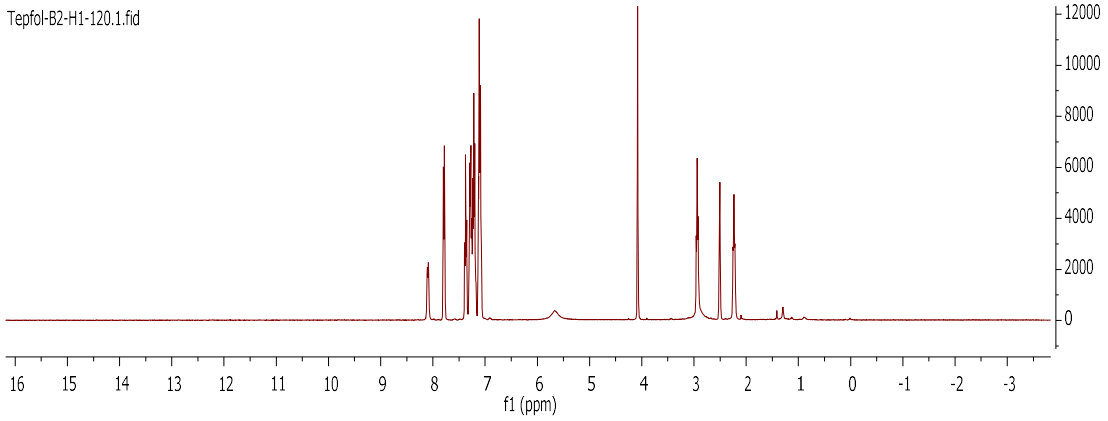
Tepfol-B2-H1-120.1.fid
f1 (ppm)

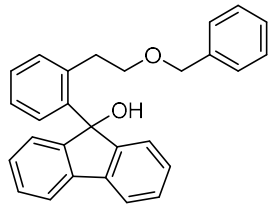
O
OH

1.39

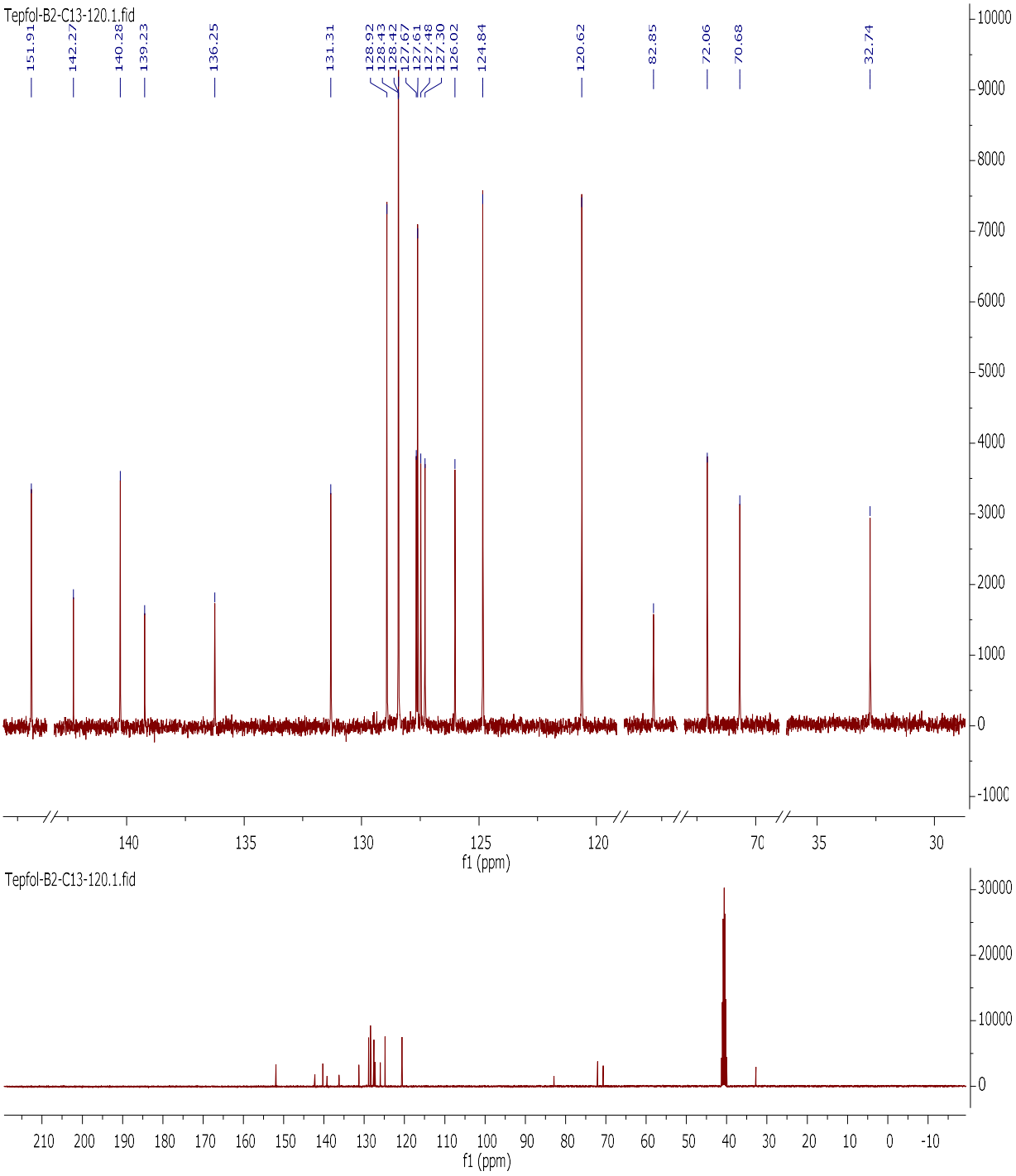
Tepfol-B2-C13-120.1.fid
151.91
142.27
140.28
139.23
136.25
131.31
128.92
128.43
128.42
127.67
127.61
127.48
127.30
126.02
124.84
120.62
82.85
72.06
70.68
32.74
f1 (ppm)
Tepfol-B2-C13-120.1.fid
f1 (ppm)

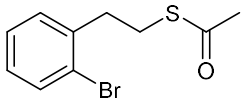
S
O
Br

1.41

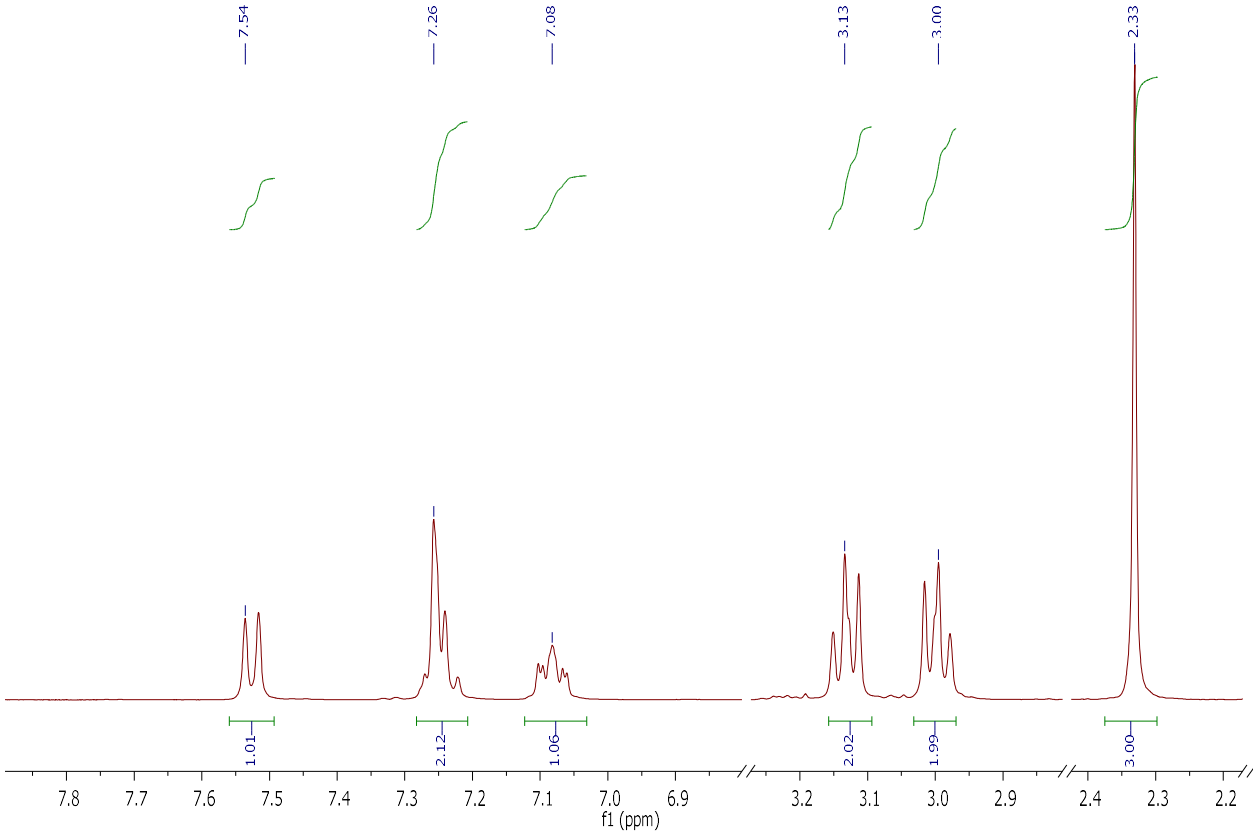
7.54
7.26
7.08
3.13
3.00
2.33
1.01
2.12
1.06
2.02
1.99
3.00
7.8 7.7 7.6 7.5 7.4 7.3 7.2 7.1 7.0 6.9 3.2 3.1 3.0 2.9 2.4 2.3 2.2
f1 (ppm)

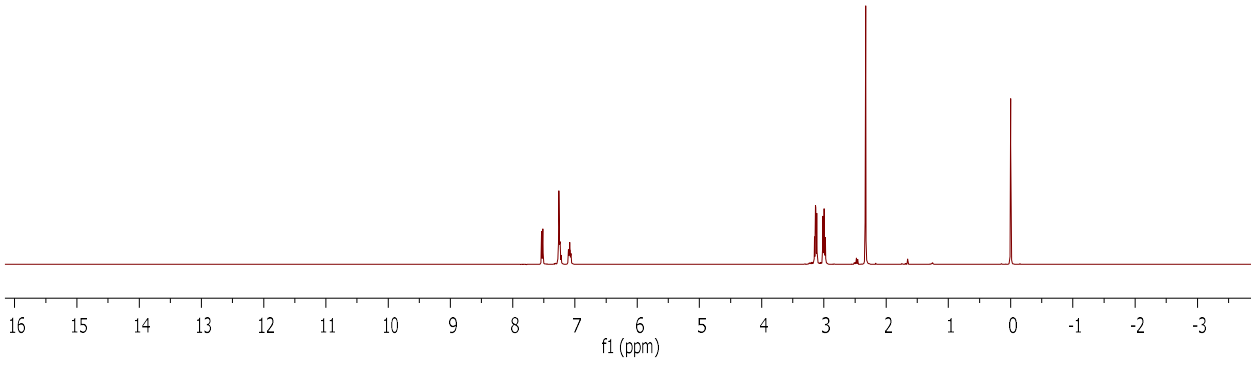
16 15 14 13 12 11 10 9 8 7 6 5 4 3 2 1 0 -1 -2 -3
f1 (ppm)

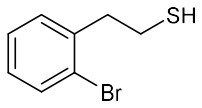
SH
Br

1.42

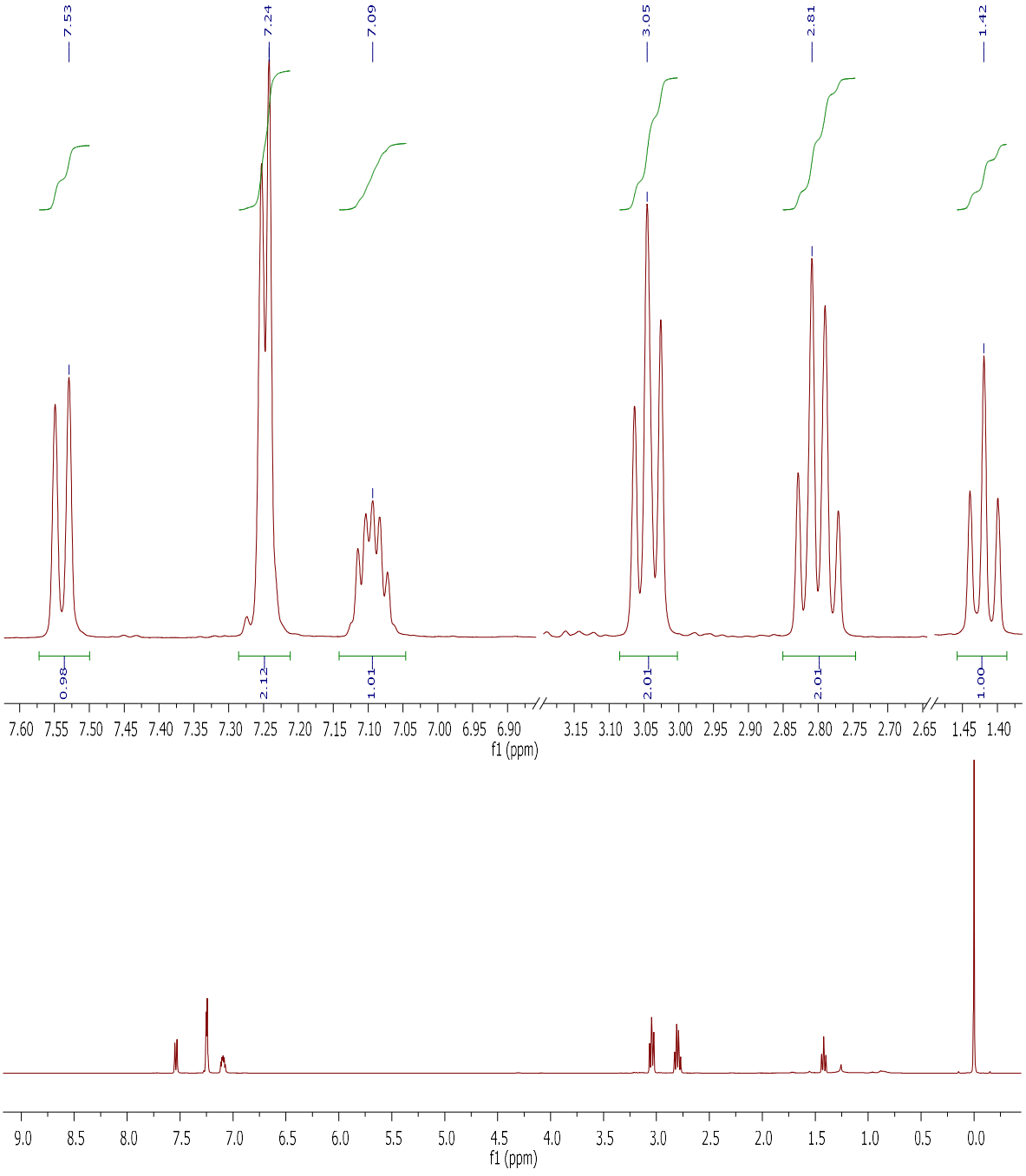
7.53
7.24
7.09
3.05
2.81
1.42
0.98
2.12
1.01
2.01
2.01
1.00
7.60 7.55 7.50 7.45 7.40 7.35 7.30 7.25 7.20 7.15 7.10 7.05 7.00 6.95 6.90
3.15 3.10 3.05 3.00 2.95 2.90 2.85 2.80 2.75 2.70 2.65
1.45 1.40
f1 (ppm)
9.0 8.5 8.0 7.5 7.0 6.5 6.0 5.5 5.0 4.5 4.0 3.5 3.0 2.5 2.0 1.5 1.0 0.5 0.0
f1 (ppm)

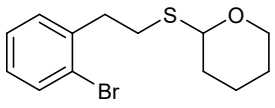
S
O
Br

1.43

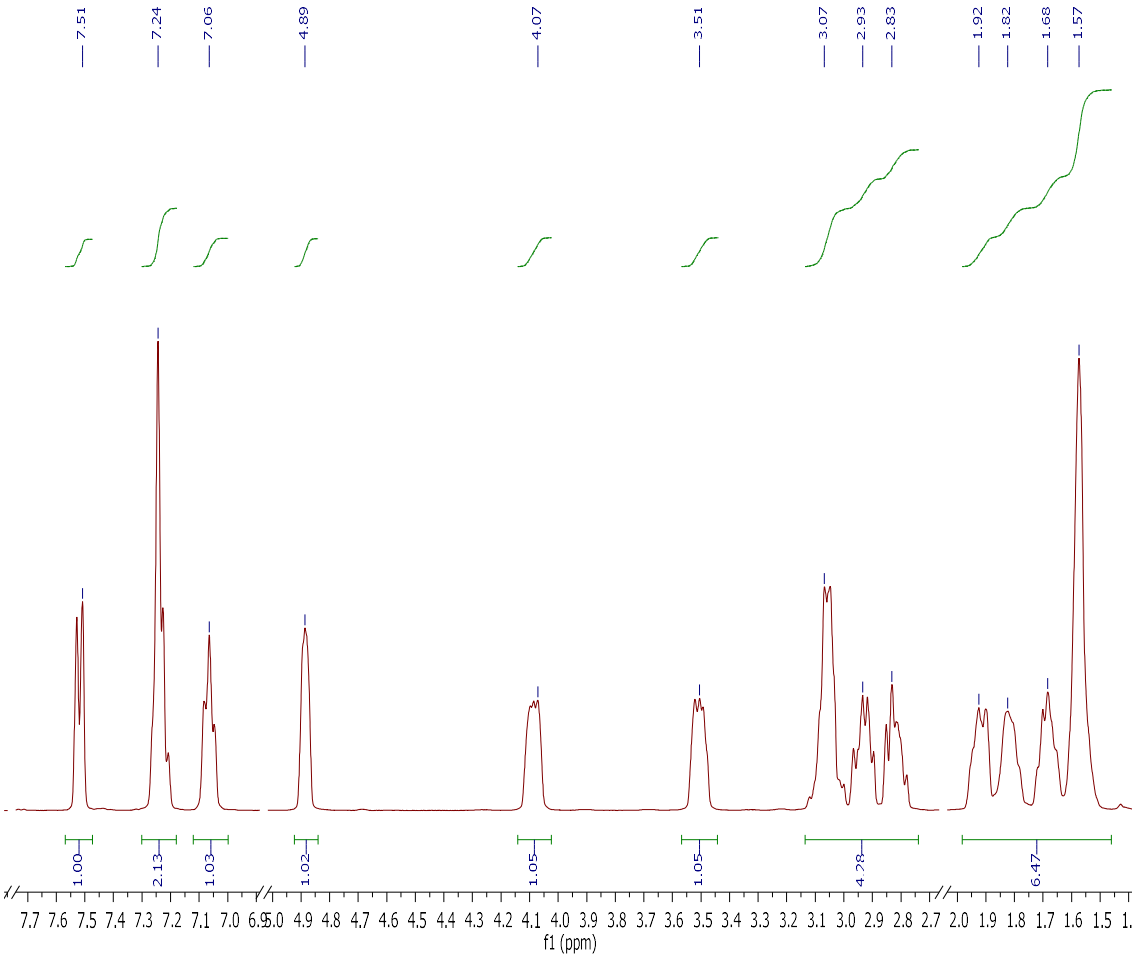
7.51
7.24
7.06
4.89
4.07
3.51
3.07
2.93
2.83
1.92
1.82
1.68
1.57
1.00
2.13
1.03
1.02
1.05
1.05
4.28
6.47
f1 (ppm)

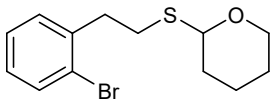
S
O
Br

1.43

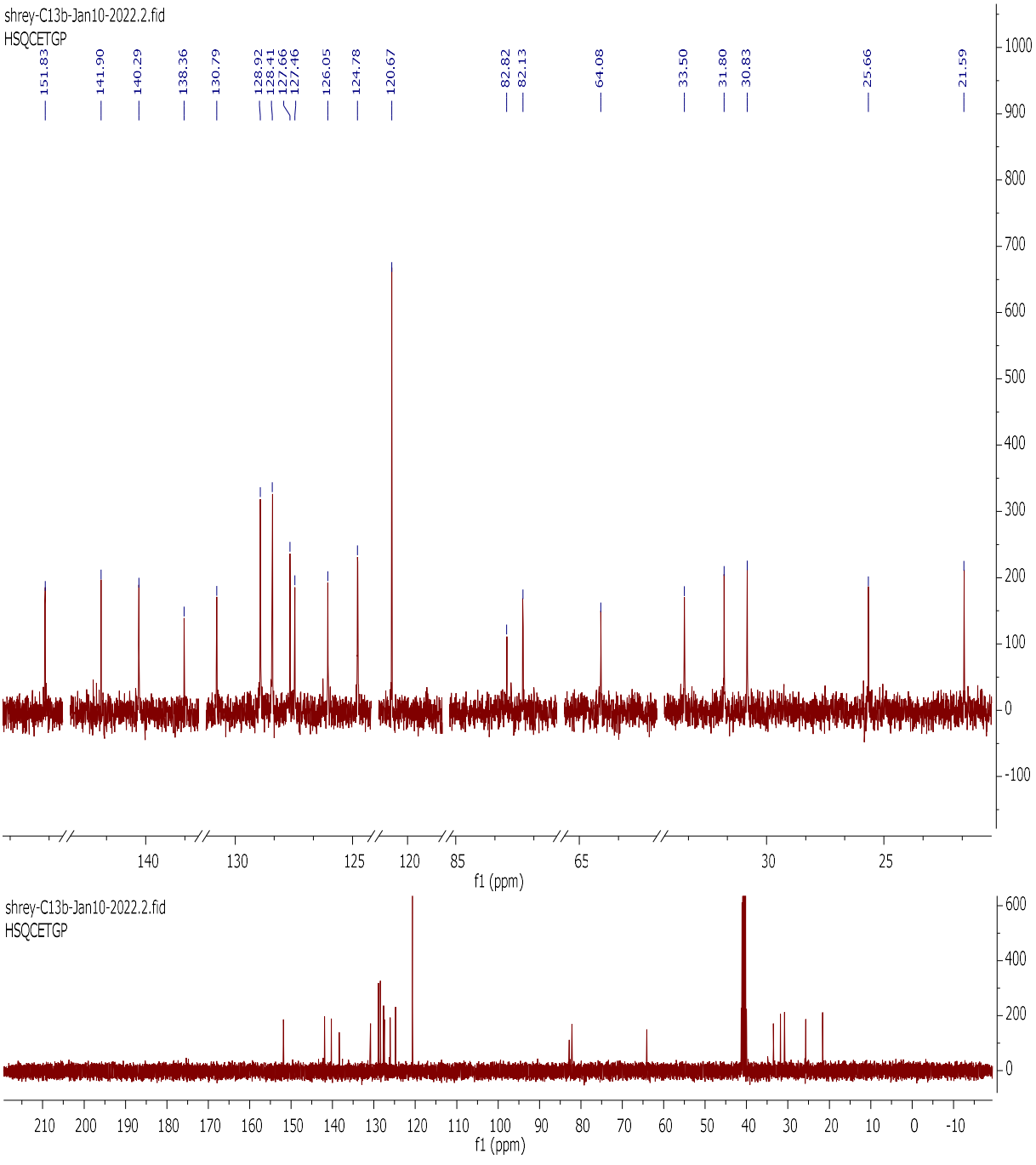
shrey-C13b-Jan10-2022.2.fid
HSQCETGP
151.83
141.90
140.29
138.36
130.79
128.92
128.41
127.66
127.46
126.05
124.78
120.67
82.82
82.13
64.08
33.50
31.80
30.83
25.66
21.59
f1 (ppm)
shrey-C13b-Jan10-2022.2.fid
HSQCETGP
f1 (ppm)

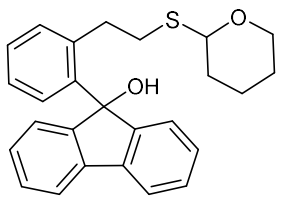
S
O
OH

1.44

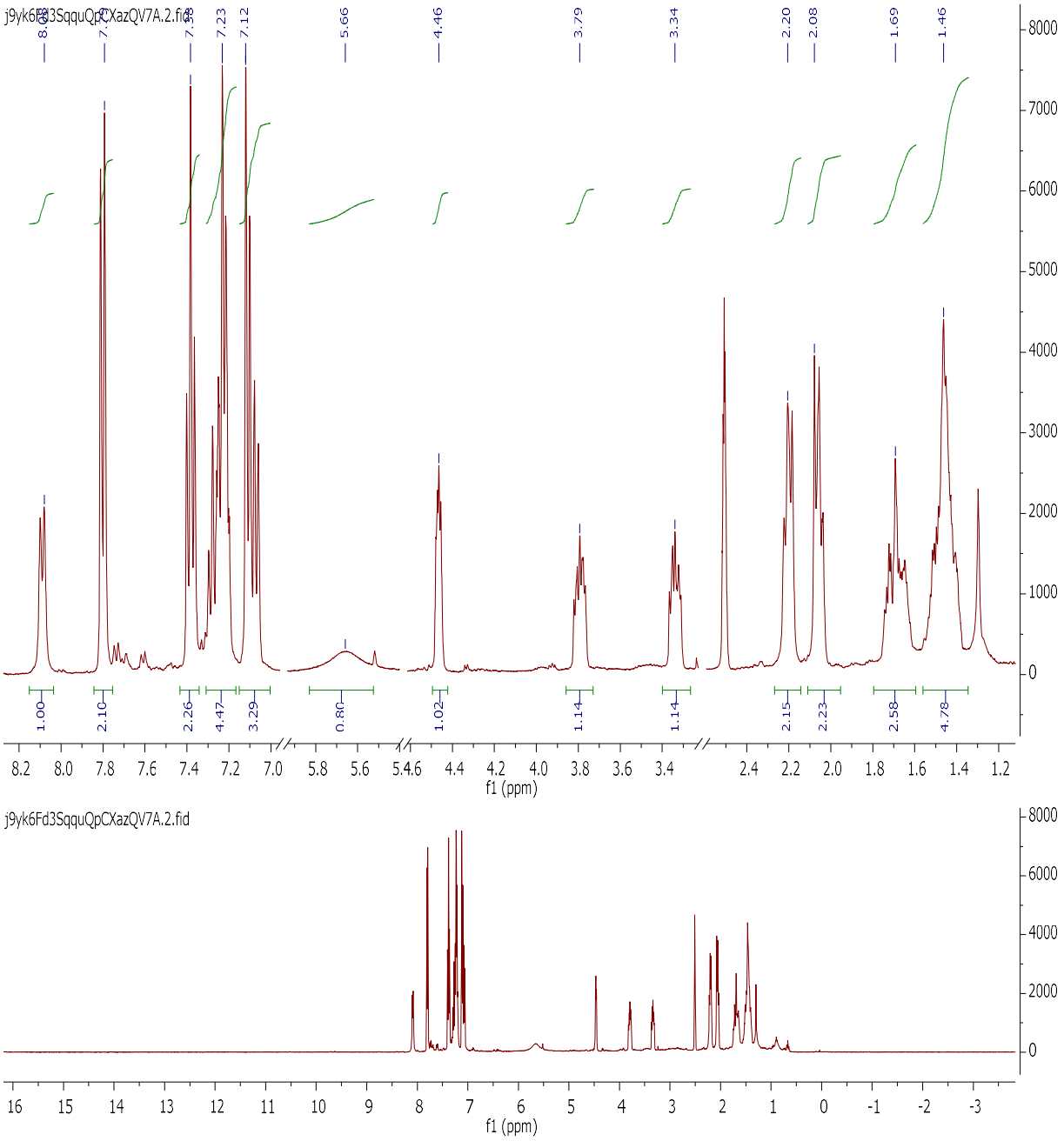
j9yk6Fd3SqquQpCXazQV7A.2.fid
8.03
7.78
7.38
7.23
7.12
5.66
4.46
3.79
3.34
2.20
2.08
1.69
1.46
1.00
2.10
2.26
4.47
3.29
0.80
1.02
1.14
1.14
2.15
2.23
2.58
4.78
f1 (ppm)
j9yk6Fd3SqquQpCXazQV7A.2.fid
f1 (ppm)

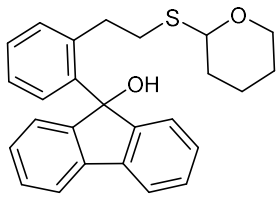
S
O
OH

1.44

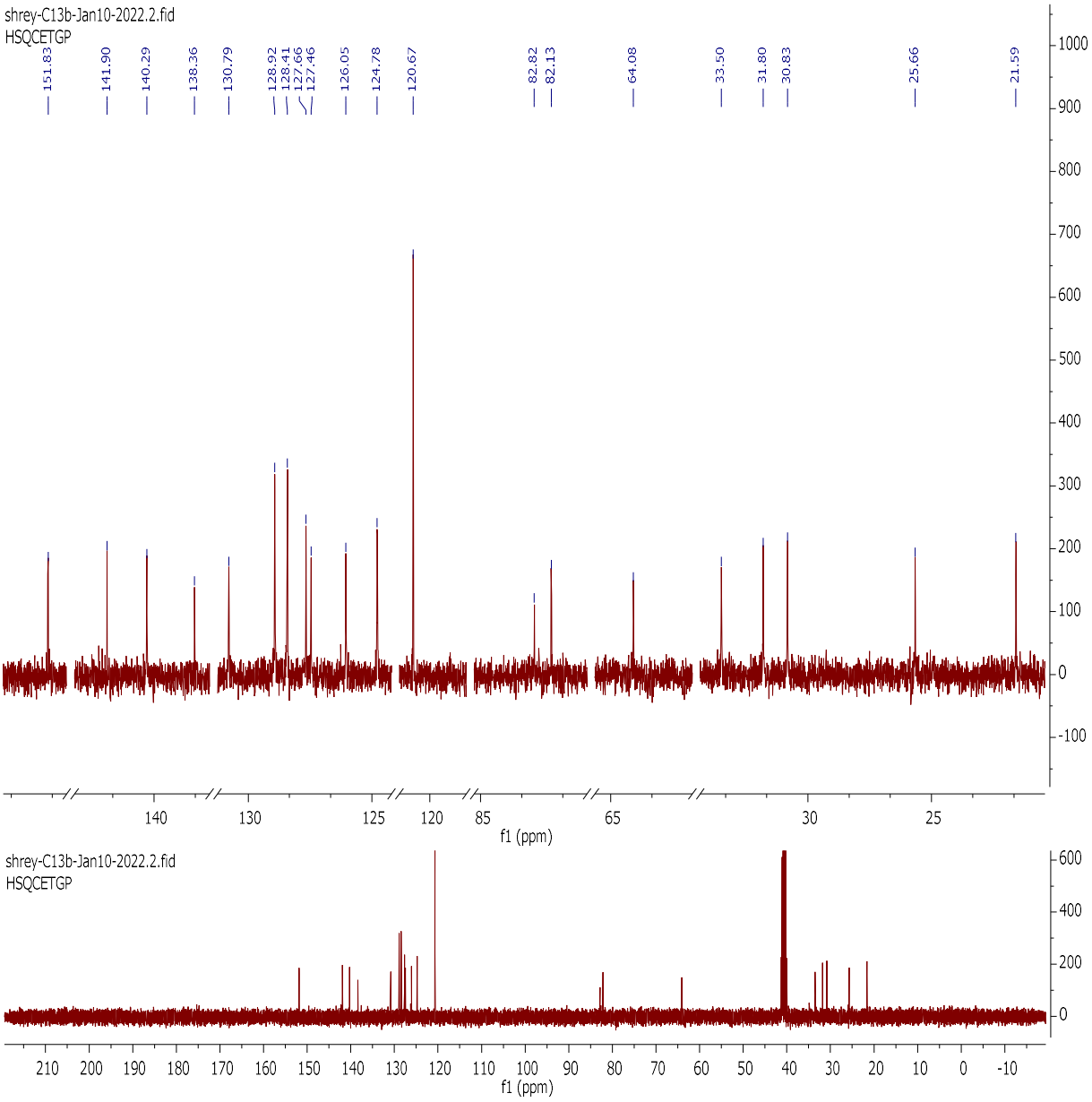
shrey-C13b-Jan10-2022.2.fid
HSQCETGP
151.83
141.90
140.29
138.36
130.79
128.92
128.41
127.66
127.46
126.05
124.78
120.67
82.82
82.13
64.08
33.50
31.80
30.83
25.66
21.59
f1 (ppm)
shrey-C13b-Jan10-2022.2.fid
HSQCETGP
f1 (ppm)

APPENDIX B

Mass Spectra of Non-synthesized Photochemical Products from GC/MS

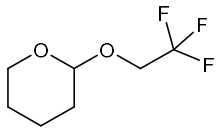

1.15

m/z M^+ = 183

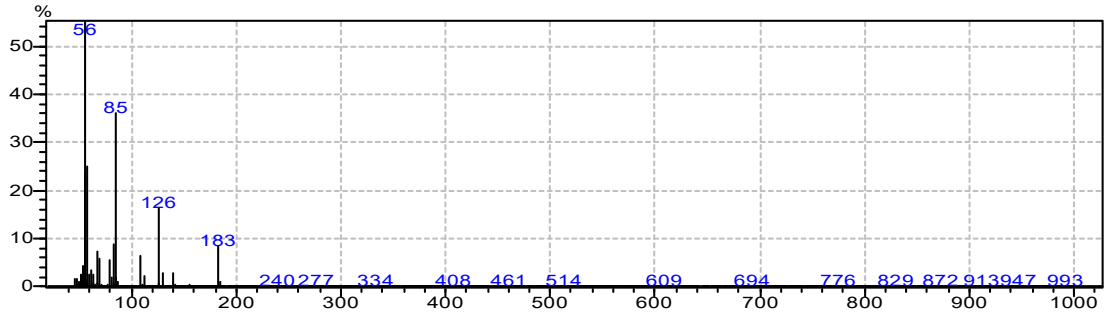

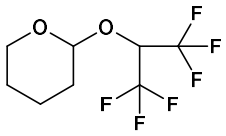

1.16

m/z M^+ = 252

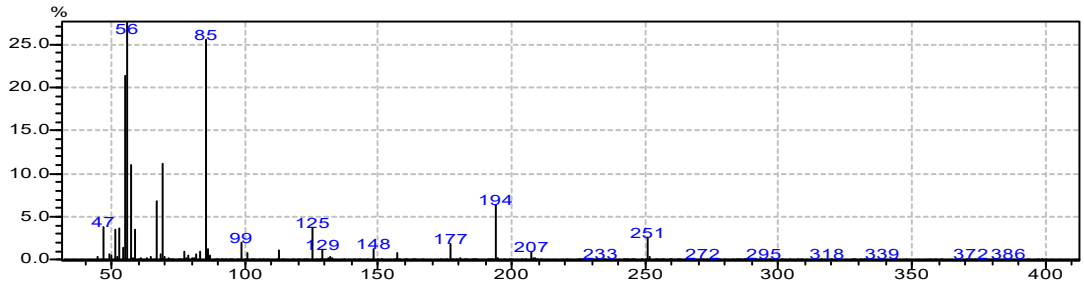

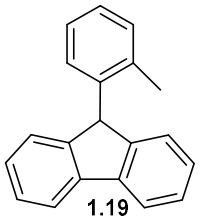

m/z M^+ = 256

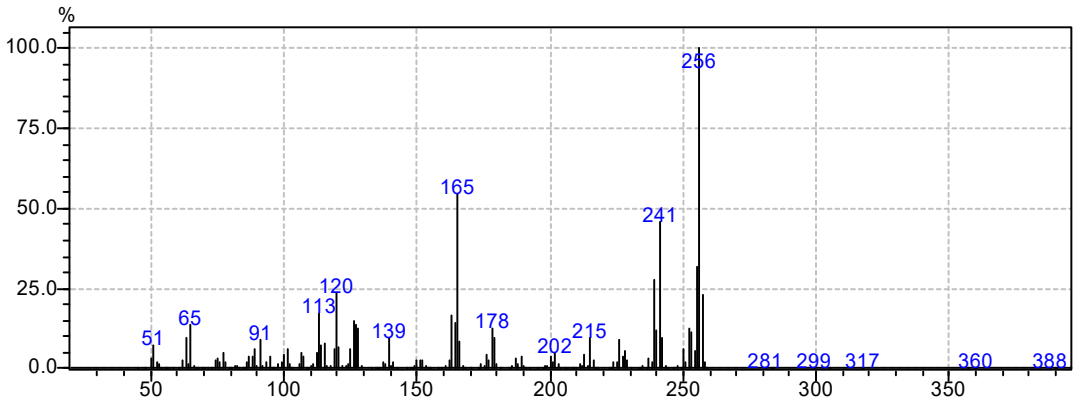

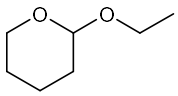

m/z M^+ = 129

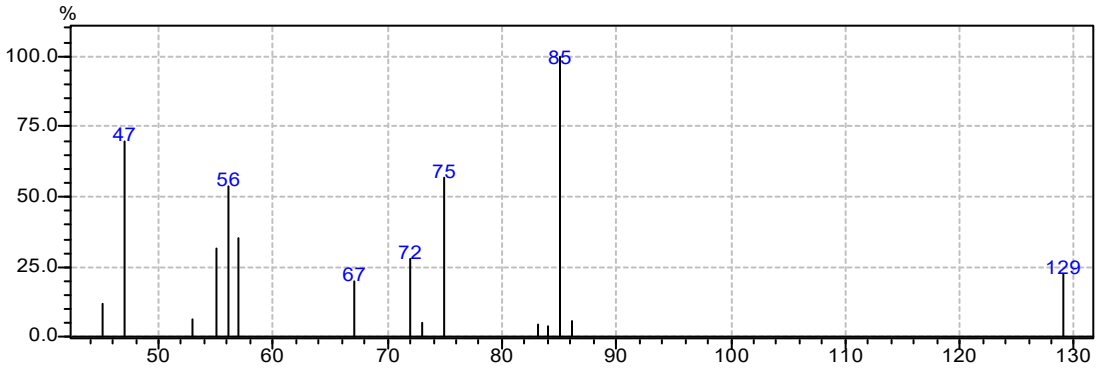

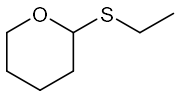

m/z M^+ = 146

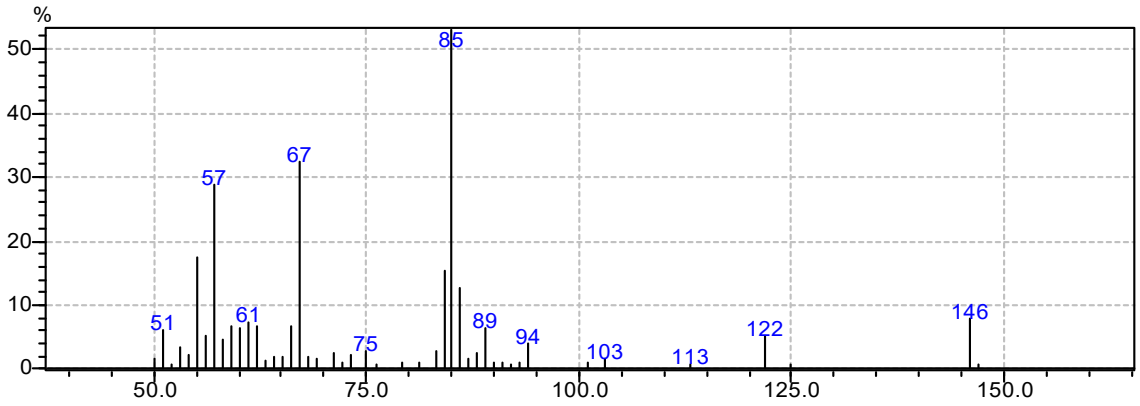

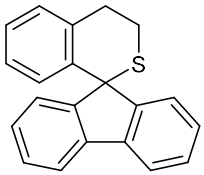

1.45

m/z M^+ = 146

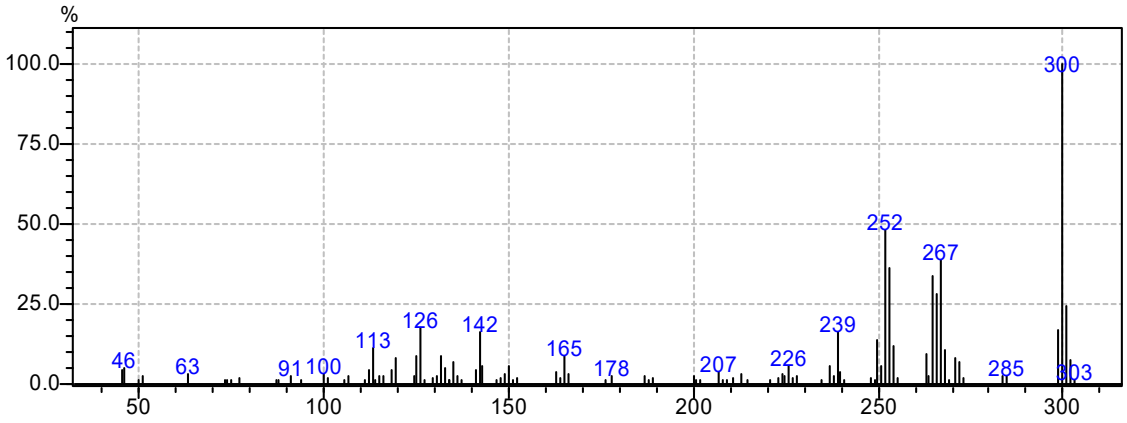

APPENDIX C

Quantum Yield Calculation of HEPFOL-THP in DCM

Actinometer reaction:

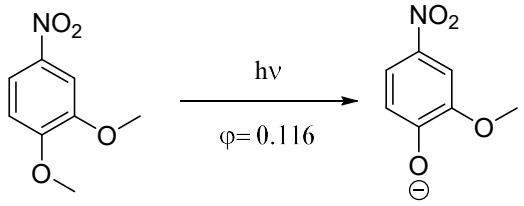

0.16 mM of 1,2-dimethoxy-4-nitrobenzene in 0.5 M KOH was used (Abs @ 300 nm = 0.810)

Photochemical reaction:

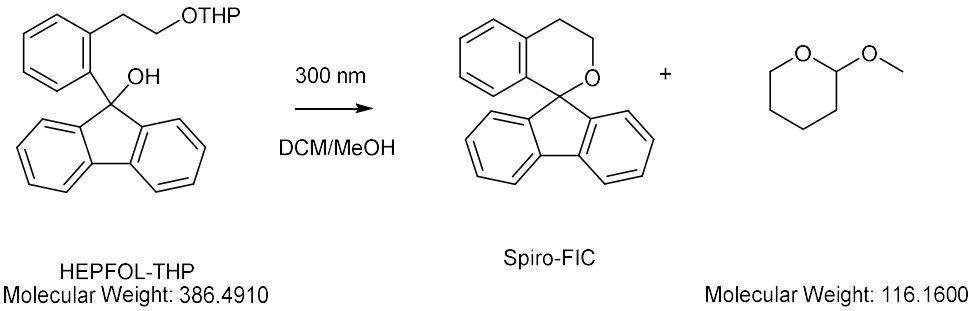

Sample preparation: 0.15 mM HEPFOL-THP in dry DCM with 40 mM MeOH (250 eq.)

Absorbance @ 300 nm = 0.785

Irradiation conditions: Small rayonet with two 300 nm lamps while stirring.

Quantum yield = Number of moles consumed / Number of photons absorbed

Actinometer (Total volume: 3 mL)

Irradiation time	Absorbance at 450 nm
0 sec	0.0040
15 sec	0.0450
Δ Abs	0.041
Δ Concentration (ε = 3040 M^{-1} cm^{-1})	1.35 x 10^{-5}
Number of moles (Volume = 3 mL)	4.05 x 10^{-8}
Number of photons absorbed	3.49 x 10^{-7}

HEPFOL-THP Photoreaction (Total volume: 1 mL)

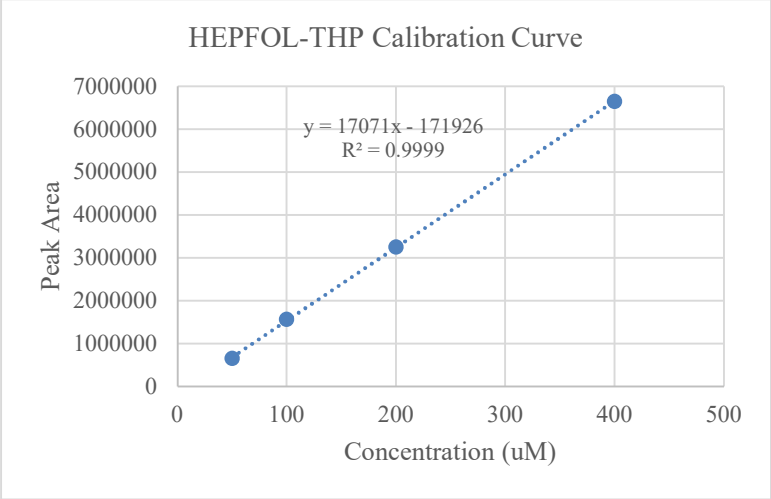

Irradiation time	HPLC Peak Area
0 sec	2583789
15 sec	2290599
Δ peak area	293190
Δ Concentration	2.72 x 10^{-5}
Number of moles (Volume = 1 mL)	2.72 x 10^{-8}

$$\frac{2.72\ x\ 10^{-8}}{3.49\ x\ 10^{-7}} = \varphi = 0.077$$